Land Use Regulations, Migration and Rising House Price Dispersion in the U.S.*

Wukuang Cun
USC Dornsife INET, University of Southern California

M. Hashem Pesaran
Department of Economics & USC Dornsife INET,
University of Southern California, USA and Trinity College, Cambridge, UK

April 2, 2018

Abstract

This paper develops a dynamic spatial equilibrium model of regional housing markets in which house prices are jointly determined with migration flows. Agents optimize period-by-period and decide whether to remain where they are or migrate to a new location at the start of each period. The gain from migration depends on the differences in incomes, housing and migration costs. The agent's optimal location choice and the resultant migration process is shown to be Markovian with the transition probabilities across all location pairs given as non-linear functions of income and housing cost differentials, which are endogenously determined. On the supply side, in each location the construction firms build new houses by combing land and residential structures. The regional land supplies are exogenously given. When a tightening of regional land-use regulation reduces local housing supply, upward pressure on house prices created by excess housing demand cascades to other locations via migration. It is shown that the deterministic version of the model has a unique equilibrium and a unique balanced growth path. We estimate the state-level supplies of new residential land from the model using housing market and urban land acreage data. These estimates are shown to be significantly negatively correlated with the Wharton Residential Land Use Regulatory Index. The model can simultaneously account for the rise in house price dispersion and the interstate migration in the U.S. during the period 1976-2014. Counterfactual simulations suggest that reducing either land supply differentials or migration costs could significantly lower house price dispersion. The model predicts substantially smaller impacts of land-use deregulation on population reallocation as compared to recent existing models of housing and migration that assume population are perfectly mobile.

JEL Classification: E0, R23, R31;
Keywords: house price dispersion, endogenous location choice, interstate migration, land-use restriction, spatial equilibrium

*We are grateful to Alexander Chudik and Ron Smith for helpful comments.

1 Introduction

The secular increase in the house price dispersion across U.S. states has been the ongoing focus of empirical and theoretical research.[1] Van Nieuwerburgh and Weill (2010) and Gyourko et al. (2013) attribute the increase in house price dispersion to rising income dispersion.[2] However, the increase in income disparities across states can only explain a small fraction of the substantial rise in house price dispersion observed since 1970s . Even after adjusting house prices for income differences, we are still left with a substantial secular rise in the dispersion of house prices relative to incomes.[3] Glaeser and Gyourko (2003), Glaeser et al. (2005) and Quigley and Raphael (2005) find that areas with faster than average growth in house prices tend to have more restrictions on residential land-use. However, the positive relationship between land-use regulation and house price growth observed across locations cannot be rationalized by the canonical spatial equilibrium models that assume perfect population mobility across locations.[4] When agents are perfectly mobile, migration equalizes utility across locations and consequently differences in house prices only reflect differences in incomes and amenities, and differences in land supplies do not impact the spatial equilibrium of house prices. Recently, Hsieh and Moretti (2015) and Herkenhoff et al. (2018), go beyond the analysis of house prices and examine the impact of land-use regulations on spatial labor allocation. They argue that the tightened land-use regulations in the high-productivity U.S. cities raise local housing costs, which deter migration flows towards these cities and lead to labor misallocation. Their models predict that land-use deregulation can lead to substantial population reallocations to high-productivity cities and a considerable increase in the average labor productivity.[5] However, since their models are built on the assumption of perfect labor mobility, the effects of deregulation might be over-estimated. Degree of population mobility is an important factor in determining the extent to which spatial heterogeneity in land-use regulation results in rising house price dispersion and/or migration towards low housing cost locations.

This paper contributes to the literature by developing a dynamic spatial equilibrium model of regional housing markets in which house prices are jointly determined with migration flows. At the start of each period agents decide whether to remain where they are or migrate to a different location. The expected gain from migration depends on the expected differences in incomes and housing costs between the origin and the destination and

[1] Similar increases in house price dispersion have also been documented across Metropolitan Statistical Areas (MSAs). But a decomposition of house price dispersion within and between states clearly show that the increases in house price dispersion at the MSA level are mainly due to increases in between-state dispersion, as the within-state dispersion has not increased that much (see details in Appendix D.2).

[2] For example, Van Nieuwerburgh and Weill (2010) find that the rise in wage dispersion across MSAs is large enough to account for the rise in house price dispersion during 1975–2004. Gyourko et al. (2013) show that an increase in the number of high-income households nationally can lead to house price dispersion.

[3] See Figure 1 in Section 2.

[4] For example, the spatial equilibrium models studied in Glaeser and Tobio (2008) and Gyourko et al. (2010) are built on the assumption that capital and labor are perfectly mobile.

[5] In addition, Parkhomenko (2016) studies how regional housing supply regulations are endogenously determined in political processes, and the implications of rising housing supply regulations for spatial labor allocations and aggregate output.

the migration cost that consists of a route-specific and a stochastic idiosyncratic component. The agent's optimal location choice and the resultant migration process is shown to be Markovian with the transition probabilities across all location pairs given as non-linear functions of income and housing cost differentials, which are endogenously determined. In each location, the construction firms build new houses by combining land and residential structures. The regional land supplies are exogenously given. When a tightening of regional land-use regulation reduces the local land supply, upward pressure on house prices created by excess housing demand cascades to other locations via migration. It is shown that the deterministic version of the model has a unique balanced growth path, on which no location ends up with zero population.

In this paper we focus on the spatial equilibrium of regional housing markets, and abstract from modelling the production sectors by assuming that the spatial distribution of wage rates is given exogenously. This assumption is made for expositional simplicity and can be relaxed by allowing for capital and agglomeration effects in location-specific production functions, following the studies by Ciccone and Hall (1996) and Davis et al. (2014). Such an extension is considered in Section S2 of the online supplement, where it is shown that our main theoretical results on the existence and uniqueness of the long-run equilibrium continue to hold, and the quantitative results obtained inclusive of capital and agglomeration effects (rendering the wage rates endogenous) are qualitatively similar to the ones reported in the paper that abstract from such effects.

Our modelling approach is to be distinguished from existing Rosen-Roback style static spatial equilibrium models, such as, Gyourko et al. (2010) and Hsieh and Moretti (2015), and from the static population allocation models adopted in the studies on spatial labor allocations by Davis et al. (2014) and Herkenhoff et al. (2018), among others.[6] These studies abstract from the dynamics of location-to-location migration flows, and rely on static models of population allocation as an outcome of spatial arbitrage process under perfect population mobility, or consider a representative household that centrally allocates household members (population) across locations. Since it is assumed that labor mobility is perfect, then increases in spatial heterogeneity in land-use regulation tend to have substantial impacts on population reallocation but little impact on house price dispersion. In contrast, we allow for imperfect labor mobility determined by variations in migration costs across origin-destination pairs.[7] Thus, in our model, spatial heterogeneity in land-use regulation simultaneously affects house price dispersion and migration.[8] In addition, when a tightening of regional land-use regulations reduces local housing supply, upward pressure on house prices created by excess housing demand spills over and cascades to other locations via migration. The route-specific migration costs determine the magnitudes and the directions of the spillover effects. Furthermore, we explicitly modelled the dynamic interactions between migration and local housing

[6] The models adopted in Gyourko et al. (2010) and Hsieh and Moretti (2015) are built on the static spatial equilibrium set up developed by Rosen (1979) and Roback (1982).

[7] The rate of migration is not uniform across the U.S.. The extent of migration between two neighboring states or between the East and the West Coasts is considerably higher than between other states, which implies that mobility may vary substantially across different origin/destination state pairs.

[8] As shown in Section S6 of the online supplement, spatial heterogeneity in land-use regulation leads to secular rise in house price dispersion only in the presence of non-zero migration costs.

markets, which also distinguishes our work from their studies. The dynamic nature of our model allows us to analyze the evolutions of the U.S. regional housing markets between the short run and the long run equilibrium.[9] To our knowledge, the present paper is the first to explicitly model migration as the source of spatial spillover effects in regional housing markets.

Our paper also differs from demographic studies on migration that use Markov chain models as Fuguitt (1965) and Tarver and Gurley (1965). These studies assume that transition probabilities across locations are exogenously given, whilst in our study we allow migration flows to interact with local housing markets through endogenous and nonlinear variations in transition probabilities across location pairs and over time.

We calibrate our model on a panel of 49 states (including the District of Columbia) in the U.S. mainland over the period 1976-2014. The route-specific migration costs are estimated using the combined state-to-state migration flows and state level incomes and housing costs data. Parameters that govern local housing supplies are calibrated using state level housing market data. We estimate the state-level supplies of new residential land from the model using housing market and urban land acreage data. These estimates are shown to be significantly negatively correlated with the Wharton Residential Land Use Regulatory Index (WRI henceforth).

In the baseline simulation exercise, we examine the performance of the model in accounting for the observed rise in house price dispersion during the period 1976-2014, taking the realized state level income processes as given. We are able to simultaneously account for the rise in house price dispersion and the interstate migration in the U.S. during the sample period. In addition to land supply differentials, we also consider the roles of other forms of spatial heterogeneities in this process. The results of counterfactual exercises show that land supply differentials are the major factor behind the rising house price dispersion in the U.S.. To examine how land supply differentials and migration costs jointly contribute to the rise in house price dispersion, we carry out simulations assuming different levels of land supply differentials and migration costs. The results indicate that both land supply differentials and migration costs play significant roles in driving up price dispersion; reducing either of them can significantly lower house price dispersion in the U.S.. In addition, increases in land supply differentials would lead to a larger rise in house price dispersion when migration costs are larger.

According to Gyourko et al. (2015), the residential land-use regulatory environments of some areas in the U.S. started to become stricter from 1970s onward. Land-use regulations can have important implications not only for local house prices, but also for the composition of population across U.S. states. Deregulating in states with stricter land-use restrictions can affect population movements between states through the house price channel (Herkenhoff et al. (2018)). To examine the impacts of local land-use regulations on house prices and populations, we consider two counterfactual exercise: a land-use deregulation in California and a tightening of land-use regulation in Texas. These exercises show that changes in

[9] The U.S. regional housing markets are unlikely to be in their long run equilibrium, considering the secular rise of house price dispersion in the U.S. since 1970s. Some parts of the observed house price differences across locations can be due to disequilibrium, which should diminish overtime with population re-location.

local land-use regulations can affect population allocation via the house price channel, but its effects tend to be relatively moderate as compared to predictions obtained from recent existing models of housing and migration, which assume population are perfectly mobile, as in studies by Hsieh and Moretti (2015) and Herkenhoff et al. (2018), for instance. We find that house prices are much more affected by changes in land use regulations as compared to their effects on allocation of population. For example, our model predicts that increasing the average land supply growth rate of California to the national average induces the population of California to rise by one million (around 2 per cent in 2014 values), whilst such a deregulations could reduce the average rate of increase in real house prices from 2.5 per cent realized during 1976-2014 to a mere 0.23 per cent counterfactually. On the opposite extreme, reducing the average land supply growth rate of Texas to the national average reduces Texas's population by 0.7 million (around 3 per cent in 2014 values), but increases the average growth rate of real house prices from a realized negative value of -0.114 per cent to a positive rate of 0.868 per cent.

The dynamic and spatial nature of our model also allows us to examine the migration linkages between U.S. states, and their evolution over times. We investigate the impulse responses of state level house prices and population to regional shocks, and take a negative regional productivity shock to California as an example. As local productivity drops, agents migrate out from California to other states, which raises housing demand and house prices in these states. However, the responses of house prices in the neighboring states of California are faster and stronger than those of the other states. In addition, migration flows between California and its neighboring states are also more responsive to the shock. The impulse responses of the model economy to regional productivity shocks to New York, Illinois, Florida and Texas also have similar patterns. These results suggest, perhaps not surprisingly, that migrations between states that are geographically close are more responsive to changes in income and housing cost differentials, which tends to keep the house price differences between them from increasing. This partially explains why the model can replicate a substantial rise in dispersion of house prices in the U.S. at a regional level, combined with only moderate increases of house price dispersions within the regions.

The present paper is closely related to Herkenhoff et al. (2018), which studies the impacts of land-use regulations on the spatial allocations of labor and capital across U.S. states. Tough the two papers study similar issues, they have very different theoretical underpinnings and empirical focus. First, Herkenhoff et al. (2018) solve the problem of allocations of labor and capital across locations, and between production and housing sectors, using a single representative household in the economy who centrally and frictionlessly allocates labor and capital. In contrast, the present paper explicitly models the dynamics of location-to-location migration flows allowing for migration costs, and develops an inter-temporal model of housing supplies and considers the evolution of the model economy towards its long-run spatial equilibrium. Also in Herkenhoff et al. (2018) the tightness of land-use regulations are measured as the productivities of existing land in the production of housing services, whilst the present uses state level growth rates of newly released residential land to measure tightness directly, which is shown to significantly negatively correlated with the WRI. Third, both papers consider the effects of land-use regulations on housing and spatial labor allocation over the past few decades; however, they have adopted very different quantitative approaches. Herkenhoff et al. (2018) compares the different steady states of the model with the tightness of land-use regulations being set to different historical levels. In contrast, the present paper simulates the transition path of the model economy over the period 1976-2014 without assuming steady state. We believe that the U.S. regional housing markets are unlikely to have been in their long run equilibrium during this period, considering the secular rise of house price dispersion. Finally, the present paper predicts substantially smaller impacts of land-use deregulations on population reallocation as compared to Herkenhoff et al. (2018) in which labor are reallocated frictionlessly.

In our analysis population mobility plays the key role in determining how land-use regulations affect house price dispersion and migration, which relates our work to the literature on location choice and migration. This strand of literature can be dated back to Mcfadden (1978), who argues that population mobility can be imperfect due to the substantial variation of migration cost across individuals. Skill sorting, which is applied in some recent works on house price dispersion, such as, Van Nieuwerburgh and Weill (2010) and Gyourko et al. (2013), can be an example of heterogeneous migration costs. These authors assume that workers have different skill types and high-skilled workers can better exploit their skills only at high-productivity locations. Therefore, high-skilled workers face relatively higher costs to move out of high productivity locations, and are thus less responsive to rising housing costs. In this paper, we focus on the variation of mobility across space and its implications for house price dispersion and migration, rather than the factors or mechanisms behind the imperfect mobility, which is motivated by the observation that the extent of migration flow varies substantially across location pairs in the U.S..[10]

Our paper also relates to empirical studies that find strong spatial spill-over effects in house price changes in the U.S. Holly et al. (2010) show that house price-to-income ratios across U.S. states are spatially correlated. Bailey et al. (2016) show that common national and regional factors are important explanations of house prices changes across U.S. MSAs and spatial spill-over effects are still present in de-factored house price changes. Cohen et al. (2016) also report significant spatial effects in house price dynamics, and further find that spatial pill-over effects are magnified in the aftermath of the 2007-2008 housing crash. Sinai (2012) finds that the booms and busts in the U.S. regional housing markets are geographically clustered. Cotter et al. (2011) identify the statistical jumps in house prices in the U.S. MSAs and find that the jump correlations are especially high between MSAs in California. DeFusco et al. (2017) finds that house prices in the neighboring MSAs have significant effects on the local house prices. In our model, regional housing markets interact with each other via migration flows, which function as a source of spatial spill-over effects.

The rest of the paper is organized as follows. Section 2 describes the data and summarizes the statistical patterns of house price dispersion across U.S. states and interstate migration. Section 3 presents the model. Section 4 characterizes the equilibrium and proves the existence

[10] Recently, considerable attention is paid to the effects of housing on mobility. In particular, Ferreira et al. (2010), Head and Lloyd-Ellis (2012), Davis et al. (2013), Nenov (2015) and Sterk (2015) examine how housing market liquidity can affect labor mobility. In addition, Ouazad and Ranciere (2017) investigate how residents' accesses to mortgage loans can affect their mobility.

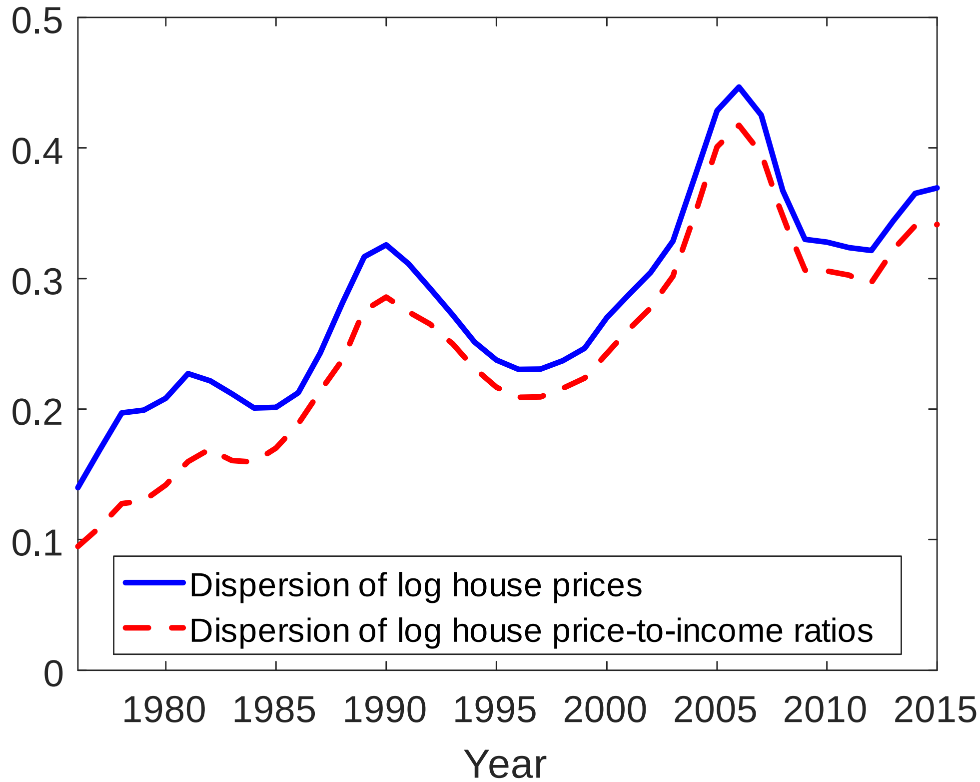

Figure 1: Dispersions of log house prices and log house price-to-income ratios across U.S. states

Notes: The solid line shows the standard deviation of log real house prices across U.S. states. The dashed line shows the standard deviation of log house price-to-income ratios across U.S. states.

and the uniqueness of the equilibrium and the balanced growth path. Section 5 calibrates the model. Section 6 presents of the compact form of the system of equations. Section 7 provides the quantitative analyses. Section 8 concludes. Extensions of the baseline model are discussed in the online supplement.[11]

2 House price dispersion and migration in the U.S.

We begin by documenting several patterns of house price dispersion across U.S. states:

- *Fact 1: The dispersion of house prices across U.S. states has substantially increased during* 1976-2014*.*
- *Fact 2: The rise in the dispersion of house prices cannot be explained in terms of*

[11] In this paper, we focus on the reasons behind the upward trend in house price dispersion. However, our model can also account for the cyclical fluctuations in house price dispersion after being extended to allow for mortgage loans and credit supply shocks. The details are provided in Section S3 of the online supplement.

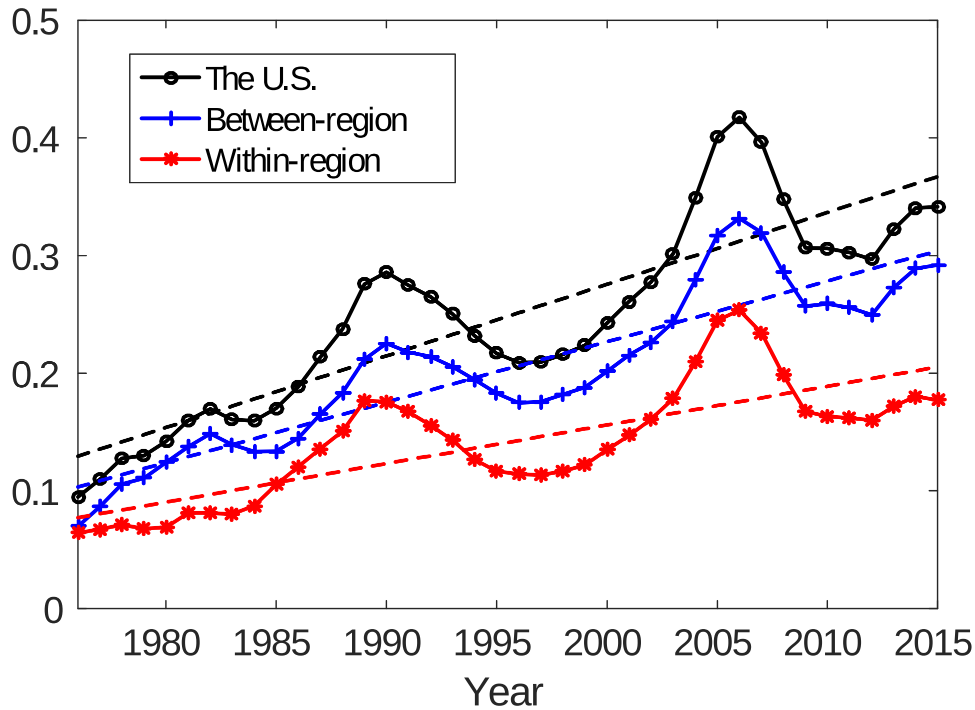

Figure 2: Dispersions of log house price-to-income ratios within and between U.S. regions

Notes: The line designated with 'o' shows the dispersion of log house price-to-income ratios across the 48 states and the District of Columbia in the U.S. mainland. The line designated with '+' shows the dispersion of log house price-to-income ratios across the five U.S. regions. The line designated with '*' shows the average of within-region dispersions, where within-region dispersion is the standard deviation of log house price-to-income ratios across the states that are within a given region.

the rise in the dispersion of incomes, and the house price-to-income ratio continues to exhibit secular trends over the 1976-2014 *period.*

- *Fact 3*: *The dynamics of house price-to-income ratios dispersion have significant cyclical patterns.*
- *Fact 4: The rise in house price dispersion is basically a between-region phenomenon.*

As shown in Figure 1, the dispersion of log real house prices across U.S. states has been increasing over the past decades. In addition, the increases in income dispersion can only account for a very small portion of the rise in house price dispersion since the dispersion of log house price-to-income ratios has also been rising over the 1976-2014 period.

We divided the 49 states/districts in the U.S. main land into five groups following the regional categorization by the National Geographic Society.[12] We decomposed the dispersion across U.S. states into dispersions within- and between- regions.[13] As shown in Figure 2, the

[12]For further information on the regional categorization by the National Geographic Society, see `http://www.nationalgeographic.org/maps/united-states-regions/`.

[13]For the derivations of the dispersion decomposition formula, see Section S5 of the online supplement.

average within-region dispersion has been increasing much slower than the between-region dispersion. The increase in the dispersion between regions is mainly due to the increasing differences in house price-to-income ratios between the West Coast and the Southern states.

A natural concern about using state level house price data is that it ignores price differences between cities and rural areas, and price dispersion between cities within a state. However, only a very small portion of U.S. population live in rural areas.[14] We constructed an alternative measure for between-state dispersion using MSA level data, where state level house prices are measured by aggregated MSA level prices. These two measures look quite similar during 1975-2007.[15] In addition, after decomposing between-MSA dispersion into within- and between- state dispersions, we find that the increases in within-State dispersions contributed very little in the rise in between-MSA dispersion.[16] Thus, we think it is not necessary to impose a higher level of disaggregation beyond the state level.

In addition, we decompose population changes of U.S. states into an intrinsic component, defined by net birth plus international migration inflows, and an extrinsic component defined by net inflows of migrants from other states.[17]

- *Fact 5: The Southern states have been attracting population from the rest of the country, known as* "the rise of the Sunbelt" (Glaeser and Tobio (2008)).

During recent decades, the growth of house prices in the Southern states have been substantially lower than the average growth rate house prices at the national level. The rate of increase in house prices in Southern states has also been below the average growth of real incomes in these states. The relatively low housing costs in these states have been attracting migrants from other states. However, the size of migration in-flows has not been sufficiently large to significantly narrow down the discrepancy of house price changes between the southern states and the rest of the country.

- *Fact 6: Migration flows between two states that are geographically close are substantially larger than between two distant states.*

Around 75% of migrants migrate to states that are within a 1000-mile radius. Around 50% of migrants migrate to adjacent states.

3 A dynamic spatial equilibrium model

In this section, we develop a dynamic spatial model of housing building on the work of Glaeser and Tobio (2008). We extended their model in two important respects. We provide

[14] In the U.S., around 86% of its population live in MSAs. In the five most populated states, such as, California, New York, Texas, Illinois, and Florida, more than 95% of their population live in MSAs.

[15] For further details, see Appendix D.2.

[16] House prices in cities that are geographically close to each other tend to co-move due to spatial contagion effects between housing markets of neighboring MSAs (Sinai (2012),DeFusco et al. (2017)). These effects help keep house price differences between cities within a state from increasing.

[17] See Appendix B.1 for further details.

a dynamic version of Glaeser and Tobio's static framework, and explicitly model the location-to-location migration choices of agents at the start of each period. In this way, we provide a simultaneously determination of house prices and migration flows over time and across space. This theoretical model can also be viewed as an example of a dynamic network where the strength of the connections are endogenously determined.

3.1 Geography and migration flows

Time, denoted by t, is discrete and the horizon is infinite, so that $t = 0, 1, 2, ...$ There are n locations, and the collection of locations is represented by $\mathcal{I} = \{1, 2, ..., n\}$, where n is fixed but possibly large ($n \geq 2$). The economy is populated by workers who consume goods and housing services, and live for only one period. At the start of each period, workers decide whether to reside at locations where they are born, or migrate to a new location. Denote by $l_{ij}(t)$ the number of workers who are born at location i in period t, and who choose to reside at location j, where i and $j \in \mathcal{I}_n$. Denote the population of workers born at location i at the start of period t by $l_{i\cdot}(t)$. Then

$$l_{i\cdot}(t) = \sum_{j=1}^{n} l_{ij}(t), \tag{1}$$

and the number of workers who choose to reside at location j in period t, denoted by $l_{\cdot j}(t)$, is given by

$$l_{\cdot j}(t) = \sum_{i=1}^{n} l_{ij}(t). \tag{2}$$

The number of workers who are born at location i at the start of period t equals to the number of workers at that location in period $t - 1$, plus an intrinsic exogenously given population change.[18] Denote the intrinsic rate of population change (growth rate if positive) of location i in period t by $g_{l,it}$. Thus, the number of workers born in location i at the start of period t is given by

$$l_{i\cdot}(t) = e^{g_{l,it}} l_{\cdot i}(t - 1), \tag{3}$$

where it is assumed that $g_{l,it}$ follows an exogenously given deterministic process, for $i \in \mathcal{I}_n$, to be specified below.

We model migration probabilities as a Markov process. The probability that an individual worker born at location i chooses to reside at location j in period t is denoted by $\rho_{ij}(t)$, where $\rho_{ij}(t) \geqslant 0$ and $\sum_{j=1}^{n} \rho_{ij}(t) = 1$. Workers' location choices are assumed to be conditionally independent given the location-specific incomes and housing service prices. Thus, according to the law of large numbers, the fraction of workers born in location i who choose to reside at location j converges to $\rho_{ij}(t)$ as population tends to infinity. We ignore any randomness due to finite population and assume the migration flow from location i to location j is determined

[18] The intrinsic population changes are made up of, for example, the net natural population increases (i.e. birth minus death) and the net migration flows from foreign countries.

as

$$\rho_{ij}(t) = \frac{l_{ij}(t)}{l_{i\cdot}(t)}. \tag{4}$$

Thus, the migration flows can be obtained by combining (2), (3) and (4), to obtain

$$\begin{aligned} l_{\cdot j}(t) &= \sum_{i=1}^{n} l_{i\cdot}(t)\rho_{ij}(t), \\ &= \sum_{i=1}^{n} e^{g_{l,it}} l_{\cdot i}(t-1)\rho_{ij}(t), \quad \text{for } j = 1, 2, ..., n. \end{aligned} \tag{5}$$

The above system of equations can be re-written more compactly as

$$\boldsymbol{l}(t) = \boldsymbol{l}(t-1)\mathbf{G}(t)\mathbf{R}(t), \tag{6}$$

where $\boldsymbol{l}(t)$ is the $1 \times n$ (row) vector of location-specific population, defined by

$$\boldsymbol{l}(t) \equiv [l_{\cdot 1}(t), l_{\cdot 2}(t), ..., l_{\cdot n}(t)], \tag{7}$$

and $\mathbf{G}(t)$ is the $n \times n$ diagonal matrix of population growth rates and $\mathbf{R}(t)$ is the $n \times n$ Markovian migration probability matrix, defined by

$$\mathbf{G}(t) \equiv \begin{pmatrix} e^{g_{l,1t}} & 0 & \cdots & 0 \\ 0 & e^{g_{l,2t}} & \cdots & 0 \\ \vdots & \vdots & \ddots & \vdots \\ 0 & 0 & \cdots & e^{g_{l,nt}} \end{pmatrix}, \text{ and } \mathbf{R}(t) \equiv \begin{pmatrix} \rho_{11}(t) & \rho_{12}(t) & \cdots & \rho_{1n}(t) \\ \rho_{21}(t) & \rho_{22}(t) & \cdots & \rho_{2n}(t) \\ \vdots & \vdots & \ddots & \vdots \\ \rho_{n1}(t) & \rho_{n2}(t) & \cdots & \rho_{nn}(t) \end{pmatrix}. \tag{8}$$

In the standard Markov chain model of migration, transition matrix is exogenously given. However, in our model, we allow $\mathbf{R}(t)$ to be time varying and endogenously determined. We consider the endogenous determination of $\mathbf{R}(t)$ in the following sections.

3.2 Location choice

At the start of each period, workers decide where to reside by maximizing their utilities in terms of consumption and housing services across all locations, and then choose the location that gives them the highest level of utility. Consider an individual worker τ who is born at location i in period t, and considers moving to location $j \in \mathcal{I}_n$, where j could be i (namely not moving). We adopt a log-linear utility function and assume that if the worker decides to reside in location j, then her utility will be given by

$$U_{\tau,t,ij} = (1-\eta)\ln c_{\tau,t,ij} + \eta \ln s_{\tau,t,ij} - \psi \ln \alpha_{ij} + \varepsilon_{\tau,t,ij}, \tag{9}$$

where $c_{\tau,t,ij}$ and $s_{\tau,t,ij}$ are her consumption of goods and housing services, respectively, η represents the relative preference for housing service to consumption goods with $\eta \in (0,1)$, $\ln \alpha_{ij}$ is the route-specific migration cost, ψ is the relative weight of migration costs in utility function, and $\varepsilon_{\tau,t,ij}$ represents the idiosyncratic component of worker's relative location preference, over (i,j) location pair. We assume $\alpha_{ij} > 1$, if $j \neq i$, and, $\alpha_{ij} = 1$, if $j = i$.[19] In addition, suppose that $\varepsilon_{\tau,t,ij}$ is distributed independently of $c_{\tau,t,ij}$ and $s_{\tau,t,ij}$, and over time t. Also, following the literature on utility-based multiple choice decision problem, we shall assume that at each point in t, $\varepsilon_{\tau,t,ij}$ are independently and identically distributed (IID) as extreme value distribution. (see, for example, Mcfadden (1978)).

Each worker inelastically supplies one unit of labor and allocate her wage income between consumption goods and housing services. Denoting the wage rate and the price of housing services at location j in period t by w_{jt} and q_{jt} respectively, the budget constraint of the worker is given as

$$c_{\tau,t,ij} + q_{jt}s_{\tau,t,ij} = w_{jt}.$$

The utility maximization is done in two steps. *First*, the worker maximizes her utility in terms of consumption and housing services across locations. Denote by $\tilde{U}_{\tau,t,ij}$ the maximized utility of worker τ if she chooses to reside at location j. It is given as

$$\tilde{U}_{\tau,t,ij} = u_{jt} - \psi \ln \alpha_{ij} + \varepsilon_{\tau,t,ij}, \tag{10}$$

where u_{jt} is the maximal utility in terms of consumption and housing services one can get in location j, which is determined as

$$\begin{aligned} u_{jt} \equiv & \max_{\{c_{\tau,t,ij},\ s_{\tau,t,ij}\}} (1-\eta)\ln c_{\tau,t,ij} + \eta \ln s_{\tau,t,ij}, \\ & s.t. \qquad c_{\tau,t,ij} + q_{jt}s_{\tau,t,ij} = w_{jt}. \end{aligned} \tag{11}$$

By solving the above optimization problem, we obtain:

$$c_{jt} = (1-\eta)w_{jt}, \tag{12}$$

$$s_{jt} = \frac{\eta w_{jt}}{q_{jt}}, \tag{13}$$

where the subscripts τ and i of $c_{\tau,t,ij}$ and $s_{\tau,t,ij}$ are dropped for convenience, since the optimal levels of consumption of goods and housing services of each worker only depend on j and t. Thus, the indirect utility function associated with location j can be obtained by substituting (12) and (13) into (11) to yield:

$$u_{jt} = u_0 + \ln w_{jt} - \eta \ln q_{jt}, \tag{14}$$

where $u_0 \equiv (1-\eta)\ln(1-\eta) + \eta \ln \eta$ is a scalar. The above indirect utility function of location j is the same as that in Glaeser and Tobio (2008).

Second, the worker chooses the location with the highest utility. Using (10), the net utility gain of worker τ migrating to location j, denoted by $v_{\tau,t,ij}$, is given by

[19] It is shown that allowing for migration costs is essential for our model to generate a secular rise in the dispersion of house price-to-income ratio. See details in Section S6 of the online supplement.

$$
\begin{aligned}
v_{\tau,t,ij} &= \tilde{U}_{\tau,t,ij} - \tilde{U}_{\tau,t,ii}, \\
&= (\ln w_{jt} - \ln w_{it}) - \eta\,(\ln q_{jt} - \ln q_{it}) + (\varepsilon_{\tau,t,ij} - \varepsilon_{\tau,t,ii}) - \psi \ln \alpha_{ij}.
\end{aligned}
$$

Given the realizations of $\{\varepsilon_{\tau,t,ij}\}_{j=1}^{n}$, the worker chooses the destination with the highest $v_{\tau,t,ij}$. Let $j^*_{\tau,t,i}$ denote the location chosen by the worker. Then,

$$
j^*_{\tau,t,i} = arg \max_{j \in \mathcal{I}_n} \; v_{\tau,t,ij}.
$$

Since by assumption $\varepsilon_{\tau,t,ij}$ is distributed as IID extreme value, it can be shown that the probability for the worker in location i to migrate to location j is given by (see Appendix A.1 for a derivation)

$$
\rho_{ij}(t) = \frac{e^{v_{t,ij}}}{\sum_{s=1}^{n} e^{v_{t,is}}}, \tag{15}
$$

where

$$
v_{t,ij} \equiv (\ln w_{jt} - \ln w_{it}) - \eta\,(\ln q_{jt} - \ln q_{it}) - \psi \ln \alpha_{ij}. \tag{16}
$$

Then, the migration probability matrix $\mathbf{R}_t$, defined by (8), can be written as:

$$
\mathbf{R}(t) \equiv \begin{pmatrix} \varpi_{1t} & 0 & \cdots & 0 \\ 0 & \varpi_{2t} & \cdots & 0 \\ \vdots & \vdots & \ddots & \vdots \\ 0 & 0 & \cdots & \varpi_{nt} \end{pmatrix}^{-1} \begin{pmatrix} e^{v_{t,11}} & e^{v_{t,12}} & \cdots & e^{v_{t,1n}} \\ e^{v_{t,21}} & e^{v_{t,22}} & \cdots & e^{v_{t,2n}} \\ \vdots & \vdots & \ddots & \vdots \\ e^{v_{t,n1}} & e^{v_{t,n2}} & \cdots & e^{v_{t,nn}} \end{pmatrix},
$$

where $\varpi_{it} \equiv \sum_{s=1}^{n} e^{v_{t,is}}$ and $v_{t,ij}$ is a function of wage rate differentials, $\ln w_{jt} - \ln w_{it}$, and housing service price differentials, $\ln q_{jt} - \ln q_{it}$, as in (16). We will discuss how w_{it} and q_{it} are determined in the following section.

3.3 Wage rates and housing service prices

3.3.1 Production and wage rates

Location-specific wage rates are competitively determined in local labor markets. We assume the production of consumption goods is linear in labor inputs and is subject to a location-specific productivity shock:

$$
y_{it} = a_{it} l^{y}_{i\cdot}(t), \tag{17}
$$

where y_{it} is the output of consumption goods in location i in period t, a_{it} is the location-specific productivity shock, and $l^{y}_{i\cdot}(t)$ is the number of workers who work in the consumption goods sector in the location i. Let w_{it} be the wage rate at location i in period t, and assume that in equilibrium wage rates are set by labor productivities, namely

$$
w_{it} = a_{it}. \tag{18}
$$

Thus, wage rates, w_{it}, are exogenously given and do not respond to migration flows or house price changes. This assumption can be relaxed by allowing for capital and agglomeration effects in the production function as in Davis et al. (2014) and Herkenhoff et al. (2018). See Section S2 of the online supplement for details, where it is shown that such an extension does not alter our main conclusions and that the extended model has a unique long-run equilibrium. But to simplify the exposition we abstract from capital and agglomeration effects, and focus on a_{it} as the main driver of local wages. Accordingly, we adopt a relatively general specification of a_{it} and assume that $\ln a_{it}$ comprises of a linear trend component, $\ln a_i + g_a t$, a national common (unobserved) component, f_t, and a local component $z_{a,it}$:

$$\ln a_{it} = \ln a_i + g_a t + \lambda_i f_t + z_{a,it}, \tag{19}$$

where g_a is the national growth rate of labor productivity, and λ_i is the location-specific coefficient on the national component, with $E(\lambda_i) > 0$. In addition, $z_{a,it}$ and f_t are assumed to follow first-order autoregressive (AR(1)) processes:

$$f_t = \rho_f f_{t-1} + \sigma_f \varepsilon_{f,t}, \tag{20}$$

$$z_{a,it} = \rho_{z_a,i} z_{a,i,t-1} + \sigma_{z_a,i} \varepsilon_{z_a,it}. \tag{21}$$

where $\varepsilon_{f,t}$ and $\varepsilon_{z_a,it}$ are IID across locations and over time.

3.3.2 Housing service prices

Location-specific housing service prices are competitively determined in local rental markets. Assume that each unit of existing houses provides a unit of housing services in each period, while new houses begin to provide housing services a period after they are built. Thus, the market clearing condition is given by

$$h_{i,t-1} = \eta \left(\frac{w_{it}}{q_{it}} \right) l_{\cdot i}(t). \tag{22}$$

where $h_{i,t-1}$ is the quantity of houses that are available for rent at location i in period t, $\eta w_{it}/q_{it}$ is the per capita consumption of housing services given by (13). We will discuss how the housing stocks h_{it} are determined in the following sections.

3.4 Housing construction

In period t, a representative contractor is endowed with $\kappa_{it} > 0$ units of unused or reclaimed land in location i that can be used for new house construction. New houses are constructed by combing residential land and residential structures, denoted by st_{it}, using a Cobb-Douglas technology. Denote the amount of new houses built at location i in period t by x_{it}, and note that

$$x_{it} = \tau_{x,i} (\kappa_{it})^{\alpha_{\kappa,i}} (st_{it})^{1-\alpha_{\kappa,i}}, \tag{23}$$

where $\tau_{x,i} > 0$ is a scalar constant and $\alpha_{\kappa,i} \in (0,1)$ is the share of land in construction costs. By dividing both sides of (23) by κ_{it}, we obtain the production function of new houses per unit of land:

$$\frac{x_{it}}{\kappa_{it}} = \tau_{x,i} \left(\frac{st_{it}}{\kappa_{it}} \right)^{1-\alpha_{\kappa,i}}, \tag{24}$$

where x_{it}/κ_{it} and st_{it}/κ_{it} are the amounts of new houses and residential structures per unit of land, respectively. Thus, $1 - \alpha_{\kappa,i}$ are the elasticities of new house supplies with respect to non-land inputs on each unit of land. It is similar to the housing supply function in Glaeser and Tobio (2008). However, we allow $\alpha_{\kappa,i}$ to vary across locations, which reflects the fact that it is more costly to build new houses at some locations as compared to other locations.

Residential structure st_{it} is produced by combing construction labor, denoted by $l^c_{\cdot i}(t)$, and materials, denoted by m_{it}, using the following Cobb-Douglas technology:

$$st_{it} = \tau_s \left(l^c_{\cdot i}(t) \right)^{\alpha_l} \left(m_{it} \right)^{\alpha_m}, \tag{25}$$

where $\tau_s > 0$ is a scalar, and α_l and α_m are the shares of labor and materials in the production costs of residential structures, which are common to all locations. We assume that α_l and $\alpha_m \in (0, 1)$, and $\alpha_l + \alpha_m = 1$.

By combing (23) and (25), we obtain the following housing construction function:

$$x_{it} = \tau_{x,i} \left(\kappa_{it} \right)^{\alpha_{\kappa,i}} \left[\tau_s \left(l^c_{\cdot i}(t) \right)^{\alpha_l} \left(m_{it} \right)^{\alpha_m} \right]^{1-\alpha_{\kappa,i}}. \tag{26}$$

Contractors are assumed to be homogeneous and operate competitively across locations, and their behavior is modelled by a 'representative' contractor who maximizes her profits period-by-period and consumes all realized profits at the end of each period. The profit of the representative contractor in period t, denoted by π^c_t, is given as

$$\pi^c_t = \sum_{i=1}^{n} p_{it} x_{it} - m_{it} - w_{it} l^c_{\cdot i}(t).$$

The contractor chooses $\{x_{it}, m_{it}, l^c_{\cdot i}(t)\}_{i=1}^n$ to maximize her profit subject to house construction technology, (26), while taking the new land supplies, κ_{it}, as given. The first order conditions for m_{it} and $l^c_{\cdot i}(t)$ are given by

$$\begin{aligned} 1 &= \frac{\alpha_m (1 - \alpha_{\kappa,i}) x_{it} p_{it}}{m_{it}}, \\ w_{it} &= \frac{\alpha_l (1 - \alpha_{\kappa,i}) x_{it} p_{it}}{l^c_{\cdot i}(t)}. \end{aligned} \tag{27}$$

By plugging the above two first order conditions into (26), we obtain the supply function for new houses

$$x_{it} = \tau_i \kappa_{it} \left(w_{it} \right)^{-\frac{\alpha_l (1-\alpha_{\kappa,i})}{\alpha_{\kappa,i}}} \left(p_{it} \right)^{\frac{1-\alpha_{\kappa,i}}{\alpha_{\kappa,i}}}, \tag{28}$$

where τ_i is the location-specific scalar that is defined by

$$\tau_i \equiv \tau_{x,i}^{\frac{1}{\alpha_{\kappa,i}}} \left[\tau_s (1 - \alpha_{\kappa,i}) (\alpha_l)^{\alpha_l} (\alpha_m)^{\alpha_m} \right]^{\frac{1-\alpha_{\kappa,i}}{\alpha_{\kappa,i}}}.$$

We assume that contractors consume all the profits they earn in each period. Thus, $c_t^c = \pi_t^c$, where c_t^c denotes the consumption of contractors in period t.

Finally, to close the housing construction module we assume

$$\ln \kappa_{it} = \ln \kappa_i + g_{\kappa,i} t + z_{\kappa,it} \tag{29}$$

where $g_{\kappa,i}$ is the trend growth rate of new land supplies, and $z_{\kappa,it}$ is the state-specific land supply shock assumed to follow the AR(1) process:

$$z_{\kappa,it} = \rho_{z_\kappa,i} z_{\kappa,i,t-1} + \sigma_{z_\kappa,i} \varepsilon_{z_\kappa,it}, \tag{30}$$

where $\varepsilon_{z_\kappa,it}$ are IID across locations and over time.

3.5 Housing investment

In each location, homogeneous landlords own local housing stocks and rent them to workers, and derive utility from consuming their profits. The population of landlords in location i, denoted by l_{it}^o, grows over time at the common rate of g_l, where $g_l > 0$. Thus, $l_{it}^o = e^{g_l t} l_{i0}^o$, where $l_{i0}^o > 0$ is the initial population of landlords in location i. The life time utility of landlords (as a group) in location i is given by

$$E_t \sum_{s=0}^{\infty} (\beta e^{g_l})^s \ln(c_{i,t+s}^o), \tag{31}$$

where c_{it}^o is the consumption of the 'representative' landlord in location i, and $\beta e^{g_l} \in (0,1)$ is the adjusted discount factor that allows for the growing number of landlords. The realized net return on housing investment in location i in period t, denoted by r_{it}^o, is given by

$$r_{it}^o = (1-\theta_i) \left[\frac{q_{it} + (1-\delta) p_{it}}{p_{i,t-1}} \right], \tag{32}$$

where $\delta \in (0,1)$ is the depreciation rate of housing stocks, and $\theta_i \in (0,1)$ is the location-specific cost of housing investment.[20] Let h_{it} denote the amount of houses owned by the landlords in location i. The landlords' budget constraint is then given by

$$c_{it}^o l_{it}^o + p_{it} h_{it} = r_{it}^o \left(p_{i,t-1} h_{i,t-1} \right). \tag{33}$$

Landlords maximize (31) subject to (33). The Euler equation for this optimization is given by

$$E_t \left(\lambda_{i,t+1} r_{i,t+1}^o \right) = 1, \tag{34}$$

where $\lambda_{i,t+1}$ is the stochastic discount factor, defined by $\lambda_{i,t+1} = \beta \left(c_{it}^o / c_{i,t+1}^o \right)$. Pre-multiplying both sides of (34) by p_{it}, and using (32), we obtain

$$p_{it} = (1-\theta_i) E_t \left\{ \lambda_{i,t+1} \left[q_{i,t+1} + (1-\delta) p_{i,t+1} \right] \right\}.$$

[20] The costs to own and transact houses, such as, property taxes and capital gain taxes, can vary substantially across locations in the U.S..

Using the above equation, the house price, p_{it}, can be expressed as the sum of the expected present value of rents net of depreciation

$$p_{it} = \sum_{s=1}^{\infty} E_t \left[(1-\delta)^{s-1} (1-\theta_i)^s \left(\prod_{v=1}^{s} \lambda_{i,t+v} \right) q_{i,t+s} \right].$$

Since the utility function of landlords is assumed to be logarithmic, a closed form solution for landlords' optimization problem exists. The optimal rules for housing investment and consumption are given by

$$p_{it} h_{it} = \beta e^{g_l} (1-\theta_i) \left[q_{it} + (1-\delta) p_{it} \right] h_{i,t-1}, \tag{35}$$

and

$$c_{it}^o l_{i0}^o e^{g_l t} = (1-\beta e^{g_l}) (1-\theta_i) \left[q_{it} + (1-\delta) p_{it} \right] h_{i,t-1}. \tag{36}$$

3.6 Market clearing and resource constraints

The market clearing condition of housing in location i is given by

$$h_{it} = (1-\delta) h_{i,t-1} + x_{it}. \tag{37}$$

where h_{it} is equal to the housing demand in location i in period t and $(1-\delta)h_{i,t-1} + x_{it}$ is the supply of houses in that location. The resource constraint for consumption goods in the economy as a whole is given by:

$$\sum_{i=1}^{n} y_{it} = \sum_{i=1}^{n} c_{it} l_{\cdot i}(t) + \sum_{i=1}^{n} c_{it}^o l_{it}^o + c_t^c + \sum_{i=1}^{n} m_{it}, \text{ for } t = 1, 2, ...$$

where $\sum_{i=1}^{n} y_{it}$ is the total amount of consumption goods produced in the economy in period t, $\sum_{i=1}^{n} c_{it} l_{\cdot i}(t)$ is the total consumption of workers, $\sum_{i=1}^{n} c_{it}^o l_{it}^o$ is the total consumption of landlords, c_t^c is the consumption of contractors and $\sum_{i=1}^{n} m_{it}$ is the amount of goods used in housing construction. The resource constraint for labor in location i in period t is given as

$$l_{\cdot i}(t) = l_{\cdot i}^y(t) + l_{\cdot i}^c(t). \tag{38}$$

where as before $l_{\cdot i}(t)$ is the population of workers who reside at location i in period t, and $l_{\cdot i}^y(t)$ and $l_{\cdot i}^c(t)$ are the numbers of workers who work in the production and the housing construction sectors respectively.

4 Equilibrium and the balanced growth path

We now consider the *non-stochastic* version of the model economy set out in Section 3, characterize its short-run and long-run equilibria and prove the existence and uniqueness of the short-run equilibrium and the balanced growth path. The non-stochastic specification is obtained by setting to zero the innovations to the national and location-specific components of labor productivities ($\varepsilon_{f,t}$ and $\varepsilon_{z_a,it}$ in (20) and (21)), and the innovations to the location-specific land supply shock ($\varepsilon_{z_\kappa,it}$ in (30)), namely

$$\varepsilon_{f,t} = 0,\ \varepsilon_{z_a,it} = 0,\ \text{and}\ \varepsilon_{z_\kappa,it} = 0,\ \text{for}\ i = 1, 2, ...n,\ \text{and}\ t = 1, 2, ...$$

In this set up, local productivities are given by

$$a_{it} = e^{g_a t} a_i,\ \text{for}\ i = 1, 2, ...n,\ \text{and}\ t = 1, 2, ... \tag{39}$$

In addition, to obtain a balanced growth path we assume the same intrinsic population growth rate, g_l, across locations:

$$g_{l,it} = g_l,\ \text{for}\ i = 1, 2, ...n,\ \text{and}\ t = 1, 2, ... \tag{40}$$

Finally, we assume that the location-specific land supplies are given by

$$\kappa_{it} = e^{g^*_{\kappa,i} t} \kappa_i,\ \text{for}\ i = 1, 2, ...n,\ \text{and}\ t = 1, 2, ..., \tag{41}$$

where $g^*_{\kappa,i}$ is the state-specific land supply growth rate. To find conditions under which the economy has a balanced growth path, using (28) we note that

$$\ln\left(\frac{x_{it}}{x_{i,t-1}}\right) = \ln\left(\frac{\kappa_{it}}{\kappa_{i,t-1}}\right) - \left(\frac{1-\alpha_{\kappa,i}}{\alpha_{\kappa,i}}\right)\ln\left(\frac{w_{it}}{w_{i,t-1}}\right) + \alpha_l\left(\frac{1-\alpha_{\kappa,i}}{\alpha_{\kappa,i}}\right)\ln\left(\frac{p_{it}}{p_{i,t-1}}\right),$$

and on the balanced growth path by definition we have $\ln(x_{it}/x_{i,t-1}) = g_l$, $\ln(w_{it}/w_{i,t-1}) = \ln(p_{it}/p_{i,t-1}) = g_a$, and $\ln(\kappa_{it}/\kappa_{i,t-1}) = g^*_{\kappa,i}$. Hence, for a balanced growth path to exist we must have

$$g^*_{\kappa,i} = g_l - \frac{(1-\alpha_{\kappa,i})\alpha_m}{\alpha_{\kappa,i}} g_a,\ \text{for}\ i = 1, 2, ..., n, \tag{42}$$

where $\alpha_m\ (= 1-\alpha_l)$ is the share of materials in the production costs of residential structures, and $\alpha_{\kappa,i}$ is the location-specific share of land in housing construction costs. The above condition states that the growth rate of new land supplies, $g^*_{\kappa,i}$, and the growth of technical progress in production of construction materials, g_a, should ensure that enough new houses can be produced to accommodate the housing requirements of the growing population in all locations. The land supply regime under which land growth rates are given by (42) will be referred to as the *balanced growth path land supply regime.* The analysis of the equilibrium properties of the stochastic version of the model is complicated, and will be conducted by simulations. The deterministic solution provides information on the local equilibrating properties of the stochastic version for sufficiently small-size shocks.

We use bold lowercase letters with only time subscripts to denote the vectors of prices and quantities for all locations. For example, $\boldsymbol{p}_t \equiv [p_{1t}, p_{2t}, ..., p_{nt}]$, which is a $1 \times n$ vector. We denote the aggregate population by $L_t \equiv \sum_{i=1}^{n} l_{\cdot i}(t)$. In addition, we use letters with stars and time subscripts to denote the corresponding detrended variables. Specifically,

$p^*_{it} \equiv e^{-g_a t} p_{it}$, $\boldsymbol{p}^*_t \equiv [p^*_{1t}, p^*_{2t}, ..., p^*_{nt}]$, $q^*_{it} = e^{-g_a t} q_{it}$, $\boldsymbol{q}^*_t \equiv [q^*_{1t}, q^*_{2t}, ..., q^*_{nt}]$, $h^*_{it} \equiv e^{-g_l t} h_{it}$, and $\boldsymbol{h}^*_t \equiv [h^*_{1t}, h^*_{2t}, ..., h^*_{nt}]$.

In the proof of the existence and the uniqueness of the equilibrium and the balanced growth path, we focus only on the key variables that are related to migration and local housing markets, including $\boldsymbol{p}_t, \boldsymbol{q}_t, \boldsymbol{w}_t, \boldsymbol{x}_t, \boldsymbol{h}_t, \boldsymbol{l}(t)$ and $\mathbf{R}(t)$, and the subset of equilibrium conditions by which they are determined. These variables are classified into two groups:

- **Migration module.** The first block of equilibrium conditions, including (6) and (15), describe how migration probabilities, $\mathbf{R}(t)$, and local population values, $\boldsymbol{l}(t)$, are determined, given incomes and housing service prices across locations, i.e., $\boldsymbol{w}_t$ and $\boldsymbol{q}_t$.
- **Regional housing market**. The second block of equilibrium conditions, including (18), (22), (28), (35) and (37), describe how the equilibria of local housing markets are determined given local population, $\boldsymbol{l}(t)$.

Note that equilibrium conditions (6), (15), (18), (22), (28), (35) and (37) can be re-written in terms of the detrended variables as follows

$$l^*_{\cdot j}(t) = \sum_{i=1}^{n} \rho^*_{ij}(t) l^*_{\cdot i}(t-1), \text{ for } j \in \mathcal{I}_n, \tag{43}$$

$$\rho^*_{ij}(t) = \frac{(w^*_{jt}/w^*_{it})(q^*_{jt}/q^*_{it})^{-\eta}(\alpha_{ij})^{-\psi}}{\sum_{s=1}^{n}(w^*_{st}/w^*_{it})(q^*_{st}/q^*_{it})^{-\eta}(\alpha_{is})^{-\psi}}, \text{ for } i \text{ and } j \in \mathcal{I}_n, \tag{44}$$

$$h^*_{it} = (1-\delta)h^*_{i,t-1} + x^*_{it}, \text{ for } i \in \mathcal{I}_n, \tag{45}$$

$$x^*_{it} = \tau_i \kappa_i (w^*_{it})^{-\frac{\alpha_l(1-\alpha_{\kappa,i})}{\alpha_{\kappa,i}}} (p^*_{it})^{\frac{1-\alpha_{\kappa,i}}{\alpha_{\kappa,i}}}, \text{ for } i \in \mathcal{I}_n, \tag{46}$$

$$q^*_{it} = \frac{\eta w^*_{it} l^*_{\cdot i}(t)}{h^*_{i,t-1}}, \text{ for } i \in \mathcal{I}_n, \tag{47}$$

$$p^*_{it} h^*_{it} = \beta(1-\theta_i)\left[q^*_{it} + (1-\delta)p^*_{it}\right] h^*_{i,t-1}, \text{ for } i \in \mathcal{I}_n, \tag{48}$$

$$w^*_{it} = a_i, \text{ for } i \in \mathcal{I}_n. \tag{49}$$

Then the short-run and the balancd growth path equilibria of the economy can be defined in terms of the above detrended variables as follows:

Definition 1 ***(Short-run equilibrium)*** *Consider the dynamic spatial equilibrium model set up in Section 3 by equations (6), (15), (18), (22), (28), (35) and (37), which can be written equivalently in terms of detrended variables by equations (43) to (49). Suppose that the vectors of exogenous processes for labor productivities, $\boldsymbol{a}_t$, land supplies, $\boldsymbol{\kappa}_t$, and the intrinsic population growth rates, $\boldsymbol{g}_{lt}$, for $t = 1, 2, ...$, are given by (39)-(41), condition (42) holds, and the initial values for local population and housing stocks ($\boldsymbol{l}_0$ and $\boldsymbol{h}_0$) are strictly positive. Then, a short-run equilibrium is defined as series of non-negative prices $[\boldsymbol{p}^*_t, \boldsymbol{q}^*_t, \boldsymbol{w}^*_t]$ and allocations $[\boldsymbol{l}^*(t), \boldsymbol{x}^*_t, \boldsymbol{h}^*_t]$ that solve the system of equations (43)-(49), for given values $l^*_{\cdot i}(t-1)$ and $h^*_{i,t-1}$, for $i \in \mathcal{I}_n$.*

Definition 2 ***(Balanced growth path equilibrium)*** *Consider the dynamic spatial equilibrium model set up in Section 3 by equations (6), (15), (18), (22), (28), (35) and (37), which can be written equivalently in terms of detrended variables by equations (43) to (49). Suppose that the vectors of exogenous processes for labor productivities, $\boldsymbol{a}_t$, land supplies, $\boldsymbol{\kappa}_t$, and the intrinsic population growth rates, $\boldsymbol{g}_{lt}$, for $t = 1, 2, ...,$ are given by (39)-(41), condition (42) holds, and the initial values for local population and housing stocks ($\boldsymbol{l}_0$ and $\boldsymbol{h}_0$) are strictly positive. Then, a balanced growth path equilibrium is defined as a path on which the economy is in short-run equilibrium in the sense set out in Definition 1 in each period, and the de-trended prices $[\boldsymbol{p}_t^*, \boldsymbol{q}_t^*, \boldsymbol{w}_t^*]$ and quantities $[\boldsymbol{l}^*(t), \boldsymbol{x}_t^*, \boldsymbol{h}_t^*]$ converge to non-negative limits as $t \to \infty$.*

The existence and uniqueness of the short-run equilibrium is established in the online supplement (see Section S1). In what follows we focus on the existence and uniqueness of the long-run balanced growth path which plays a more fundamental role in our simulation exercises.

Proposition 1 ***(Existence and uniqueness of the long-run balanced growth path)*** *Consider the dynamic spatial equilibrium model set up in Section 3 by (6), (15), (18), (22), (28), (35) and (37). Suppose that the vectors of exogenous processes for labor productivities, $\boldsymbol{a}_t$, land supplies, $\boldsymbol{\kappa}_t$, and intrinsic population growth rates, $\boldsymbol{g}_{lt}$, for $t = 1, 2, ...,$ are given by (39)-(41), and condition (42) holds, and the initial values for local population and housing stocks ($\boldsymbol{l}_0$ and $\boldsymbol{h}_0$) are strictly positive. Then the model has a unique balanced growth path as set out in Definition 2.*

Proof: We start by re-writing the equilibrium conditions in terms of detrended variables. Recall that we use letters with stars and time subscripts to denote the corresponding detrended variables. Note that the detrended exogenous variables are time invariant by construction (see (39)-(42)). For example, $a_{it}^* = a_i$ and $\kappa_{it}^* = \kappa_i$. Note also that in the model, wage rates are pinned down by labor productivities, i.e. $w_{it} = a_{it}$ (see (18)). Thus, the detrended wage rates are also constant over time, i.e., $w_{it}^* = a_i$. Further, note that (6) can be re-written in terms of the detrended variables as

$$\boldsymbol{l}^*(t) = \boldsymbol{l}^*(t-1)\mathbf{R}^*(t), \tag{50}$$

where $\mathbf{R}^*(t) = (\rho_{ij}^*(t))$ is the $n \times n$ matrix with non-negative (i, j) elements

$$\rho_{ij}^*(t) = \frac{(\alpha_{ij})^{-\psi}(w_{jt}^*/w_{it}^*)(q_{jt}^*/q_{it}^*)^{-\eta}}{\sum_{s=1}^{n}(\alpha_{is})^{-\psi}(w_{st}^*/w_{it}^*)(q_{st}^*/q_{it}^*)^{-\eta}} \geq 0, \tag{51}$$

and rows that sum to unity.[21] Thus, by post-multiplying both sides of (50) by $\boldsymbol{\tau}$, an $n \times 1$ vector of ones, we have

$$L_t^* = \boldsymbol{l}^*(t)\boldsymbol{\tau} = \boldsymbol{l}^*(t-1)\mathbf{R}^*(t)\boldsymbol{\tau} = \boldsymbol{l}^*(t-1)\boldsymbol{\tau} = L_{t-1}^*,$$

[21] This result follows from (15) and (16), and using de-trended variables denoted by $*$.

which implies

$$L_t^* = L_{t-1}^*, ..., = L_1^* = L_0, \tag{52}$$

where L_0 is the detrended aggregate population for $t = 0, 1, ...$ Using (50), $\boldsymbol{l}^*(t)$ can be written as

$$\boldsymbol{l}^*(t) = \boldsymbol{l}(0)\left[\Pi_{s=1}^t \mathbf{R}^*(s)\right], \tag{53}$$

where $\boldsymbol{l}(0) > 0$ is the vector of the initial local populations, and $\mathbf{R}^*(1), \mathbf{R}^*(2), ..., \mathbf{R}^*(t)$, are a series of stochastic matrices. Lemma A1 in Appendix A.3 establishes the existence of the balanced growth path by showing that $\boldsymbol{l}^*(t)$ converges to some time invariant non-negative population vector $\boldsymbol{l}^*$, as $t \to \infty$. To establish that $\boldsymbol{l}^*$is unique, we note that the detrended aggregate population remains constant over time, as shown in (52), namely

$$\sum_{i=1}^n l_{\cdot i}^* = L_0. \tag{54}$$

By imposing the balance growth path conditions, the equilibrium conditions (6), (15), (18), (28), (35), (22) and (37) can be written in terms of the detrended variables as follows

$$l_{\cdot j}^* = \sum_{i=1}^n \rho_{ij}^* l_{\cdot i}^*, \text{ for } j \in \mathcal{I}_n, \tag{55}$$

$$\rho_{ij}^* = \frac{(w_j^*/w_i^*)(q_j^*/q_i^*)^{-\eta}(\alpha_{ij})^{-\psi}}{\sum_{s=1}^n (w_s^*/w_i^*)(q_s^*/q_i^*)^{-\eta}(\alpha_{is})^{-\psi}}, \text{ for } i \text{ and } j \in \mathcal{I}_n, \tag{56}$$

$$x_i^* = \delta h_i^*, \text{ for } i \in \mathcal{I}_n, \tag{57}$$

$$x_i^* = \tau_i \kappa_i (w_i^*)^{-\frac{\alpha_l(1-\alpha_{\kappa,i})}{\alpha_{\kappa,i}}} (p_i^*)^{\frac{1-\alpha_{\kappa,i}}{\alpha_{\kappa,i}}}, \text{ for } i \in \mathcal{I}_n, \tag{58}$$

$$q_i^* = \frac{\eta w_i^* l_{\cdot i}^*}{h_i^*}, \text{ for } i \in \mathcal{I}_n, \tag{59}$$

$$p_i^* = \beta(1-\theta_i)\left[q_i^* + (1-\delta)p_i^*\right], \text{ for } i \in \mathcal{I}_n, \tag{60}$$

$$w_i^* = a_i, \text{ for } i \in \mathcal{I}_n. \tag{61}$$

Thus, to prove the uniqueness of the balanced growth path, in what follows we show that the system of equations given by (54)-(61), has a *unique positive* solution. Note that wage rates are pinned down by labor productivities, i.e., $\boldsymbol{w}^* = \boldsymbol{a}$ (see (61)). In the rest of the proof, we show that given $L_0, \boldsymbol{\kappa}$ and $\boldsymbol{w}^*$, then $\boldsymbol{p}^*, \boldsymbol{q}^*, \boldsymbol{x}^*, \boldsymbol{h}^*, \boldsymbol{l}^*$ and $\mathbf{R}^*$ are uniquely determined. We first show that for given values of $\boldsymbol{l}^*, \boldsymbol{\kappa}$ and $\boldsymbol{w}^*$, the solution for $\boldsymbol{p}^*, \boldsymbol{q}^*, \boldsymbol{x}^*$ and $\boldsymbol{h}^*$ is unique and can be obtained using (57), (58), (59) and (60). We first observe that the long run rent-to-price ratio in location i can be obtained from (60) and is given by

$$\frac{q_i^*}{p_i^*} = \Gamma_i, \tag{62}$$

where Γ_i is given by

$$\Gamma_i = \frac{1}{\beta(1-\theta_i)} - (1-\delta). \tag{63}$$

Note that β and $\theta_i \in (0,1)$, which implies $\beta^{-1}(1-\theta_i)^{-1} > 1$. Since $\delta > 0$, it follows that $\Gamma_i > \delta > 0$. Using this result in (59), we obtain the long-run demand function for housing in location i:

$$h_i^* = \frac{\eta w_i^* l_{\cdot i}^*}{\Gamma_i p_i^*} \tag{64}$$

By substituting (57) into (58), we obtain the long-run housing supply function in location i:

$$h_i^* = \delta^{-1}\tau_i\kappa_i (w_i^*)^{-\frac{\alpha_l(1-\alpha_{\kappa,i})}{\alpha_{\kappa,i}}} (p_i^*)^{\frac{1-\alpha_{\kappa,i}}{\alpha_{\kappa,i}}}. \tag{65}$$

Therefore, p_i^*, q_i^*, x_i^* and h_i^* can be obtained uniquely in terms of $l_{\cdot i}^*, w_i^*$,and κ_i using (57), and (62) - (65):

$$\begin{aligned}
p_i^* &= \left(\frac{\delta\eta}{\tau_i\kappa_i}\right)^{\alpha_{\kappa,i}} \Gamma_i^{-\alpha_{\kappa,i}} (l_{\cdot i}^*)^{\alpha_{\kappa,i}} (w_i^*)^{\alpha_{\kappa,i}+\alpha_l(1-\alpha_{\kappa,i})}, &(66)\\
q_i^* &= \left(\frac{\delta\eta}{\tau_i\kappa_i}\right)^{\alpha_{\kappa,i}} \Gamma_i^{1-\alpha_{\kappa,i}} (l_{\cdot i}^*)^{\alpha_{\kappa,i}} (w_i^*)^{\alpha_{\kappa,i}+\alpha_l(1-\alpha_{\kappa,i})}, &(67)\\
h_i^* &= \left(\frac{\delta}{\tau_i\kappa_i}\right)^{-\alpha_{\kappa,i}} \left(\frac{\eta}{\Gamma_i}\right)^{1-\alpha_{\kappa,i}} (l_{\cdot i}^*)^{1-\alpha_{\kappa,i}} (w_i^*)^{(1-\alpha_l)(1-\alpha_{\kappa,i})}, &(68)\\
x_i^* &= \left(\frac{1}{\tau_i\kappa_i}\right)^{-\alpha_{\kappa,i}} \left(\frac{\delta\eta}{\Gamma_i}\right)^{1-\alpha_{\kappa,i}} (l_{\cdot i}^*)^{1-\alpha_{\kappa,i}} (w_i^*)^{(1-\alpha_l)(1-\alpha_{\kappa,i})}, &(69)
\end{aligned}$$

where Γ_i is defined by (63).[22] By substituting (67) into (56) for q_i^*, then ρ_{ij}^* can be written as a function of $\boldsymbol{l}^*$:

$$\rho_{ij}^* = \frac{\psi_{ij}\left(l_{\cdot j}^*\right)^{-\varphi_j}}{\sum_{s=1}^n \psi_{is}\left(l_{\cdot s}^*\right)^{-\varphi_s}}, \tag{70}$$

where

$$\begin{aligned}
\varphi_j &= \eta\alpha_{\kappa,j},\\
\psi_{ij} &= \alpha_{ij}^{-\psi}\left(\frac{\delta\eta}{\tau_j\kappa_j}\right)^{-\eta\alpha_{\kappa,j}} \Gamma_j^{-\eta(1-\alpha_{\kappa,j})}\left(w_j^*\right)^{1-\eta[\alpha_{\kappa,j}+\alpha_l(1-\alpha_{\kappa,j})]}.
\end{aligned}$$

Since η and $\alpha_{\kappa,j} \in (0,1)$, it follows that $\varphi_j > 0$, for any $i \in \mathcal{I}_n$. In addition, note that $\psi_{ij} > 0$, for any i and $j \in \mathcal{I}_n$, since $\alpha_{ij}, \delta, \eta, \tau_j, \kappa_j$ and $w_j^* > 0$, and Γ_j, given by (63), is strictly positive as previously shown. Recall that $\mathbf{R}^*$ is the migration probability matrix on the balanced growth path, with a typical element ρ_{ij}^* given by (70). Thus, $\mathbf{R}^*$ can be written as a function of $\boldsymbol{l}^*$, namely $\mathbf{R}^* \equiv \mathbf{R}(\boldsymbol{l}^*)$. Then, (55) can be written more compactly as

$$\boldsymbol{l}^* = \boldsymbol{l}^*\mathbf{R}(\boldsymbol{l}^*), \tag{71}$$

[22] For the detail of the derivations, see Appendix A.2.

which is a system of non-linear equations in $\boldsymbol{l}^*$. Lemma A1 in the Appendix establishes that there exists a $\boldsymbol{l}^*$ that solves (71). Lemma A2 establishes that (71) cannot have more than one solution. Therefore, $\boldsymbol{l}^*$ exists and is unique. Then, using the solution of $\boldsymbol{l}^*$, the other variables of the model, namely, $\boldsymbol{p}^*$, $\boldsymbol{q}^*$, $\boldsymbol{x}^*$, $\boldsymbol{h}^*$and $\mathbf{R}^*$, can be solved for using equations (66) to (70).■

5 Calibration and estimation of model's parameters

We now consider whether the model can quantitatively account for the observed rise in the house price dispersion in the U.S.. To this end, we estimate the model using the combined interstate migration flows and state level housing market data, and then use the estimated model for several simulation excises in the next section. We calibrate some of the parameters, and then estimate the rest of them using the panel data of the 49 states (including the District of Columbia) in the U.S. mainland with yearly observations over the period 1976-2014. Thus, the period indexed by 0 (i.e., the initial period) corresponds to 1976, and the periods indexed by $1, 2, ..., T$ correspond to the years 1977 to 2014.

The model parameters can be divided into five groups, which include the parameters that characterize preferences, migration flows, housing supplies and investment, and the exogenous per capita incomes and new land supply processes. In what follows we consider these five sets of parameters in turn.

5.1 Preference parameters

The relative weight of housing in workers' utility function (11), η, is set to 0.24, as estimated by Davis and Ortalo-Magné (2011).[23] The discount factor of landlord β is set to 0.98 to match the risk-free annual real interest rate of the U.S. over the period 1962-2014, which is estimated to be around 2 per cent. The spreads between the risk-free interest rate and the location-specific returns on housing investments are captured by the parameters θ_i, which will be calibrated in Section 5.3 below.

5.2 Migration and intrinsic population growth rates

To estimate route-specific migration cost parameters, α_{ij}, using (15), we first note that

$$\frac{\rho_{ij}(t)}{\rho_{ii}(t)} = \frac{\alpha_{ij}^{-\psi} w_{jt} q_{jt}^{-\eta}}{\alpha_{ii}^{-\psi} w_{it} q_{it}^{-\eta}}, \Rightarrow \alpha_{ij}^{\psi} = \left(\frac{w_{jt} q_{jt}^{-\eta}}{w_{it} q_{it}^{-\eta}} \right) \left(\frac{\rho_{ii}(t)}{\rho_{ij}(t)} \right) \alpha_{ii}^{\psi}.$$

Also from (4), we have $\rho_{ij}(t) = l_{ij}(t)/l_{i\cdot}(t)$, and therefore

$$\alpha_{ij}^{\psi} = \left(\frac{w_{jt} q_{jt}^{-\eta}}{w_{it} q_{it}^{-\eta}} \right) \left(\frac{l_{ii}(t)}{l_{ij}(t)} \right) \alpha_{ii}^{\psi}.$$

[23]These authors also provide evidence that the share of expenditure on housing are constant over time and across U.S. MSAs.

We set ψ to unity, and normalize α_{ii} to one, for $i = 1, 2, ..., n$. Note that the Internal Revenue Service (IRS) migration flow data that we will be using are only available for the period 1990-2014. Thus, we estimate α_{ij} using the above equation as follows:

$$\hat{\alpha}_{ij} = \frac{1}{25} \sum_{t=t_{1990}}^{t_{2014}} \frac{w_{jt} q_{jt}^{-\eta}}{w_{it} q_{it}^{-\eta}} \frac{l_{ii}(t)}{l_{ij}(t)}, \quad \text{for } i \neq j, \text{ and } i \text{ and } j \in \mathcal{I}_n, \tag{72}$$

where t_{1990} and t_{2014} are the time indices corresponding to 1990 and 2014, respectively, η is calibrated in Section 5.1, and w_{it}, q_{it} and $l_{ij}(t)$ are observed data.

In addition, the balanced growth path intrinsic population growth rate, g_l, defined by (40), is set to 1%, which is the average growth rate of the U.S. population over the period 1977-2014. The actual state-level intrinsic population growth rates, $g_{l,it}$, over the period 1977-2014 are measured using the IRS and the Census data. For further details, see Appendix B.1.

5.3 Housing supplies and investment

Following Van Nieuwerburgh and Weill (2010), we estimate the housing depreciation rate, δ, as the average ratio of aggregate depreciation to aggregate housing stock over the period 1977-2014 using the data from the Fixed Assets Tables compiled by the Bureau of Economic Analysis (BEA), and obtain $\hat{\delta} = 2\%$. To calibrate the state-specific supply functions for new houses, given by (28), we follow Davis and Heathcote (2005) and set the share of material in the value of residential structure, α_m, assumed to be common to all states, to 0.53. This estimate matches the national share of value added of non-construction sectors in the total value of residential investments. The share of construction labor in residential structure value added, α_l, is then set to 0.47 to ensure that $\alpha_l + \alpha_m = 1$. Finally, we estimate, $\alpha_{\kappa,i}$, location-specific share of land in construction costs, by the state level average land values relative to total value of housing stocks over the 1977-2014 period.[24]

The location-specific housing investment cost parameter, θ_i, is estimated as follows. Using the rent-to-price ratio on the balanced growth path given by (62), we have

$$\theta_i = 1 - \frac{1}{\beta} \left[\frac{q_i^*}{p_i^*} + (1 - \delta) \right]^{-1},$$

which suggests the following estimate

$$\hat{\theta}_i = 1 - \frac{1}{\beta} \left[\frac{1}{\frac{1}{T} \sum_{t=1}^{T} q_{it}/p_{it} + (1 - \hat{\delta})} \right], \tag{73}$$

where periods 1 and T correspond to 1977 and 2014, respectively, β and δ are previously calibrated and estimated, and q_{it} and p_{it} are observed data.

[24] The data on state level land share in home values are obtained from Davis and Heathcote (2007).

5.4 Income processes

Wage rates are set by labor productivities in equilibrium: $w_{it} = a_{it}$, and since we abstract from capital, wage is the only source of income for households. Thus, we measure a_{it} using the realized state level real per capita disposable income during the 1977-2014 period. To estimate the stochastic process of a_{it}, defined by (19), (20) and (21), recall that a_{it} is given by

$$\ln a_{it} = \ln a_i + g_a t + \lambda_i f_t + z_{a,it}, \tag{74}$$

where $t = 1, 2, ..., T$ (1977-2014). To identify the unobserved common factor, f_t, we impose the following restrictions:

$$n^{-1} \sum_{i=1}^{n} \lambda_i = 1. \tag{75}$$

and

$$T^{-1} \sum_{t=1}^{T} f_t = 0, \tag{76}$$

Restriction (75) is required to distinguish between scales of λ_i and f_t, and (76) is required to separate the linear trend from the common factor. We take the common growth rate of state-level incomes, g_a, as a known parameter, and set it to match the average annual growth rate of the U.S. real per capita income during the period 1977-2014, which is around 0.018. Then, in view of (76), we estimate a_i by

$$\hat{a}_i = \exp\left[T^{-1} \sum_{t=1}^{T} (\ln a_{it} - \hat{g}_a t)\right]. \tag{77}$$

Let $e_{a,it}$ be the deviation of $\ln a_{it}$ from its trend, which is given by

$$e_{a,it} = \lambda_i f_t + z_{a,it}, \tag{78}$$

and estimated as

$$\hat{e}_{a,it} = \ln a_{it} - \ln \hat{a}_i - \hat{g}_a t,$$

for $t = 0, 1, 2, ..., T$. To estimate f_t, we first note that $n^{-1} \sum_{i=1}^{n} \lambda_i = 1$ (see (75)). By summing up both sides of (78), we have

$$n^{-1} \sum_{i=1}^{n} e_{a,it} = f_t + n^{-1} \sum_{i=1}^{n} z_{a,it},$$

where by assumption $z_{a,it}$ are cross-sectionally independent. As a result,

$$f_t = n^{-1} \sum_{i=1}^{n} \hat{e}_{a,it} + O_p\left(T^{-\frac{1}{2}}\right) + O_p\left(n^{-\frac{1}{2}}\right),$$

which gives a consistent estimator of f_t:

$$\hat{f}_t = n^{-1} \sum_{i=1}^{n} \hat{e}_{a,it}. \tag{79}$$

The parameters ρ_f and σ_f in (20) are estimated by running the OLS regression of $\hat{f}_t$ on $\hat{f}_{t-1}$, for $t = 1, 2, ..., T$. To estimate the associated loading coefficients, λ_i, for each i we run the OLS regressions of $\hat{e}_{a,it}$ on $\hat{f}_t$, and obtain the residuals, $\hat{z}_{a,it}$, for $t = 0, 1, 2, ..., T$. Then, we estimate $\rho_{z_{a,i}}$ and $\sigma_{z_{a,i}}$ in (21) by running OLS regressions of $\hat{z}_{a,it}$ on $\hat{z}_{a,i,t-1}$, over the period $t = 1, 2, ..., T$.

5.5 Land supplies

To estimate κ_{it}, we first note that equilibrium conditions (22), (28), (35) and (37) imply

$$\kappa_{it} = \frac{\gamma_{it}}{\tau_i}, \tag{80}$$

where[25]

$$\gamma_{it} = \frac{\left\{\beta e^{g_l} (1-\theta_i) \left[\frac{q_{it}}{p_{it}} + (1-\delta)\right] - (1-\delta)\right\} \eta \left(\frac{w_{it}}{q_{it}}\right) l_{\cdot i}(t)}{(w_{it})^{-\alpha_l (1-\alpha_{\kappa,i})/\alpha_{\kappa,i}} (p_{it})^{(1-\alpha_{\kappa,i})/\alpha_{\kappa,i}}}. \tag{81}$$

Note that $\beta, g_l, \theta_i, \eta, \alpha_l, \alpha_{\kappa,i}$ and δ are previously calibrated and estimated, and that $l_{\cdot i}(t), w_{it}, q_{it}$ and p_{it} are observed data. Thus, an estimator of γ_{it} can be obtained by evaluating (81) using the parameter estimates and realized values of $l_{\cdot i}(t), w_{it}, q_{it}$ and p_{it}, for $t = 0, 1, ..., T$, which corresponds to the period of 1976-2014.

We assume that *used land*, denoted by UR_{it}, is turned into *unused land* when houses on these lands are depreciated. Thus, UR_{it} would shrink at rate δ in the absence of any new constructions. Therefore, UR_{it} follows as:

$$UR_{it} = \kappa_{it} + (1-\delta) UR_{i,t-1}. \tag{82}$$

To estimate τ_i in (80), we make use of published data on major land uses in the U.S. compiled by the U.S. Department of Agriculture (USDA). We consider only the observations from 2002 onward, which are available for the years 2002, 2007 and 2012, since earlier data are not compatible in concept and scope.[26] Thus, we estimate τ_i using the USDA urban area size data for 2002 and 2012 as follows. Note that (82) implies

$$UR_{i,t_{2012}} = \sum_{t=t_{2003}}^{t_{2012}} (1-\delta)^{t_{2012}-t} \kappa_{i,t} + (1-\delta)^{10} UR_{i,t_{2002}}, \tag{83}$$

[25] For details of the derivations, see Appendix A.4.

[26] For further information on the USDA data on land uses in the U.S., see `https://www.ers.usda.gov/data-products/major-land-uses`..

where t_{2002}, t_{2003} and t_{2012} are the time indices for 2002, 2003, and 2004. Using (80) in (83) to eliminate κ_{it}, we obtain the following estimator of τ_i:

$$\hat{\tau}_i = \frac{\sum_{t=t_{2003}}^{t_{2012}} (1-\delta)^{t_{2012}-t} \hat{\gamma}_{i,t}}{UR_{i,t_{2012}} - \left(1-\hat{\delta}\right)^{10} UR_{i,t_{2002}}}. \tag{84}$$

Then, we compute $\hat{\kappa}_{it}$ using (80) as

$$\ln \hat{\kappa}_{it} = \ln \hat{\gamma}_{it} - \ln \hat{\tau}_i, \text{ for } i = 1, 2, ..., n \text{ and } t = 0, 1, ..., T. \tag{85}$$

We estimate κ_i and $g_{\kappa,i}$ in (29) by running OLS regressions of $\ln \hat{\kappa}_{it}$ on a linear time trend (including a constant), for $i = 1, 2, ..., n$, and obtain the residuals, $\hat{z}_{\kappa,it}$, for $t = 0, 1, ..., T$.[27] Finally, for each i we estimate $\rho_{z_\kappa,i}$ and $\sigma_{z_\kappa,i}$ by running OLS regressions of $\hat{z}_{\kappa,it}$ on $\hat{z}_{\kappa,i,t-1}$, over the period $t = 1, 2, ..., T$.

Figure 3 plots $\hat{g}_{\kappa,i}$ versus the state level Wharton Residential Land Use Regulatory Index, which are complied by Gyourko et al. (2008) and denoted by WRI_i, for the 48 states on the U.S. mainland. Washington, D.C. is excluded since its WRI data is not available. Note that WRI_i is an index constructed from surveys carried out in 2004 and is intended to characterizes the local residential land-use regulatory environment, which increases with the tightness of land-use regulation.[28] Therefore, the data used to construct WRI_i have little overlap with the time series data and parameter calibrations we employ to back out κ_{it}. Thus, the significant negative correlation between $\hat{g}_{\kappa,i}$ and WRI_i, as shown in Figure 3, indicates that the land use regulation can be an important factor that affects local house prices through the supplies of new land. By running an OLS regression of $\hat{g}_{\kappa,i}$ on WRI_i, for the 48 states on the U.S. mainland, we obtain

$$\hat{g}_\kappa (WRI_i) = \underset{(0.0059)}{0.0310} - \underset{(0.0060)}{0.0373} WRI_i, \;\; R^2 = 0.46 \tag{86}$$

where $\hat{g}_\kappa (WRI_i)$ is the fitted value, R^2 is the squared correlation coefficient, and the figures in brackets are standard errors of the estimated coefficients.

[27] It is worth noting that our estimates of $g_{\kappa,i}$ reflect the average tightness of state-level land-use regulations over the period 1977-2014, and need not to be good proxies for particular years or sub-periods.

[28] More specifically, the Wharton Residential Land Use Regulatory Index is based on the Wharton survey on land-use regulations conducted in 2004, and complied by Gyourko et al. (2008), who use factor analysis to create the aggregate index, which is then standardized so that its sample mean is zero and its standard deviation equals one. Since Alaska and Hawaii are excluded from our analysis, we re-scale the WRIs of the remaining states so that the mean and the standard deviation of the sub-sample we use are zero and one, respectively.

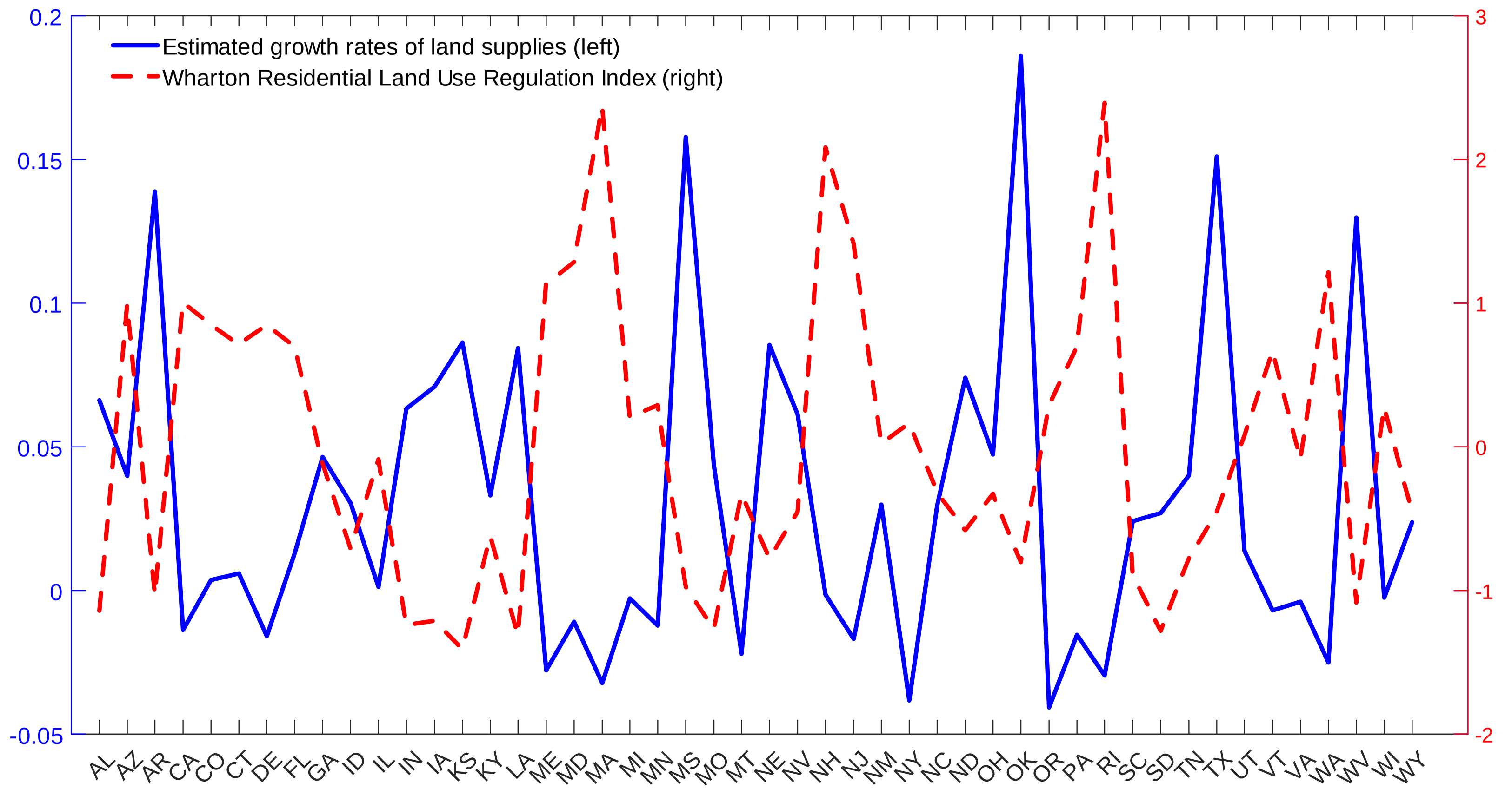

Figure 3: Estimated land supply growth rates and the WRI

Notes: This figure shows the estimated state level growth rates of land supplies and the state level Wharton Residential Land Use Regulatory Index (WRI), complied by Gyourko et al. (2008), of the 48 states on the U.S. mainland. Washington, D.C. is excluded since its WRI data is not available.

6 Dynamic system of equations

Here we set out the equations used in simulation exercises. We first note that since location-specific production functions are linear in labor, the wage rates are always equal to the labor productivities, i.e., $w_{it} = a_{it}$. By substituting a_{it} for w_{it}, the equilibrium conditions that define the model economy are given by:

$$\boldsymbol{l}(t) = \boldsymbol{l}(t-1)\mathbf{G}(t)\mathbf{R}(t), \tag{87}$$

where $\mathbf{G}(t) \equiv \mathbf{diag}\left(e^{g_{l,1t}}, e^{g_{l,2t}}, ..., e^{g_{l,nt}}\right)$ is the $n \times n$ diagonal matrix of intrinsic population growth rates, $\mathbf{R}(t) \equiv \left(\rho_{ij}(t)\right)$ is the $n \times n$ matrix of migration probabilities, and

$$\rho_{ij}(t) = \frac{\alpha_{ij}^{-\psi} \left(q_{jt}/q_{it}\right)^{-\eta} \left(a_{jt}/a_{it}\right)}{\sum_{s=1}^{n} \alpha_{is}^{-\psi} \left(q_{st}/q_{it}\right)^{-\eta} \left(a_{st}/a_{it}\right)}, \tag{88}$$

and,

$$\begin{aligned} h_{i,t-1} &= \eta \left(\frac{a_{it}}{q_{it}}\right) l_{\cdot i}(t), & (89)\\ x_{it} &= \tau_i \kappa_{it} \left(a_{it}\right)^{-\frac{\alpha_l(1-\alpha_{\kappa,i})}{\alpha_{\kappa,i}}} \left(p_{it}\right)^{\frac{1-\alpha_{\kappa,i}}{\alpha_{\kappa,i}}}, & (90)\\ p_{it} h_{it} &= \beta e^{g_l} \left(1-\theta_i\right) \left[q_{it} + (1-\delta) p_{it}\right] h_{i,t-1}, & (91)\\ h_{it} &= (1-\delta) h_{i,t-1} + x_{it}. & (92) \end{aligned}$$

To write the equilibrium conditions in a compact form, using (91), we note that

$$p_{it} = \frac{\beta e^{g_l} \left(1-\theta_i\right) q_{it}}{h_{it}/h_{i,t-1} - \beta e^{g_l} \left(1-\theta_i\right)\left(1-\delta\right)}. \tag{93}$$

Also, by substituting (90) into (92), we have

$$h_{it} = (1-\delta) h_{i,t-1} + \tau_i \kappa_{it} \left(a_{it}\right)^{-\frac{\alpha_l(1-\alpha_{\kappa,i})}{\alpha_{\kappa,i}}} \left(p_{it}\right)^{\frac{1-\alpha_{\kappa,i}}{\alpha_{\kappa,i}}}. \tag{94}$$

Then, substituting (93) into (94) we obtain

$$\begin{aligned} h_{it} = {} & (1-\delta) h_{i,t-1} + \\ & \tau_i \kappa_{it} \left(a_{it}\right)^{-\frac{\alpha_l(1-\alpha_{\kappa,i})}{\alpha_{\kappa,i}}} \left[\frac{\beta e^{g_l} \left(1-\theta_i\right) q_{it}}{h_{it}/h_{i,t-1} - \beta e^{g_l} \left(1-\theta_i\right)\left(1-\delta\right)}\right]^{\frac{1-\alpha_{\kappa,i}}{\alpha_{\kappa,i}}}. \end{aligned} \tag{95}$$

Then, by substituting (89) into (95), we can eliminate h_{it} and $h_{i,t-1}$, and after lagging the resultant equation by one period we have

$$\eta\left(\frac{a_{it}}{q_{it}}\right)l_{\cdot i}(t)=(1-\delta)\eta\left(\frac{a_{i,t-1}}{q_{i,t-1}}\right)l_{\cdot i}(t-1)+ \\ \tau_i\kappa_{i,t-1}\left(a_{i,t-1}\right)^{-\frac{\alpha_l(1-\alpha_{\kappa,i})}{\alpha_{\kappa,i}}}\left[\frac{\beta e^{g_l}\left(1-\theta_i\right)q_{i,t-1}}{\left(\frac{a_{it}}{a_{i,t-1}}\right)\left(\frac{l_{\cdot i}(t)}{l_{\cdot i}(t-1)}\right)\left(\frac{q_{i,t-1}}{q_{it}}\right)-\beta e^{g_l}\left(1-\theta_i\right)(1-\delta)}\right]^{\frac{1-\alpha_{\kappa,i}}{\alpha_{\kappa,i}}}. \tag{96}$$

Equations (87) and (88), together with (96), provide $2n$ non-linear dynamic equations in $l_{\cdot i}(t)$, $i=1,2,...,n$, and q_{it}, $i=1,2,...,n$, which can be written compactly as:

$$\boldsymbol{\zeta}_t=\boldsymbol{f}\left(\boldsymbol{\zeta}_{t-1},\boldsymbol{a}_t,\boldsymbol{a}_{t-1},\boldsymbol{\kappa}_{t-1},\boldsymbol{g}_{l,t};\Theta\right), \tag{97}$$

where Θ is a row vector that contains all the parameters, $\boldsymbol{\zeta}_t=[\boldsymbol{l}(t),\boldsymbol{q}_t]$ is a $1\times 2n$ vector. In addition, using (89) in (94) and (93) to eliminate $h_{i,t-1}$, we have

$$p_{it} = \frac{\beta e^{g_l}\left(1-\theta_i\right)q_{it}}{h_{it}q_{it}/\left(\eta a_{it}l_{\cdot i}(t)\right)-\beta e^{g_l}\left(1-\theta_i\right)(1-\delta)}, \tag{98}$$

$$h_{it} = (1-\delta)\eta\left(\frac{a_{it}}{q_{it}}\right)l_{\cdot i}(t)+\tau_i\kappa_{it}\left(a_{it}\right)^{-\frac{\alpha_l(1-\alpha_{\kappa,i})}{\alpha_{\kappa,i}}}\left(p_{it}\right)^{\frac{1-\alpha_{\kappa,i}}{\alpha_{\kappa,i}}}. \tag{99}$$

Note that using (98) and (99), we can solve for p_{it} and h_{it}, for given values of $l_{\cdot i}(t), q_{it}, a_{it}$ and k_{it}. Thus, $\boldsymbol{p}_t$ and $\boldsymbol{h}_t$ are functions of $\boldsymbol{l}(t)$, $\boldsymbol{q}_t$, $\boldsymbol{a}_t$ and $\boldsymbol{k}_t$:

$$\boldsymbol{\chi}_t=\boldsymbol{g}\left(\boldsymbol{\zeta}_t,\boldsymbol{a}_t,\boldsymbol{\kappa}_t;\Theta\right), \tag{100}$$

where $\boldsymbol{\chi}_t=[\boldsymbol{p}_t,\boldsymbol{h}_t]$ is a $1\times 2n$ vector.

The stochastic processes of $\boldsymbol{a}_t$ are defined as

$$\begin{aligned}
\ln\boldsymbol{a}_t &= \ln\boldsymbol{a}+\boldsymbol{g}_a t+\boldsymbol{\lambda}f_t+\boldsymbol{z}_{a,t},\\
f_t &= \rho_f f_{t-1}+\sigma_f\varepsilon_{f,t},\\
\boldsymbol{z}_{a,t} &= \boldsymbol{z}_{a,t-1}\mathbf{diag}(\rho_{z_a,1},\rho_{z_a,2},...\rho_{z_a,n})+\boldsymbol{\varepsilon}_{z_a,t}\mathbf{diag}(\sigma_{z_a,1},\sigma_{z_a,2},...\sigma_{z_a,n}),
\end{aligned}$$

and the stochastic processes of $\boldsymbol{\kappa}_t$ are given by

$$\begin{aligned}
\ln\boldsymbol{\kappa}_t &= \ln\boldsymbol{\kappa}+\boldsymbol{g}_\kappa t+\boldsymbol{z}_{\kappa,t},\\
\boldsymbol{z}_{\kappa,t} &= \boldsymbol{z}_{\kappa,t-1}\mathbf{diag}(\rho_{z_\kappa,1},\rho_{z_\kappa,2},...\rho_{z_\kappa,n})+\boldsymbol{\varepsilon}_{z_\kappa,t}\mathbf{diag}(\sigma_{z_\kappa,1},\sigma_{z_\kappa,2},...\sigma_{z_\kappa,n}).
\end{aligned}$$

and the values of $\boldsymbol{g}_{l,t}$, for $t=1,2,...$, are exogenously given.

7 Simulation exercises

To examine the ability of the model in explaining the observed rise in house price dispersion in the U.S., we simulate the model using the realized state level incomes and land supplies. In addition, we conduct a series of counterfactual exercises to examine the relative contributions of different types of spatial heterogeneities in driving up house price dispersion. Third, to investigate how land supply growth rate differentials and migration costs jointly contribute to the rising house price dispersion, we carry out additional simulations by varying land supply growth rates and levels of migration costs. Fourth, to investigate the impacts of the land-use regulations in California and Texas on local house prices and populations, we conduct counterfactual simulations by varying the land supply growth rates of California and Texas, in turn.

Note that to simulate the model given by (97) and (100), we need to set the initial values, $\boldsymbol{\zeta}_0$, and the exogenous variables, $\boldsymbol{a}_t, \boldsymbol{\kappa}_t$ and $\boldsymbol{g}_{l,t}$. Thus, we start each of our simulations by specifying the values used for $\boldsymbol{\zeta}_0$, $\boldsymbol{a}_t, \boldsymbol{\kappa}_t$ and $\boldsymbol{g}_{l,t}$, for $t = 1, 2, ..., T$.

7.1 Baseline simulations

To examine the model's ability in explaining the rise in house price dispersion, we simulate the model using the realized state level incomes and land supplies. To do so, we take the state level productivities and land supplies, i.e., $\boldsymbol{a}_t$ and $\boldsymbol{\kappa}_t$, as deterministic exogenous variables in the following simulations. Furthermore, we set $\boldsymbol{a}_t$, for $t = 0, 1, ..., T$, to their realized values, which are measured using the realized state level real per capita disposable income, and set $\boldsymbol{\kappa}_t$ equal to the trend components of their realized values:

$$\boldsymbol{\kappa}_t = \hat{\boldsymbol{\kappa}} \ \mathbf{diag}(e^{\hat{g}_{\kappa,1}t}, e^{\hat{g}_{\kappa,2}t}, ...e^{\hat{g}_{\kappa,n}t}), \text{ for } t = 0, 1, ..., T,$$

where $\hat{\boldsymbol{\kappa}}$ and $\hat{\boldsymbol{g}}_\kappa$ are estimated in Section 5.5. The state level intrinsic population growth rates, $\boldsymbol{g}_{l,t}$, are set to their actual values, which are estimated in Sections 5.2. The initial values correspond to the actual 1976 economy, and $\boldsymbol{l}(0)$ and $\boldsymbol{q}_0$ are observed data. The simulation results are summarized as follows:

First, the model can capture the trends in the house price-to-income ratios at both the national and the regional levels as shown in Figure 4. In particular, it captures the rise in house price-to-income ratio in the West and the falls in the Southeast, the Midwest and the Southwest. Due to the fast growth of land supplies, house prices in the southern states increase at a slower pace than local incomes, leading to significant drops in house price-to-income ratios. In addition, the model generates the slight observed decline in the national house price-to-income ratio.

Second, the model replicates reasonably well the trends in the dispersions of house price-to-income ratios at both national and regional levels, as shown in Figure 5. The model generates between-state dispersion increases from 0.11 to 0.39 during the period 1976-2014, while the counterpart realized value rises from 0.09 to 0.34 (Table 1). In addition, the model captures the different trends at different geographical levels, i.e., the substantial increase in the between-region dispersion and the moderate increases of within-region dispersions. As will be shown in Section 7.5, this can be partially due to the stronger migration linkages between states that are geographically close, which tends to prevent the house price differences between these states from increasing.

Third, the model matches the observed trends in the interstate migration. Figure 6 compares the actual accumulated net migration inflows of the U.S. states during the period 1990-2014 with the model generated counterparts.[29] As can be seen, the model captures the significant migration outflows from states with rising house price-to-income ratios, such as CA, IL, and NY, and the substantial inflows towards states with decreasing house price-to-income ratios, such as, FL and TX.

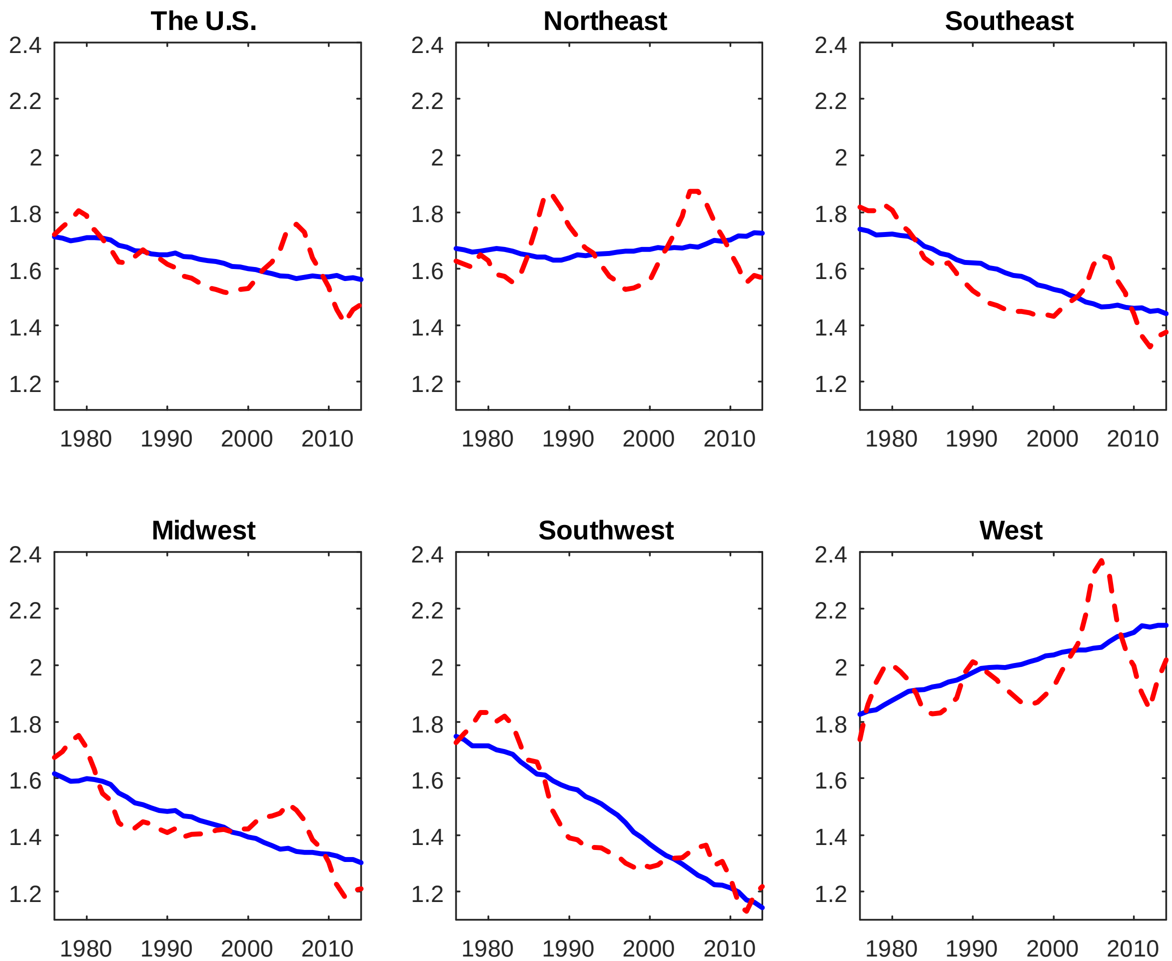

Figure 4: Log house price-to-income ratios of U.S. regions
(Solid-blue: simulated; Dashed-red: data)

Notes: This figure plots the realized and simulated log house price-to-income ratios of the U.S. and U.S. regions.

[29]Note that the IRS migration data are only available for the period 1990-2014.

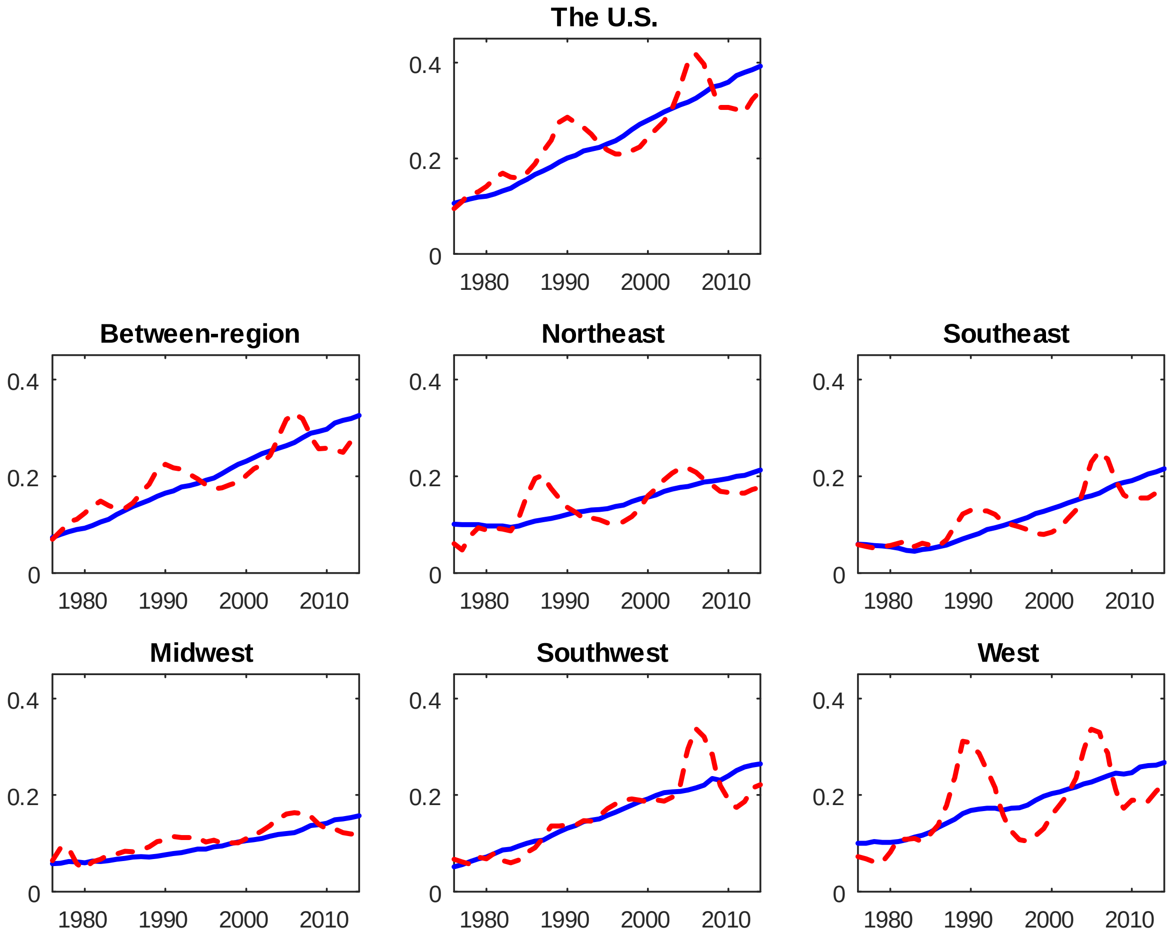

Figure 5: Dispersions of log house price-to-income ratios between- and within- U.S. regions (Solid-blue: simulated; Dashed-red: data)

Notes: This figure plots the realized and simulated dispersions of log house price-to-income ratios between- and within- U.S. regions.

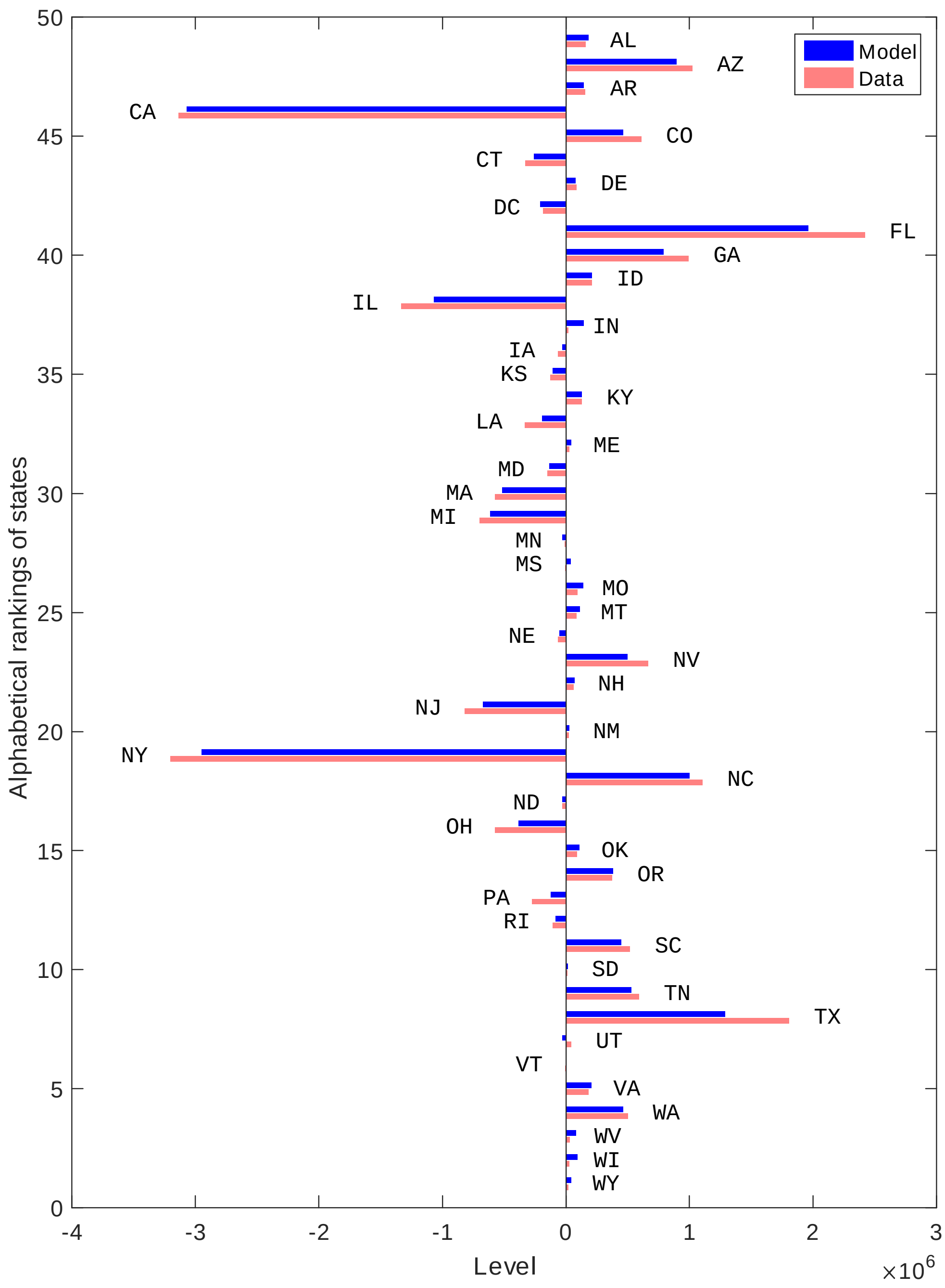

Figure 6: Net inward migration flows by states during 1990-2014
(Upper-blue: simulated; Lower-red: data)

Notes: This figure shows the realized and simulated accumulated net migration inflows towards U.S. states during the period 1990-2014. States are arranged from top to bottom in alphabetical order.

7.2 Spatial heterogeneities and house price dispersion

Land supply growth rates proxied by the WRI: The results of the baseline simulation have shown that the spatial heterogeneity in the growth rate of new land supplies can explain the trends in the house price dispersions during the period 1977-2014, given the realized incomes and intrinsic population growth rates. In addition, the estimated state level land supply growth rates, $\hat{g}_{\kappa,i}$, are highly correlated with WRI_i as shown in Figure 3. To examine the extent to which the heterogeneity in regulatory environments that are measured by WRI_i can explain the rising house price dispersion, we use WRI_i to proxy the state level growth rates of land supplies according to (86).[30] Then, we conduct a counterfactual simulation using the proxied land supply growth rates, while keeping everything else the same as in the baseline simulation. As shown in the Panel (3) of Table 1, the results are not changed much from those of the baseline simulation, which implies that the rising house price dispersion can be largely explained by the spatial heterogeneity in land-use regulations.

Homogeneous land supply growth rates: To examine the importance of the spatial heterogeneity in land supply growth rates across U.S. states in driving up the house price dispersion, we conduct a counterfactual simulation in which land supply growth rates of all states are set equal to their national average

$$g_{\kappa,i} = \bar{\hat{g}}_{\kappa}, \text{ for } i = 1, 2, ..., n,$$

where

$$\bar{\hat{g}}_{\kappa} = \frac{1}{n} \textstyle\sum_{i=1}^{n} \hat{g}_{\kappa,i}, \tag{101}$$

and $\hat{g}_{\kappa,i}$ is the actual state-specific land supply growth rate estimated in Section 5.5, while keeping everything else the same as in the baseline simulation. As shown in Panel (4) of Table 1, the model fails to capture the upward trends in house price-to-income ratio dispersions when land supply growth rates are homogeneous, which suggests that spatial heterogeneity in land supply growth rates is an essential factor behind the increasing house price dispersion.

Homogeneous intrinsic population growth rates: In addition, the intrinsic population growth rate varies substantially across U.S. states. To examine the importance of the spatial heterogeneity in intrinsic population growth rate in driving up house price dispersion, we conduct a counterfactual simulation in which the intrinsic population growth rates of all states are set to the national average population growth rate over the sample period:

$$g_{l,it} = \hat{g}_l, \text{ for } i = 1, 2, ..., n, \text{ and } t = 0, 1, ..., T,$$

where $\hat{g}_l$ is the average growth rate of the national population over the period 1977-2014. At the same time, we keep everything else the same as in the baseline simulation. However, the results are not changed much as shown in Panel (5) of Table 1. Thus, we conclude that heterogeneity in intrinsic population growth rate may not be an important reason for the rise in house price dispersion.

[30] Since the WRI data is not available for Washington, D.C., we keep its land supply growth rate as it is in the baseline simulation, i.e., $\hat{g}_{\kappa,DC}$.

7.3 Land supply growth differentials, mobility and dispersion

As previously discussed, population mobility plays a key role in determining the impacts of land supply growth differentials on house price dispersion. To examine how land supply growth differentials and migration costs jointly contribute to the rise in house price dispersion, we carry out simulations assuming different levels of land supply growth differentials and migration costs. We adjust the weight of migration costs in utility function through ψ (see (16)). As ψ increases, population mobility drops. In addition, we adjust the degree of land supply growth differentials by letting the state-specific land supply growth rates vary between their actual levels and the national average. Let ϱ denote the counterfactual land supply regime. Under regime ϱ, the growth rates of land supplies are given by

$$g_{\kappa,i}(\varrho) = (1-\varrho)\bar{\bar{g}}_{\kappa} + \varrho \hat{g}_{\kappa,i}, \text{ for } i = 1, 2, ..., n, \tag{102}$$

where $\bar{\bar{g}}_{\kappa}$ is the national average of land supply growth rate defined by (101) in Section 7.2, $\varrho \in [0, 1]$, and a higher ϱ corresponds to a higher level of land supply growth differentials.

We simulate the model for different pairs of (ϱ and ψ) $= (0.60, 0.80, 1, 1.2,\ 1.4)$, and keeping everything else the same. The results are summarized in Table 2, and show that the dispersion of log house price-to-income ratios would be significantly lower if migration costs were reduced. For example, when $\varrho = 1$, dispersion would be around 0.1 (0.2) less when ψ is reduced to 0.8 (0.6). The decreases in ψ also lower the national log house price-to-income ratio, since more people would move out of high price growth states as migration costs are reduced. However, it has much smaller impacts on the level than on the dispersion of house price-to-income ratios. In addition, both land supply growth differentials and migration costs play important roles in driving up house price dispersion; reducing either of them can significantly lower house price dispersion in the U.S.. Moreover, increases in land supply growth differentials would lead to larger rises in house price dispersion when the magnitudes of migration costs are larger. For example, when $\psi = 0.6$ dispersion increases by 0.255, from 0.192 to 0.447, as the level of land supply growth differentials, ϱ, increases from 0.6 to 1.4. But, when $\psi = 1.4$, dispersion would increase by 0.299, from 0.273 to 0.572, as ϱ increases from 0.6 to 1.4.

Table 1: The level and the dispersion of realized and simulated log house price-to-income ratios

	Actual		Simulated							
	(1) Data		(2) Baseline simulation		(3) Land supply growth rates proxied by the WRI		(4) Homogeneous land supply growth rates		(5) Homogeneous intrinsic population growth rates	
Year	*1976*	*2014*	*1976*	*2014*	*1976*	*2014*	*1976*	*2014*	*1976*	*2014*
					I. Level					
The U.S.	1.72	1.47	1.71	1.56	1.71	1.49	1.71	1.32	1.71	1.55
Northeast	1.63	1.57	1.67	1.72	1.67	1.53	1.67	1.13	1.67	1.73
Southeast	1.82	1.38	1.74	1.44	1.74	1.40	1.74	1.37	1.74	1.46
Midwest	1.67	1.21	1.62	1.30	1.62	1.20	1.62	1.26	1.62	1.32
Southwest	1.73	1.22	1.75	1.14	1.75	1.45	1.75	1.45	1.75	1.14
West	1.74	2.02	1.83	2.14	1.83	1.99	1.83	1.47	1.83	2.05
					II. Disperison					
The US	0.09	0.34	0.11	0.39	0.11	0.37	**0.11**	**0.15**	0.11	0.36
Between-region	0.07	0.29	0.07	0.33	0.07	0.26	0.07	0.12	0.07	0.29
Northeast	0.06	0.18	0.10	0.21	0.10	0.40	0.10	0.04	0.10	0.19
Southeast	0.06	0.17	0.06	0.22	0.06	0.22	0.06	0.10	0.06	0.21
Midwest	0.06	0.12	0.06	0.16	0.06	0.10	0.06	0.06	0.06	0.16
Southwest	0.07	0.22	0.05	0.26	0.05	0.24	0.05	0.13	0.05	0.26
West	0.07	0.23	0.10	0.27	0.10	0.29	0.10	0.12	0.10	0.21

Notes: This table reports the levels and the dispersions of realized and simulated log house price-to-income ratios at different geographical levels. Panel (2) reports the results from the baseline simulation. Panel (3) reports the simulation results when the growth rates of state level land supplies are proxied by the WRI as (86). Panel (4) corresponds to the counterfactual simulation in which land supply growth rates of all U.S. states are homogeneous. Panel (5) reports the simulation results when the intrinsic population growth rates of all U.S. states are homogeneous.

Table 2: The level and the dispersion of simulated 2014 log house price-to-income ratios under different parameter values

Land Supply Regime ϱ \ Migration Costs Ψ		Lower		Bechmark	Higher		Lower		Bechmark	Higher	
		0.6	*0.8*	*1.0*	*1.2*	*1.4*	*0.6*	*0.8*	*1.0*	*1.2*	*1.4*
		I. Level					II. Dispersion				
Lower	*0.6*	1.417 (0.908)	1.445 (0.926)	1.468 (0.940)	1.475 (0.945)	1.475 (0.945)	0.192 (0.490)	0.217 (0.552)	0.253 (0.645)	0.269 (0.686)	0.273 (0.695)
	0.8	1.462 (0.936)	1.491 (0.955)	1.515 (0.970)	1.522 (0.975)	1.523 (0.976)	0.249 (0.635)	0.280 (0.712)	0.321 (0.818)	0.341 (0.868)	0.346 (0.882)
Benchmark	*1.0*	1.505 (0.964)	1.535 (0.983)	**1.561** **(1.000)**	1.569 (1.005)	1.570 (1.006)	0.313 (0.799)	0.347 (0.884)	**0.393** **(1.000)**	0.414 (1.056)	0.421 (1.074)
Higher	*1.2*	1.547 (0.991)	1.579 (1.011)	1.606 (1.029)	1.615 (1.035)	1.617 (1.036)	0.380 (0.968)	0.416 (1.061)	0.465 (1.184)	0.489 (1.246)	0.497 (1.266)
	1.4	1.588 (1.017)	1.621 (1.038)	1.650 (1.057)	1.660 (1.064)	1.662 (1.065)	0.447 (1.139)	0.485 (1.237)	0.537 (1.368)	0.563 (1.435)	0.572 (1.458)

Notes: This table reports the average and the dispersion of model simulated log house price-to-income ratios across U.S. states in 2014 for different land supply regimes and migration costs. A larger ϱ corresponds to a higher level of land supply differentials. A larger Ψ corresponds to higher migration costs.

7.4 Land-use regulations in California and Texas

Land-use regulations can have important implications not only for local house prices but could also have important implications for spatial allocation of the population. Deregulating in states with stricter land-use restrictions can affect the population allocation across U.S. states through house price channel. According to Herkenhoff et al. (2018), loosening the land-use restrictions in California to its 1980s level would raise its population in 2014 by 6 million, i.e., around 20% of its actual population in 2014. However, this study assumes perfect mobility, and by not taking into account migration friction, could be overestimating the effects of land-use deregulations on population reallocation.

Here, we investigate the impacts of local land-use regulations, which are the main factors that determine the land supplies for housing, on house prices and population allocation. In particular, we consider California and Texas in our counterfactual experiments, which are at the two extreme poles of land-use regulation continuum; The former, one of the most regulated states, has experienced considerable house price rises during the 1976-2014 period, while the later, one of the least regulated states, has experienced little house price rise during the same period. In the following counterfactual simulations, we let the average land supply growth rates of California and Texas to vary between their actual values and the national average land supply growth rate. Let $g_{\kappa,CA}(\varrho)$ and $g_{\kappa,TX}(\varrho)$ denote the counterfactual land supply growth rates of California and Texas, and consider the following rates

$$g_{\kappa,i^*}(\varrho) = (1-\varrho)\hat{g}_{\kappa,i^*} + \varrho\bar{\bar{g}}_{\kappa}, \text{ for } i^* = CA, TX \tag{103}$$

where $\bar{\bar{g}}_{\kappa}$ is the national average of land supply growth rate defined by (101) in Section 7.2, $\varrho \in [0,1]$, and $\hat{g}_{\kappa,i^*}$ is the estimated actual land supply growth rate of State i^*.

We first consider a land-use deregulation in California. To this end, we simulate the model while setting the land supply growth rate of California to $g_{\kappa,CA}(\varrho)$, given by (103), for $\varrho = \{1/4, 1/2, 3/4, 1\}$, and keeping everything else the same as in the baseline simulation in Section 7.1. Note that the estimated land growth rate of California, $\hat{g}_{\kappa,CA}$, is less than the national average, $\bar{\bar{g}}_{\kappa}$. Thus, a larger ϱ corresponds to a higher degree of deregulation. As shown in Table 3, the land supply growth rate of California has considerable impacts on the local house prices, but relatively small impacts on the local population. Figure 7 shows the difference between the state level population predicted by the counterfactual simulation in which the land supply growth rate of California is raised to the national average and those predicted by the baseline simulation. As this figure shows, if the growth rate of land supply in California were raised to the national average, the 2014 population of California would increase by around 1 million, which is substantially less than the 6 million increase obtained in the deregulation experiment conducted by Herkenhoff et al. (2018).[31] In addition, the reallocation of population towards California are mainly from Texas, and the neighboring states of California, such as, Arizona, Nevada, Oregon, and Washington.

[31] But it is important to note, however, that the deregulation experiments in our paper is different from that in Herkenhoff et al. (2018). In their paper, deregulation refers to setting the level of regulation to its historical level.

Table 3: Effects of loosening of land-use regulations in California

California						
	units	Baseline	Counterfactual increases in land supply growth (ϱ)			
ϱ		0	1/4	1/2	3/4	1
Increases in land-supply growth rate	Per cent	0.00	1.12	2.24	3.36	4.48
Real house price in 2014	Thousands $	302.1	245.8	199.1	160.7	129.3
Avg. yearly growth rate of real house prices (1976-2014)	Per cent	2.467	1.924	1.370	0.806	0.234
Population in 2014	Millions	31.4	31.7	32.0	32.3	32.7
Avg. yearly growth rate of population (1976-2014)	Per cent	1.577	1.601	1.627	1.654	1.681

Notes: This table shows the impacts of land-use deregulation in California on the local house prices and population. The third column reports the results from the baseline simulation. The fourth to last columns report the results from the counterfactual simulations in which the land supply growth rate of California is set to $g_{\kappa,CA}(\varrho)$, given by (103), where $\varrho = \{1/4, 1/2, 3/4, 1\}$.

We then consider a tightening of land-use regulation in Texas. To this end, we simulate the model while setting the land supply growth rate of Texas to $g_{\kappa,TX}(\varrho)$, given by ((103), for $\varrho = \{1/4, 1/2, 3/4, 1\}$, and keeping everything else the same as in the baseline simulation in Section 7.1. Note that the estimated land growth rate of Texas, $\hat{g}_{\kappa,TX}$, is higher than the national average, $\bar{\hat{g}}_{\kappa}$. Thus, a larger ϱ corresponds to more tightened land-use regulation. Similar to the deregulation experiment in California, tightening land-use regulation in Texas significantly impact local house prices, but only has marginal effects on the State's population (see Table 4). Figure 8 shows the difference between the state level population predicted by the counterfactual simulation in which the land supply growth rate of Texas is reduced to the national average and those predicted by the baseline simulation. As this figure shows, if the growth rate of land supply in Texas were reduced to the national average, the 2014 population of Texas would decrease by around 0.6 million, and the reallocation of population from Texas are mainly towards California, Florida, and the neighboring states of Texas, such as, Louisiana and Oklahoma.

Table 4: Effects of tightening of land-use regulations in Texas

Texas						
	units	Baseline	Counterfactual decreases in land supply growth (ϱ)			
ϱ		0	1/4	1/2	3/4	1
Reductions in land-supply growth rate	Per cent	0	-3	-6	-9	-12
Real house price in 2014	Thousands $	85.2	93.5	102.7	112.7	123.7
Avg. yearly growth rate of real house prices (1976-2014)	Per cent	-0.114	0.132	0.378	0.623	0.868
Population in 2014	Millions	20.3	20.1	19.9	19.8	19.6
Avg. yearly growth rate of population (1976-2014)	Per cent	1.763	1.742	1.722	1.702	1.682

Notes: This table shows the impacts of tightening land-use regulation in Texas on the local house prices and population. The third column reports the results from the baseline simulation. The fourth to last columns report the results from the counterfactual simulations in which the land supply growth rate of Texas is set to $g_{\kappa,TX}(\varrho)$, given by (103), where $\varrho = \{1/4, 1/2, 3/4, 1\}$.

Our counterfactual exercises do show that changes in local land-use regulations can affect population allocation via the house price channel, but its effects tend to be relatively moderate as compared to recent existing models of housing and migration, which assume population are perfectly mobile, such as, Hsieh and Moretti (2015) and Herkenhoff et al. (2018). However, changes in land use regulations affect house prices much more as compared to their effects on allocation of population.

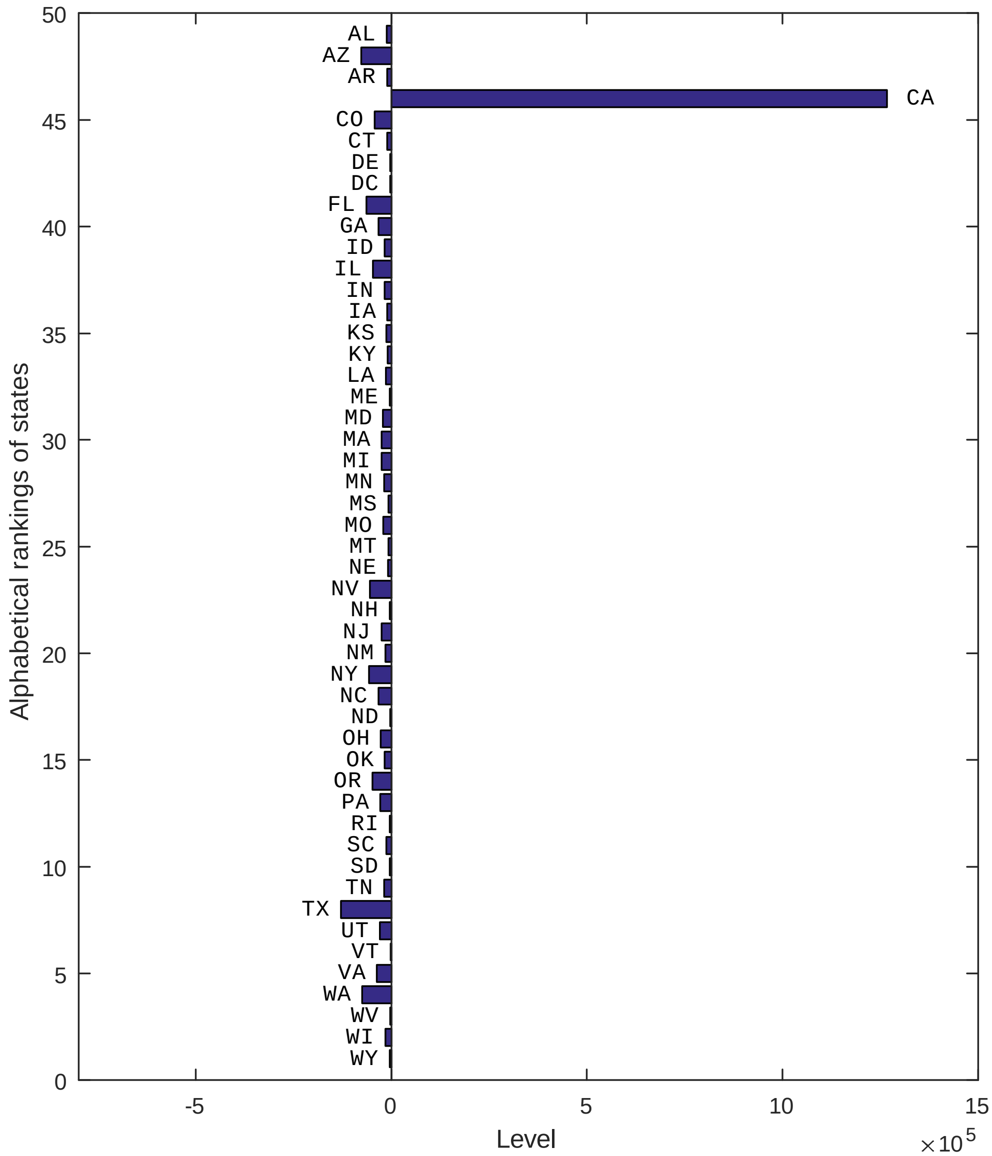

Figure 7: Effects of loosening of land-use regulations in California on population by states

Notes: This figure shows the counterfactual changes in U.S. population by states in 2014 in response to an exogenous increase in land supply growth rate of California to the national average.

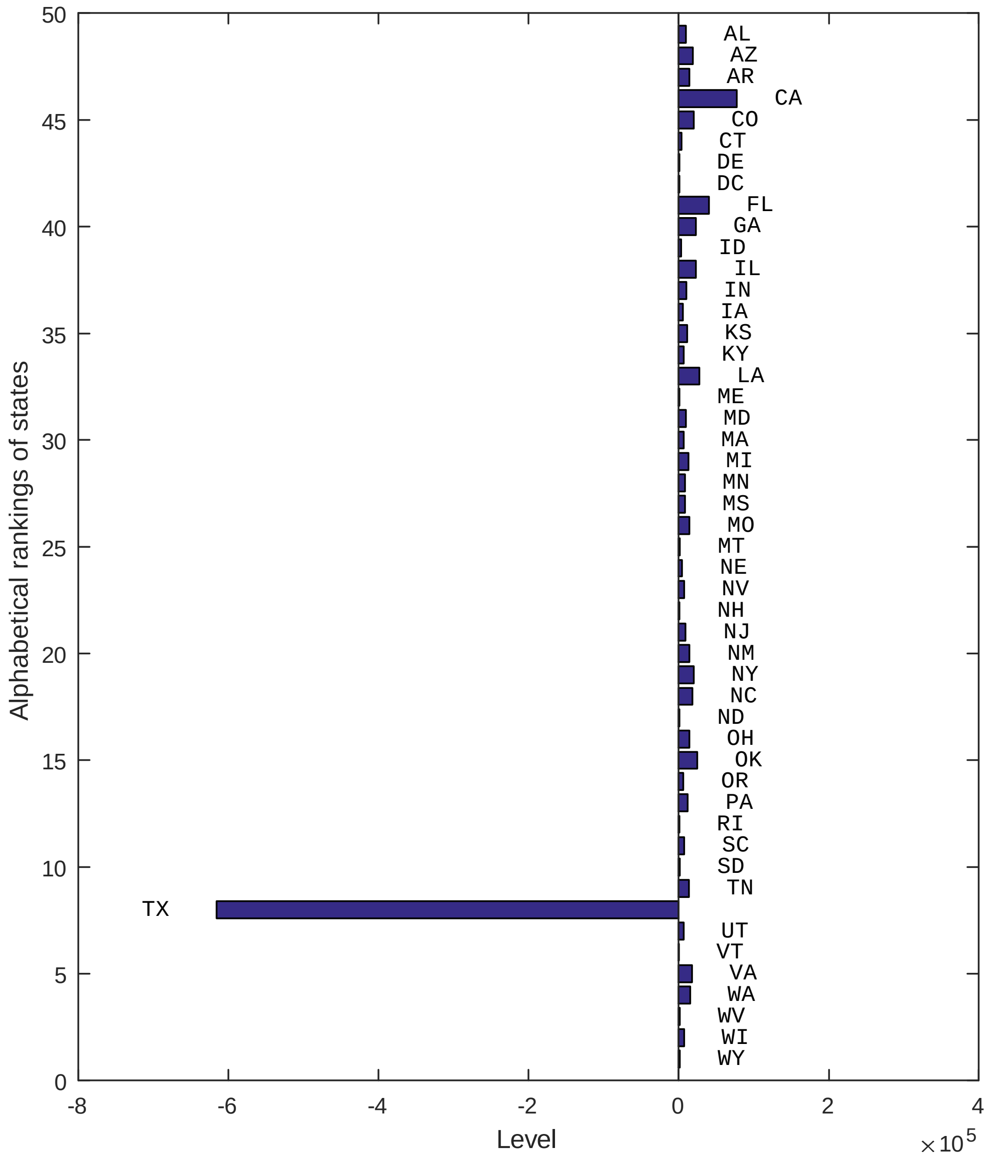

Figure 8: Effects of tightening of land-use regulations in Texas on population by states

Notes: This figure shows the counterfactual changes in U.S. population by states in 2014 in response to an exogenous decrease in land supply growth rate of Texas to the national average.

7.5 Impulse responses to a regional shock

To better understand the migration linkages between regional housing markets, we analyze the responses of the economy to a regional shock. In particular, we assume that the economy is initially on the balanced growth path and consider a one standard deviation negative regional productivity shock to California. The simulated innovations used in the computation of the impulse responses are independently drawn from the standard normal distribution. For the details of the computation of the impulse responses, see Section S4 of the online supplement. The impulse responses are shown in Figures 9, 11, 10 and 12. Figure 9 shows the responses of the house price-to-income ratio (left panel) and the population (right panel) of CA after the shock. As shown in these figures, the adjustments of population and house price to the shock are very slow, which takes decades. This is due to the slow depreciation of housing stocks and the sluggishness in the migration. Figures 10 and 11 show the responses of house price-to-income ratios and populations of U.S. states (except for CA) to the negative regional productivity shock to CA, where the states are ordered by their distances to CA. Figure 12 shows the snapshots of the responses of house price-to-income ratios of U.S. states (except for CA). Each panel shows the responses in the period noted at the top. In each panel, the horizontal axis corresponds to state's rank in terms of their geographical closeness to CA. In response to the shock, house price-to-income ratios rise in all states. However, the responses in the neighboring states (e.g., NV and AZ), and in some of the West Coast states (e.g., DC and NY) are quicker and stronger. The responses in these states reach their peaks more quickly and their peak values tend to be larger as well. Thus, the snapshots of responses are U shaped.

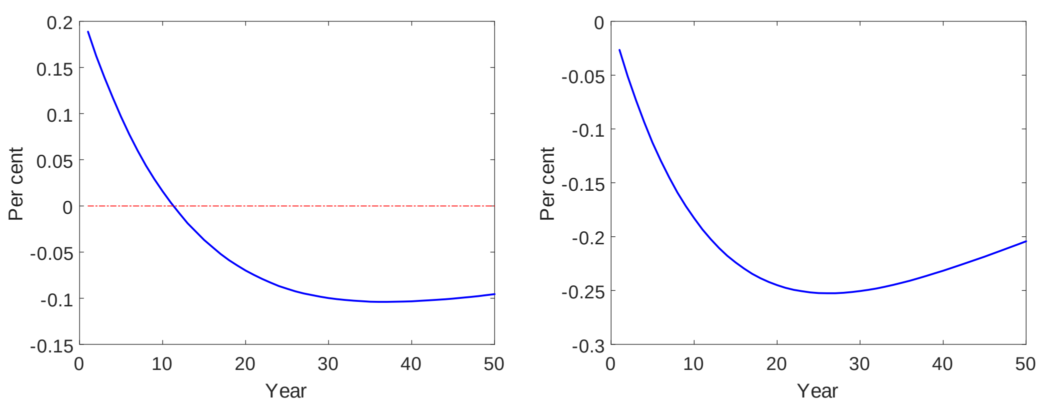

Log house price-to-income ratio   Log population

Figure 9: Reponses of CA to a negative regional shock to local productivity

Notes: This figure shows the responses of log house price-to-income ratio and log population of California to a one standard deviation negative regional shock to local productivity.

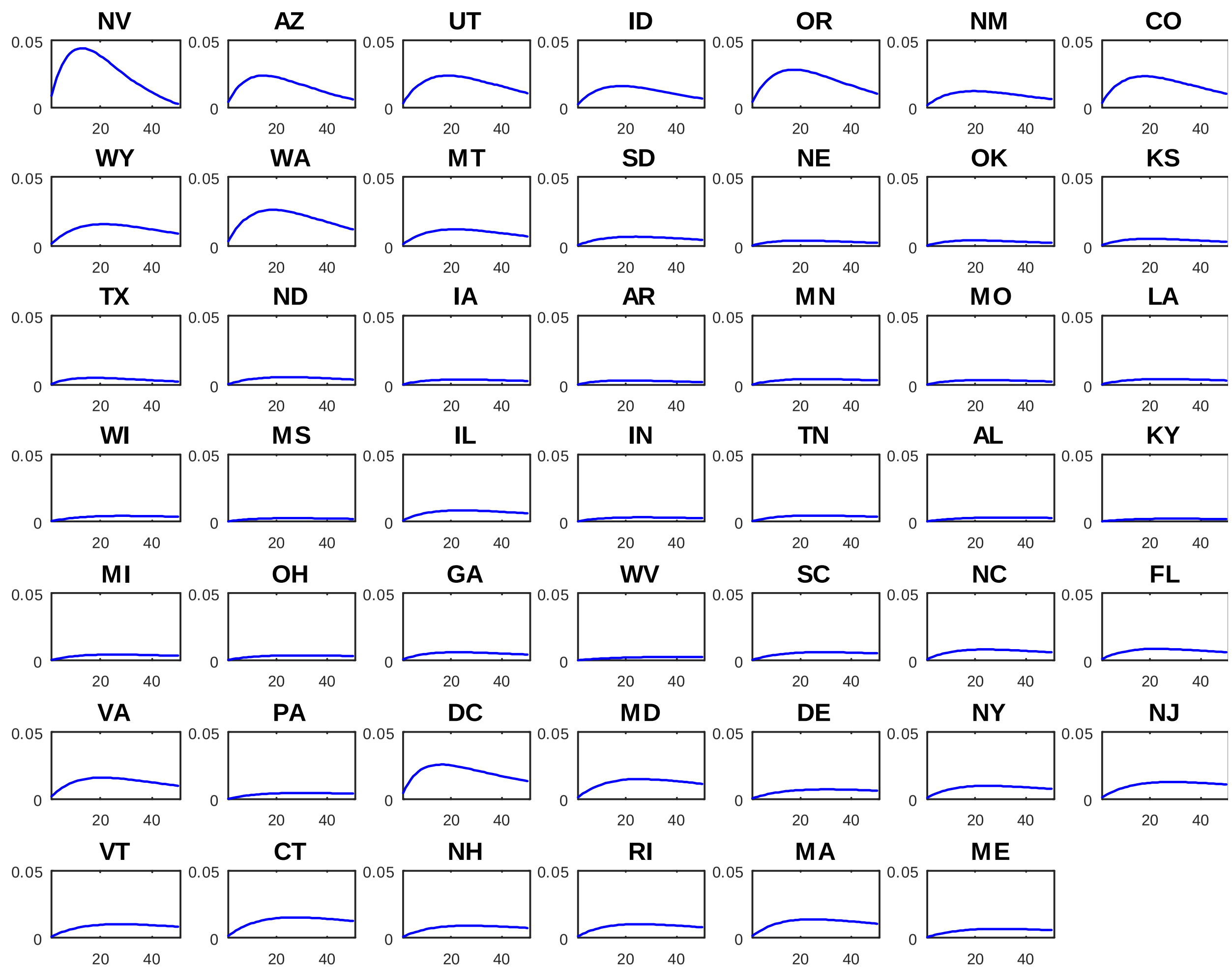

Figure 10: Responses of log house price-to-income ratios of U.S. states to a negative regional productivity shock to CA

Notes: This figure shows the responses of log house price-to-income ratios of U.S. states (except for CA) to a one standard deviation negative regional productivity shock to CA. States are ordered ascendingly by their distances to CA. The unit on the horizontal axis is year. The unit on the vertical axis is per cent.

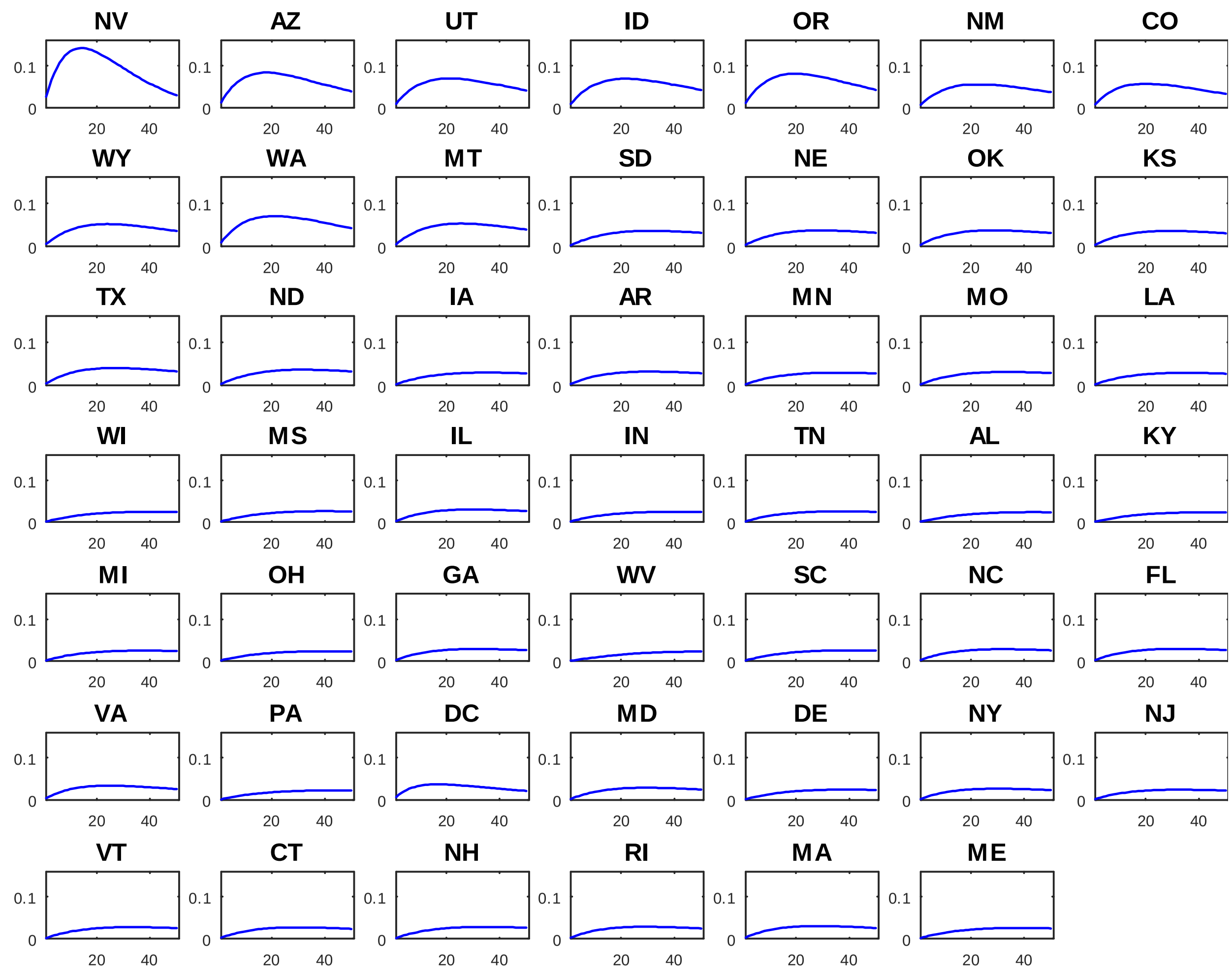

Figure 11: Responses of log populations of U.S. states to a negative regional productivity shock to CA

Notes: This figure shows the responses of log populations of U.S. states (except for CA) to a one standard deviation negative regional productivity shock to CA. States are ordered ascendingly by their distances to CA. The unit on the horizontal axis is year. The unit on the vertical axis is per cent.

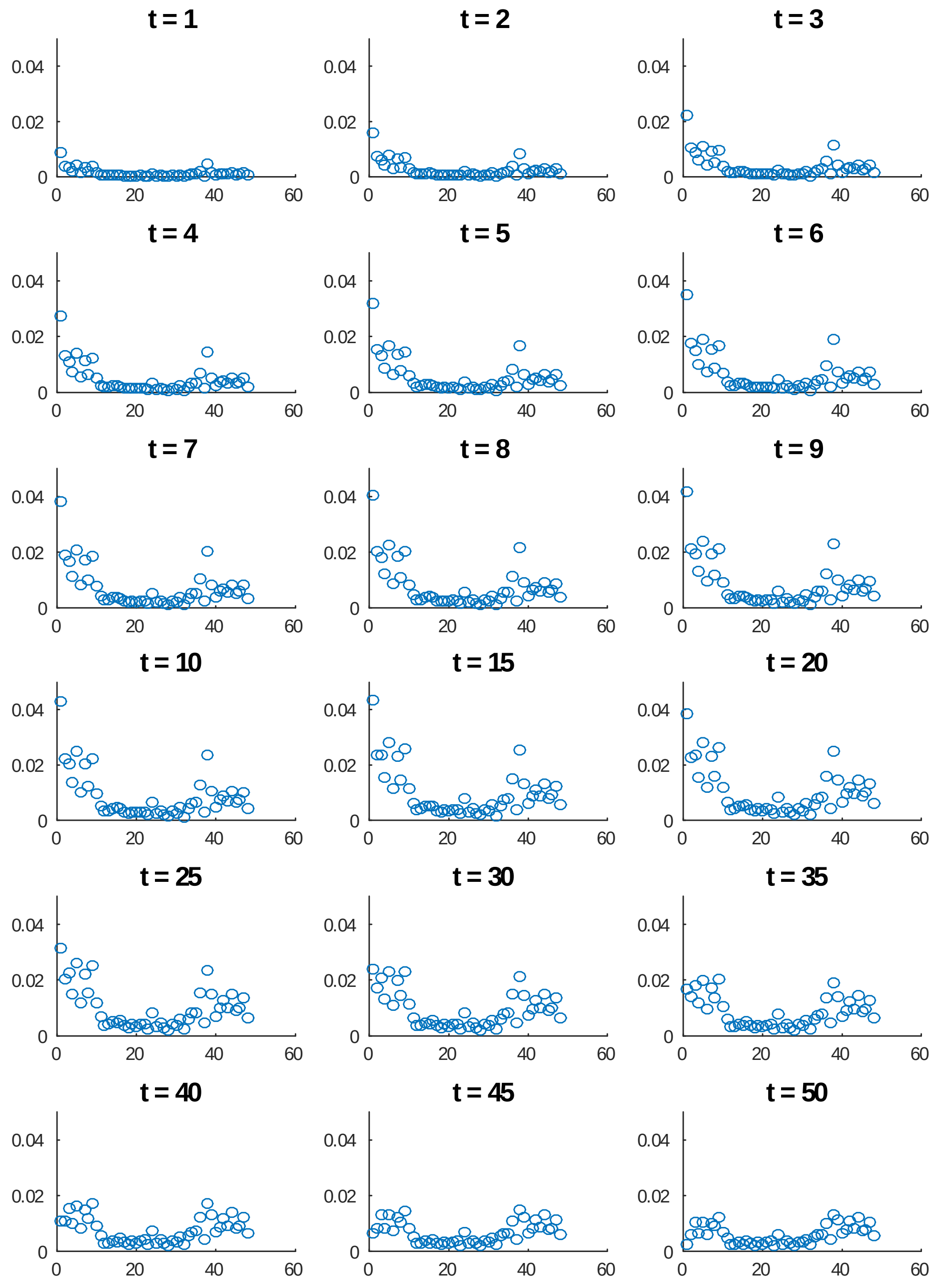

Figure 12: Snapshots of the responses of the log house price-to-income ratios of U.S. states to a negative regional productivity shock to CA

Notes: Each panel shows the responses of the log house price-to-income ratios of U.S. states (except for CA) to a one standard deviation negative regional productivity shock to CA for the period noted at the top. The unit of t is year. States are ordered ascendingly by their distances to CA. The horizontal axis corresponds state's rank in terms of distance to CA. The unit on the vertical axis is per cent.

8 Concluding remarks

This paper presents a spatial equilibrium model of regional housing markets in which regional house prices are jointly determined with migration flows. It extends existing studies by explicitly modelling location-to-location migration. Agent's optimal location choice and the resultant migration process is Markovian with the transition probabilities across all location pairs given as non-linear functions of income and housing cost differentials, which are endogenously determined. These features allow the model to simultaneously account for the observed rise in the house price dispersion and the interstate migration flows over the period 1976-2014.

Spatial heterogeneity in land-use regulation is the key driving force behind the rise in house price dispersion. Degree of population mobility is also an important factor in determining how land-use regulations affect house price dispersion and migration. Spatial house price dispersion tends to rise when mobility is low and fall when mobility is high. Furthermore, our model takes into account the substantial variation of mobility across the U.S.. Impulse response reported in the paper suggest that migrations between states that are geographically close are more responsive to changes in income and housing cost differentials, which in turn help accounting for the observed differences in trends in house price dispersions within and between regions. Our counterfactual exercises show that changes in land-use regulations do affect population allocation via the house price channel, but its effects tend to be relatively moderate as compared to recent existing models of housing and migration that assume population are perfectly mobile.

The analysis of this paper can be developed extended in a number of directions. The financial side of the housing market (briefly discussed in the online supplement) can be studied further, with the aim of investigating possible implications of rising house price dispersion for macroeconomic fluctuations. An econometrically estimated version of the model can also be used for the analysis and predication of house price diffusion across states or MSAs. Finally, given the importance of labor mobility for a stable spatial house price dispersion, it is also worth considering the factors that determine population mobility, their nature and variations overtime and across space.

Appendices

A Mathematical derivations and proofs

A.1 Derivation of migration probabilities

Here we derive the migration probability equation (15). For the worker τ who is born in location i, the probability of residing in location j^* is

$$Prob\ (j^* \text{ is chosen}) = Prob\ \left(v_{\tau,t,ij^*} > v_{\tau,t,ij}\ \forall j \neq j^*\right),$$

where

$$v_{\tau,t,ij} = (\ln w_{jt} - \ln w_{it}) - \eta\,(\ln q_{jt} - \ln q_{it}) + (\varepsilon_{\tau,t,ij} - \varepsilon_{\tau,t,ii}) - \psi \ln \alpha_{ij}.$$

Recall that $\varepsilon_{\tau,t,ij}$ is IID for all τ, t, i and j, and has an extreme value distribution, with the cumulative distribution function $F(\varepsilon) = e^{-e^{-\varepsilon}}$, and the probability density function $f(\varepsilon) = e^{-\varepsilon}e^{-e^{-\varepsilon}}$. Consider the following decomposition of $v_{\tau,t,ij}$,

$$v_{\tau,t,ij} = v_{t,ij} + (\varepsilon_{\tau,t,ij} - \varepsilon_{\tau,t,ii})$$

where

$$v_{t,ij} \equiv (\ln w_{jt} - \ln w_{it}) - \eta\,(\ln q_{jt} - \ln q_{it}) - \psi \ln \alpha_{ij}.$$

Note that $v_{t,ij}$ is known by worker τ, and will be treated as given. The probability that worker τ selects region j^* as her migration destination can be written as

$$\begin{aligned} Prob\ (j^* \text{ is chosen}) &= Prob\ \left(v_{\tau,t,ij^*} + \varepsilon_{\tau,t,ij^*} - \varepsilon_{\tau,t,ii} > v_{\tau,t,ij} + \varepsilon_{\tau,t,ij} - \varepsilon_{\tau,t,ii},\ \forall j \neq j^*\right), \\ &= Prob\ \left(\varepsilon_{\tau,t,ij^*} + v_{\tau,t,ij^*} - v_{\tau,t,ij} > \varepsilon_{\tau,t,ij},\quad \forall j \neq j^*\right). \end{aligned}$$

Conditional on $\varepsilon_{\tau,t,ij^*}$, the probability that location j^* is chosen by worker τ is given by

$$Prob\ (j^* \text{ is chosen}\ |\varepsilon_{\tau,t,ij^*}) = \prod_{j \neq j^*} F\left(\varepsilon_{\tau,t,ij^*} + v_{\tau,t,ij^*} - v_{\tau,t,ij}\right).$$

Since $\varepsilon_{\tau,t,ij^*}$ is also random, the probability that location j^* is chosen is the integral of $Prob\ (j^* \text{ is chosen}\ |\varepsilon_{\tau,t,ij^*})$ over its support and weighted by its density function, namely

$$\begin{aligned} Prob\ (j^* \text{ is chosen}) &= \int_{-\infty}^{+\infty} \left[\prod_{j \neq j^*} e^{-e^{-\left(\varepsilon + v_{\tau,t,ij^*} - v_{\tau,t,ij}\right)}}\right] e^{-\varepsilon}e^{-e^{-\varepsilon}} d\varepsilon \\ &= \int_{-\infty}^{+\infty} \left[\prod_{j \neq j^*} e^{-e^{-\left(\varepsilon + v_{\tau,t,ij^*} - v_{\tau,t,ij}\right)}}\right] e^{-\varepsilon}e^{-e^{-\left(\varepsilon + v_{\tau,t,ij^*} - v_{\tau,t,ij^*}\right)}} d\varepsilon \\ &= \int_{-\infty}^{+\infty} \left[\prod_{j} e^{-e^{-\left(\varepsilon + v_{\tau,t,ij^*} - v_{\tau,t,ij}\right)}}\right] e^{-\varepsilon} d\varepsilon \\ &= \int_{-\infty}^{+\infty} exp\left[-e^{-\varepsilon}\sum_{j} e^{-\left(v_{\tau,t,ij^*} - v_{\tau,t,ij}\right)}\right] e^{-\varepsilon} d\varepsilon. \end{aligned}$$

Define $s = e^{-\varepsilon}$. Thus, $ds = -e^{-\varepsilon} d\varepsilon$. Then,

$$
\begin{aligned}
Prob\ (j^* \text{ is chosen}) &= \int_0^{+\infty} exp\left[-s \sum_j e^{-\left(v_{\tau,t,ij*} - v_{\tau,t,ij}\right)}\right] ds \\
&= -\left.\frac{exp\left[-s \sum_j e^{-\left(v_{\tau,t,ij*} - v_{\tau,t,ij}\right)}\right]}{\sum_j e^{-\left(v_{\tau,t,ij*} - v_{\tau,t,ij}\right)}}\right|_0^{+\infty} \\
&= \frac{1}{\sum_j e^{-\left(v_{\tau,t,ij*} - v_{\tau,t,ij}\right)}} = \frac{e^{v_{\tau,t,ij*}}}{\sum_j e^{v_{\tau,t,ij}}}.
\end{aligned}
$$

A.2 Balanced growth paths

The long run rent-to-price ratio in location i can be obtained using (60):

$$\frac{q_i^*}{p_i^*} = \Gamma_i, \tag{A.1}$$

where Γ_i is defined as

$$\Gamma_i = \frac{1}{\beta\left(1-\theta_i\right)} - (1-\delta). \tag{A.2}$$

Using this result in (59), we obtain the long-run demand function for housing in location i:

$$h_i^* = \frac{\eta w_i^* l_{\cdot i}^*}{\Gamma_i p_i^*}. \tag{A.3}$$

By substituting (57) into (58), we obtain the long-run housing supply function in location i:

$$h_i^* = \delta^{-1} \tau_i \kappa_i (w_i^*)^{-\frac{\alpha_l(1-\alpha_{\kappa,i})}{\alpha_{\kappa,i}}} (p_i^*)^{\frac{1-\alpha_{\kappa,i}}{\alpha_{\kappa,i}}}. \tag{A.4}$$

By substituting (A.4) into (A.3) for h_i^*, we have

$$\delta^{-1} \tau_i \kappa_i (w_i^*)^{-\frac{\alpha_l(1-\alpha_{\kappa,i})}{\alpha_{\kappa,i}}} (p_i^*)^{\frac{1-\alpha_{\kappa,i}}{\alpha_{\kappa,i}}} = \frac{\eta w_i^* l_{\cdot i}^*}{\Gamma_i p_i^*}.$$

Using the above equation, we can solve for p_i^*

$$p_i^* = \left(\frac{\delta\eta}{\tau_i \kappa_i}\right)^{\alpha_{\kappa,i}} \Gamma_i^{-\alpha_{\kappa,i}} \left(l_{\cdot i}^*\right)^{\alpha_{\kappa,i}} \left(w_i^*\right)^{\alpha_{\kappa,i} + \alpha_l(1-\alpha_{\kappa,i})}, \tag{A.5}$$

and by substituting (A.5) into (A.1) for p_i^*, we have

$$q_i^* = \left(\frac{\delta\eta}{\tau_i \kappa_i}\right)^{\alpha_{\kappa,i}} \Gamma_i^{1-\alpha_{\kappa,i}} \left(l_{\cdot i}^*\right)^{\alpha_{\kappa,i}} \left(w_i^*\right)^{\alpha_{\kappa,i} + \alpha_l(1-\alpha_{\kappa,i})}. \tag{A.6}$$

Finally, substituting (A.5) into (A.4) for p_i^*, we obtain

$$h_i^* = \left(\frac{\delta}{\tau_i \kappa_i}\right)^{-\alpha_{\kappa,i}} \left(\frac{\eta}{\Gamma_i}\right)^{1-\alpha_{\kappa,i}} \left(l_{\cdot i}^*\right)^{1-\alpha_{\kappa,i}} \left(w_i^*\right)^{(1-\alpha_l)(1-\alpha_{\kappa,i})}. \tag{A.7}$$

A.3 Lemmas: statements and proofs

Lemma A1 *Consider the following Markovian process in* $\boldsymbol{l}^*(t)$

$$\boldsymbol{l}^*(t) = \boldsymbol{l}^*(t-1)\mathbf{R}^*(t) \tag{A.8}$$

where $\boldsymbol{l}^*(t) = [l^*_{\cdot 1}(t), l^*_{\cdot 2}(t), ..., l^*_{\cdot n}(t)]$ *is the* $1 \times n$ *row vector of detrended population values, and* $\mathbf{R}^*(t) = (\rho^*_{ij}(t))$ *is the* $n \times n$ *transition matrix with the typical element,* $\rho^*_{ij}(t)$ *defined by (51) that depends non-linearly on* $\boldsymbol{l}^*(t)$*, and* n *is a fixed integer. Suppose that the initial population vector,* $\boldsymbol{l}^*(0) = \boldsymbol{l}(0)$*, is given and satisfies the conditions* $\boldsymbol{l}(0) > 0$*, and* $\sum_{i=1}^n l_{\cdot i}(0) = L_0$*, where* $0 < L_0 < K$*. Then* $\boldsymbol{l}^*(t)$ *converges to a finite population vector,* $\boldsymbol{l}^*(\infty)$*, or simply* $\boldsymbol{l}^* = [l^*_{\cdot 1}, l^*_{\cdot 2}, ..., l^*_{\cdot n}]$*, as* $t \to \infty$*, with* $l^*_{\cdot i} \geq 0$*, and* $\sum_{i=1}^n l^*_{\cdot i} = L_0$

Proof: We first note that by construction $0 \leq \rho^*_{ij}(t) \leq 1$ for all i and j, and $\sum_{j=1}^n \rho^*_{ij}(t) = 1$, for all j. Hence, for each t, $\mathbf{R}^*(t)$ is a right stochastic matrix with $\mathbf{R}^*(t)\boldsymbol{\tau}_n = \boldsymbol{\tau}_n$, where $\boldsymbol{\tau}_n$ is an $n \times 1$ vector of ones, for all t. Recursively solving (A.8) forward from $\boldsymbol{l}^*(0)$, we have

$$\boldsymbol{l}^*(t) = \boldsymbol{l}^*(0)\left[\Pi_{s=1}^t \mathbf{R}^*(s)\right],$$

But it is easily seen that $[\Pi_{s=1}^t \mathbf{R}^*(s)]\boldsymbol{\tau}_n = \boldsymbol{\tau}_n$, and hence

$$\sum_{i=1}^n l^*_{\cdot i}(t) = \boldsymbol{l}^*(t)\boldsymbol{\tau}_n = \boldsymbol{l}^*(0)\boldsymbol{\tau}_n = L_0. \tag{A.9}$$

Also, since $\boldsymbol{l}^*(0) = \boldsymbol{l}(0) > 0$, $\rho^*_{ij}(t) \geq 0$, and n is finite, then $\boldsymbol{l}^*(t) = [l^*_{\cdot 1}(t), l^*_{\cdot 2}(t), ..., l^*_{\cdot n}(t)] \geq 0$, for all t, and in view of (A.9) we have $\sup_{it}(l^*_{\cdot i}(t)) \leq L_0 < K$. Therefore, $\boldsymbol{l}^*(t)$ must converge to some vector $\boldsymbol{l}^*$ which is bounded in t, as $t \to \infty$. ■

Lemma A2 *Consider the system of non-linear equations in* $l_{\cdot i}$*, for* $i \in \mathcal{I}_n$*:*

$$\boldsymbol{l} = \boldsymbol{l}\mathbf{R}(\boldsymbol{l}) \tag{A.10}$$

where $\boldsymbol{l} = [l_{\cdot 1}, l_{\cdot 2}, ..., l_{\cdot n}]$, $\boldsymbol{l} \geq 0$, $\sum_{i=1}^n l_{\cdot i} = L_0$, $0 < L_0 < K$, *n is fixed, and the typical element of matrix* $\mathbf{R}$ *is given by*

$$\rho_{ij} = \frac{\psi_{ij}(l_{\cdot j})^{-\varphi_j}}{\sum_{s \in \mathcal{I}_n} \psi_{is}(l_{\cdot s})^{-\varphi_s}}, \tag{A.11}$$

where ψ_{ij} *and* $\varphi_j > 0$*, for any* i *and* $j \in \mathcal{I}_n$*. Then, the solution to (A.10) must be strictly positive,* $l_{\cdot i} > 0$ *for* $i \in \mathcal{I}_n$*, and unique.*

Proof. We first show that $l_{\cdot i} > 0$, and hence $1 > \rho_{ij} > 0$, for all i and $j \in \mathcal{I}_n$. Consider a population vector $\boldsymbol{l}$ that solves (A.10). Note that $\sum_{i=1}^n l_{\cdot i} > 0$, and $l_{\cdot i}$ is non-negative for any $i \in \mathcal{I}_n$. Thus, $l_{\cdot i} > 0$ has to hold for at least one i. Without loss of generality, we assume

$$l_{\cdot 1} > 0. \tag{A.12}$$

Note also that since $l_{\cdot 1}$ is the first element in $\boldsymbol{l}$, then from (A.10) we have

$$l_{\cdot 1} = \sum_{i=1}^{n} \rho_{i1} l_{\cdot i}, \tag{A.13}$$

where, upon using (A.11), ρ_{i1} is given by

$$\rho_{i1} = \frac{1}{1 + \sum_{s \neq i} \left(\frac{\psi_{is}}{\psi_{i1}} \right) \frac{(l_{\cdot 1})^{\varphi_1}}{(l_{\cdot s})^{\varphi_s}}}, \text{ for } i = 1, 2, ..., n. \tag{A.14}$$

Note that by assumption ψ_{ij} and $\varphi_j > 0$, and it is supposed that $l_{\cdot 1} > 0$. Hence, if $l_{\cdot s} = 0$, for any $s \in \{2, 3, ..., n\}$, then $\rho_{i1} = 0$, for all $i \in \mathcal{I}_n$, and using (A.13) it follows that $l_{\cdot 1} = 0$, which contradicts our supposition. The same line of reasoning can be applied to any other elements of $\boldsymbol{l}$, and we must have $l_{\cdot i} > 0$, for any $i \in \mathcal{I}_n$.

Given that $l_{\cdot i} > 0$, for all i, we now show that (A.10) cannot have more than one solution. Suppose there exist two solutions $\boldsymbol{l}^{(1)}$ and $\boldsymbol{l}^{(2)}$, with $\boldsymbol{l}^{(1)}$ and $\boldsymbol{l}^{(2)} > 0$, $\boldsymbol{l}^{(1)} \neq \boldsymbol{l}^{(2)}$, such that $\boldsymbol{l}^{(1)} = \boldsymbol{l}^{(1)} \boldsymbol{R}\left(\boldsymbol{l}^{(1)}\right)$ and $\boldsymbol{l}^{(2)} = \boldsymbol{l}^{(2)} \boldsymbol{R}\left(\boldsymbol{l}^{(2)}\right)$. Denote the j^{th} elements of $\boldsymbol{l}^{(1)}$ and $\boldsymbol{l}^{(2)}$ by $l_{\cdot j}^{(1)}$ and $l_{\cdot j}^{(2)}$, respectively. Split the locations into two groups, $\mathcal{I}_n^+$ and $\mathcal{I}_n^-$, where $\mathcal{I}_n^+ \equiv \{j \mid l_{\cdot j}^{(2)} > l_{\cdot j}^{(1)}, j \in \mathcal{I}_n\}$, and $\mathcal{I}_n^- \equiv \{j \mid l_{\cdot j}^{(2)} \leq l_{\cdot j}^{(1)}, j \in \mathcal{I}_n\}$, and note that $\mathcal{I}_n^+ \cap \mathcal{I}_n^- = \emptyset$ and $\mathcal{I}_n^+ \cup \mathcal{I}_n^- = \mathcal{I}_n$. That is,

$$l_{\cdot j}^{(2)} \begin{cases} > l_{\cdot j}^{(1)} & \text{if } j \in \mathcal{I}_n^+ \\ \leq l_{\cdot j}^{(1)} & \text{if } j \in \mathcal{I}_n^- \end{cases}. \tag{A.15}$$

Further, since $\sum_{j=1}^{n} l_j^{(1)} = \sum_{j=1}^{n} l_j^{(2)} = L_0$, and $\boldsymbol{l}^{(1)} \neq \boldsymbol{l}^{(2)}$, it also follows that neither $\mathcal{I}_n^+$ nor $\mathcal{I}_n^-$ can be empty. Thus, we have

$$\sum_{j \in \mathcal{I}_n^+} l_{\cdot j}^{(2)} > \sum_{j \in \mathcal{I}_n^+} l_{\cdot j}^{(1)}. \tag{A.16}$$

Recall that $\rho_{ij}^{(1)}$ and $\rho_{ij}^{(2)}$ are the typical elements of $\boldsymbol{R}\left(\boldsymbol{l}^{(1)}\right)$ and $\boldsymbol{R}\left(\boldsymbol{l}^{(2)}\right)$, respectively. For any $i \in \mathcal{I}_n$, using (A.11), we have (recall that $l_{\cdot j}^{(1)} > 0$ and $l_{\cdot j}^{(2)} > 0$)

$$\frac{\sum_{j \in \mathcal{I}_n^+} \rho_{ij}^{(2)}}{\sum_{j \in \mathcal{I}_n^-} \rho_{ij}^{(2)}} = \frac{\sum_{j \in \mathcal{I}_n^+} \psi_{ij} \left(l_{\cdot j}^{(2)}\right)^{-\varphi_j}}{\sum_{j \in \mathcal{I}_n^-} \psi_{ij} \left(l_{\cdot j}^{(2)}\right)^{-\varphi_j}}, \tag{A.17}$$

$$\frac{\sum_{j \in \mathcal{I}_n^+} \rho_{ij}^{(1)}}{\sum_{j \in \mathcal{I}_n^-} \rho_{ij}^{(1)}} = \frac{\sum_{j \in \mathcal{I}_n^+} \psi_{ij} \left(l_{\cdot j}^{(1)}\right)^{-\varphi_j}}{\sum_{j \in \mathcal{I}_n^-} \psi_{ij} \left(l_{\cdot j}^{(1)}\right)^{-\varphi_j}}. \tag{A.18}$$

Since by (A.15), $l_{\cdot j}^{(2)} > l_{\cdot j}^{(1)}$, if $j \in \mathcal{I}_n^+$, and $l_{\cdot j}^{(2)} \leq l_{\cdot j}^{(1)}$, if $j \in \mathcal{I}_n^-$, then (recall that $\psi_{ij} > 0$ and $\varphi_j > 0$)

$$
\begin{aligned}
\sum_{j \in \mathcal{I}_n^+} \psi_{ij} \left(l_{\cdot j}^{(2)} \right)^{-\varphi_j} &< \sum_{j \in \mathcal{I}_n^+} \psi_{ij} \left(l_{\cdot j}^{(1)} \right)^{-\varphi_j}, \\
\sum_{j \in \mathcal{I}_n^-} \psi_{ij} \left(l_{\cdot j}^{(2)} \right)^{-\varphi_j} &\geq \sum_{j \in \mathcal{I}_n^-} \psi_{ij} \left(l_{\cdot j}^{(1)} \right)^{-\varphi_j}.
\end{aligned}
$$

Hence, using the above results in (A.17) and (A.18) we have

$$
\frac{\sum_{j \in \mathcal{I}_n^+} \rho_{ij}^{(2)}}{\sum_{j \in \mathcal{I}_n^-} \rho_{ij}^{(2)}} < \frac{\sum_{j \in \mathcal{I}_n^+} \rho_{ij}^{(1)}}{\sum_{j \in \mathcal{I}_n^-} \rho_{ij}^{(1)}}, \qquad \forall\, i \in \mathcal{I}_n,
$$

and it follows that

$$
\frac{\sum_{j \in \mathcal{I}_n^+} \rho_{ij}^{(2)} + \sum_{j \in \mathcal{I}_n^-} \rho_{ij}^{(2)}}{\sum_{j \in \mathcal{I}_n^+} \rho_{ij}^{(2)}} > \frac{\sum_{j \in \mathcal{I}_n^+} \rho_{ij}^{(1)} + \sum_{j \in \mathcal{I}_n^-} \rho_{ij}^{(1)}}{\sum_{j \in \mathcal{I}_n^+} \rho_{ij}^{(1)}}, \qquad \forall\, i \in \mathcal{I}_n.
$$

Since $\rho_{ij}^{(1)}$ and $\rho_{ij}^{(2)}$ are migration probabilities,

$$
\sum_{j \in \mathcal{I}_n^+} \rho_{ij}^{(2)} + \sum_{j \in \mathcal{I}_n^-} \rho_{ij}^{(2)} = \sum_{j \in \mathcal{I}_n^+} \rho_{ij}^{(1)} + \sum_{j \in \mathcal{I}_n^-} \rho_{ij}^{(1)} = 1.
$$

Thus, we have

$$
\sum_{j \in \mathcal{I}_n^+} \rho_{ij}^{(2)} < \sum_{j \in \mathcal{I}_n^+} \rho_{ij}^{(1)}, \qquad \forall\, i \in \mathcal{I}_n. \tag{A.19}
$$

Note that $l_{\cdot j}^{(1)}$ and $l_{\cdot j}^{(2)}$ are given by

$$
l_{\cdot j}^{(1)} = \sum_{i \in \mathcal{I}_n} \rho_{ij}^{(1)} l_{\cdot i}^{(1)} \qquad \text{and} \qquad l_{\cdot j}^{(2)} = \sum_{i \in \mathcal{I}_n} \rho_{ij}^{(2)} l_{\cdot i}^{(2)}.
$$

Thus, we have

$$
\begin{aligned}
\sum_{j \in \mathcal{I}_n^+} l_{\cdot j}^{(2)} - \sum_{j \in \mathcal{I}_n^+} l_{\cdot j}^{(1)} &= \sum_{j \in \mathcal{I}_n^+} \sum_{i \in \mathcal{I}_n} \rho_{ij}^{(2)} l_{\cdot i}^{(2)} - \sum_{j \in \mathcal{I}_n^+} \sum_{i \in \mathcal{I}_n} \rho_{ij}^{(1)} l_{\cdot i}^{(1)}, \\
&= \sum_{i \in \mathcal{I}_n} l_{\cdot i}^{(2)} \sum_{j \in \mathcal{I}_n^+} \rho_{ij}^{(2)} - \sum_{i \in \mathcal{I}_n} l_{\cdot i}^{(1)} \sum_{j \in \mathcal{I}_n^+} \rho_{ij}^{(1)}.
\end{aligned}
$$

Since $\sum_{j \in \mathcal{I}_n^+} \rho_{ij}^{(2)} < \sum_{j \in \mathcal{I}_n^+} \rho_{ij}^{(1)}$ as previously shown in (A.19), then

$$
\begin{aligned}
\sum_{j \in \mathcal{I}_n^+} l_{\cdot j}^{(2)} - \sum_{j \in \mathcal{I}_n^+} l_{\cdot j}^{(1)} &< \sum_{i \in \mathcal{I}_n} l_{\cdot i}^{(2)} \sum_{j \in \mathcal{I}_n^+} \rho_{ij}^{(1)} - \sum_{i \in \mathcal{I}_n} l_{\cdot i}^{(1)} \sum_{j \in \mathcal{I}_n^+} \rho_{ij}^{(1)}, \\
&= \sum_{i \in \mathcal{I}_n} \left[\left(l_{\cdot i}^{(2)} - l_{\cdot i}^{(1)} \right) \sum_{j \in \mathcal{I}_n^+} \rho_{ij}^{(1)} \right].
\end{aligned} \tag{A.20}
$$

Since by (A.15), $l_{\cdot i}^{(2)} > l_{\cdot i}^{(1)}$, if $i \in \mathcal{I}_n^+$, and $l_{\cdot i}^{(2)} \leq l_{\cdot i}^{(1)}$, if $i \in \mathcal{I}_n^-$, and $\sum_{j\in\mathcal{I}_n^+} \rho_{ij}^{(1)} > 0$ by construction, then

$$\begin{aligned} & \sum_{i\in\mathcal{I}_n} \left[\left(l_{\cdot i}^{(2)} - l_{\cdot i}^{(1)} \right) \sum_{j\in\mathcal{I}_n^+} \rho_{ij}^{(1)} \right] \\ = & \sum_{i\in\mathcal{I}_n^+} \left[\left(l_{\cdot i}^{(2)} - l_{\cdot i}^{(1)} \right) \sum_{j\in\mathcal{I}_n^+} \rho_{ij}^{(1)} \right] + \sum_{i\in\mathcal{I}_n^-} \left[\left(l_{\cdot i}^{(2)} - l_{\cdot i}^{(1)} \right) \sum_{j\in\mathcal{I}_n^+} \rho_{ij}^{(1)} \right], \\ < & \sum_{i\in\mathcal{I}_n^+} \left[\left(l_{\cdot i}^{(2)} - l_{\cdot i}^{(1)} \right) \sum_{j\in\mathcal{I}_n^+} \rho_{ij}^{(1)} \right]. \end{aligned}$$

Note that $\rho_{ij}^{(1)}$ are migration probabilities, and $\sum_{j\in\mathcal{I}_n^+} \rho_{ij}^{(1)} < 1$ by construction, and that $l_{\cdot i}^{(2)} - l_{\cdot i}^{(1)} > 0$, if $i \in \mathcal{I}_n^+$. Then, we have

$$\sum_{i\in\mathcal{I}_n^+} \left[\left(l_{\cdot i}^{(2)} - l_{\cdot i}^{(1)} \right) \sum_{j\in\mathcal{I}_n^+} \rho_{ij}^{(1)} \right] < \sum_{i\in\mathcal{I}_n^+} \left(l_{\cdot i}^{(2)} - l_{\cdot i}^{(1)} \right),$$

and thus

$$\sum_{i\in\mathcal{I}_n} \left[\left(l_{\cdot i}^{(2)} - l_{\cdot i}^{(1)} \right) \sum_{j\in\mathcal{I}_n^+} \rho_{ij}^{(1)} \right] < \sum_{i\in\mathcal{I}_n^+} l_{\cdot i}^{(2)} - \sum_{i\in\mathcal{I}_n^+} l_{\cdot i}^{(1)},$$

which contradicts (A.20). Thus, $\boldsymbol{l} \neq \boldsymbol{l}^*$ cannot hold.■

A.4 Derivation of new land supplies, κ_{it}

To derive (80), we first note that (22) can be re-written as

$$h_{i,t-1} = \eta \left(\frac{w_{it}}{q_{it}} \right) l_{\cdot i}(t). \tag{A.21}$$

By using the above equation in (35) to eliminate $h_{i,t-1}$, we have

$$h_{it} = \beta e^{g_l} (1 - \theta_i) \left[\frac{q_{it}}{p_{it}} + (1 - \delta) \right] \eta \left(\frac{w_{it}}{q_{it}} \right) l_{\cdot i}(t) \tag{A.22}$$

Then, by using (A.21) and (A.22) in (37), we have

$$\begin{aligned} x_{it} &= h_{it} - (1-\delta) h_{i,t-1}, \\ &= \left\{ \beta e^{g_l} (1 - \theta_i) \left[\frac{q_{it}}{p_{it}} + (1 - \delta) \right] - (1 - \delta) \right\} \eta \left(\frac{w_{it}}{q_{it}} \right) l_{\cdot i}(t). \end{aligned}$$

By combing the above equation with (28), we have

$$\kappa_{it} = \frac{x_{it}}{\tau_i \left(w_{it}\right)^{-\alpha_l(1-\alpha_{\kappa,i})/\alpha_{\kappa,i}} \left(p_{it}\right)^{(1-\alpha_{\kappa,i})/\alpha_{\kappa,i}}} = \frac{\gamma_{it}}{\tau_i},$$

where

$$\gamma_{it} = \frac{\left\{\beta e^{g_l}\left(1-\theta_i\right)\left[\frac{q_{it}}{p_{it}} + (1-\delta)\right] - (1-\delta)\right\}\eta\left(\frac{w_{it}}{q_{it}}\right) l_{\cdot i}(t)}{\left(w_{it}\right)^{-\alpha_l(1-\alpha_{\kappa,i})/\alpha_{\kappa,i}} \left(p_{it}\right)^{(1-\alpha_{\kappa,i})/\alpha_{\kappa,i}}}.$$

B Data sources and measurements

B.1 Interstate migration and population growth

Between states migration flows are measured using annual data from the Internal Revenue Service (IRS).[A1] The IRS compiles state-to-state migration data using year-to-year address changes reported on individual income tax returns filed with the IRS, which are available from 1990 to 2014.[A2] Those who file income tax returns with the IRS in two consecutive years in the same state are considered as non-migrants, and migrants otherwise. State level population for 1976-1990 are obtained from Census data.[A3] We focus on the 48 states and the District of Columbia on the U.S. mainland, and treat Alaska and Hawaii as "foreign countries" in our analysis.

B.1.1 Population growth rates by states

For the years 1990-2014, we compute migration flows and the intrinsic population growth rates of U.S. states using the IRS state-to-state migration flow data. Migrants are considered as the residents of the destination states for the year they migrate.[A4] Thus, the population of State j in year t is measured as the number of tax filers (and their dependents) who report a home address in State j at the start of year $t+1$ as recorded by the IRS for the period from t to $t+1$. We decompose the population changes of U.S. states into an intrinsic component (due to births and deaths) and a net inward migration component. Let

$$l_{i\cdot}(t) \equiv \sum_{j=1}^{n} l_{ij}(t), \text{ and } l_{\cdot j}(t) \equiv \sum_{i=1}^{n} l_{ij}(t), \tag{A.23}$$

where for $i \neq j$, $l_{ij}(t)$ denotes the population flow from State i to State j in year t, measured using the IRS data (see also (1) and (2)). The number that remain in State i is denoted by

[A1] For further information on the IRS migration flow data, see `https://www.irs.gov/uac/soi-tax-stats-migration-data`.

[A2] The total number of exemptions recorded by the IRS each year is around 80% of the U.S. population.

[A3] For further information on the Census population data, see `https://www.census.gov/topics/population.html`.

[A4] For example, suppose a person files income tax returns with the IRS at the starts of year t and year $t+1$, and the two addresses reported are in State i and State j respectively. If $i = j$, this person is considered as a resident in State j in year t. However, if $i \neq j$, the time she migrates to State j can be any point between the starts of year t and year $t+1$. In our analysis, we consider this person as a resident in State j for year t.

$l_{ii}(t)$. $l_{i\cdot}(t) - l_{ii}(t)$ measures the outward migration from State i, and $l_{\cdot i}(t) - l_{ii}(t)$, measures the inward migration to State i. The change in population of State i in period t, defined by $l_{\cdot i}(t) - l_{\cdot i}(t-1)$ can now be decomposed as:

$$l_{\cdot i}(t) - l_{\cdot i}(t-1) = [l_{\cdot i}(t) - l_{i\cdot}(t)] + [l_{i\cdot}(t) - l_{\cdot i}(t-1)]\,. \tag{A.24}$$

where the first component $l_{\cdot i}(t) - l_{i\cdot}(t)$ is the net inward migration to State i, and the reminder term, $l_{i\cdot}(t) - l_{\cdot i}(t-1)$, which we refer to as the intrinsic population change of State i. We decompose the population growths at both state and regional levels using the above formula. At the regional level, the Southeast and the Southwest have been attracting population from the rest of the country, while the West, the Midwest, and especially the Northeast have experienced substantial population outflows, as shown in Figure 13. For the five most populated states in the U.S., Florida and Texas have experienced considerable population inflows, while New York and California have experienced substantial population outflows, as shown in Figure 14.

In addition, the actual state level intrinsic population growth rates, $\hat{g}_{l,1t}$, for $i = 1, 2, ..., n$, are measured as

$$\hat{g}_{l,it} = \frac{l_{\cdot i}(t) - l_{\cdot i}(t-1)}{\sum_{i=1}^{n} l_{\cdot i}(t-1)} \tag{A.25}$$

For the period of 1976-1990, state level populations are measured using Census population data, which are scaled such that their 1990 values match those implied by the IRS migration flow data. The intrinsic population growth rates of U.S. states during this period are inferred using the migration equation (6), which can be re-written as

$$\boldsymbol{l}(t-1)\mathbf{G}(t)\mathbf{R}(t) = \boldsymbol{l}(t).$$

Note that $\mathbf{R}(t)$, which is a stochastic matrix, is invertible. Thus, we have

$$\boldsymbol{l}(t-1)\mathbf{G}(t) = \boldsymbol{l}(t)\mathbf{R}(t)^{-1}.$$

By right multiplying both sides of the above equation by a $n \times n$ identity matrix, $\mathbf{I}_n$, we have

$$\boldsymbol{l}(t-1)\mathbf{G}(t)\mathbf{I}_n = \boldsymbol{l}(t)\mathbf{R}(t)^{-1}\mathbf{I}_n \Rightarrow \mathbf{diag}\left(\boldsymbol{l}(t-1)\mathbf{G}(t)\right) = \mathbf{diag}\left(\boldsymbol{l}(t)\mathbf{R}(t)^{-1}\right)$$

Recall that $\mathbf{G}(t) = \mathbf{diag}\left(g_{l,1t}, g_{l,2t}, ..., g_{l,nt}\right)$, is a diagonal matrix, and $\boldsymbol{l}(t-1)$ is a $1 \times n$ row vector. Thus, $\mathbf{diag}\left(\boldsymbol{l}(t-1)\mathbf{G}(t)\right) = \mathbf{diag}\left(\boldsymbol{l}(t-1)\right)\mathbf{G}(t)$. Thus, we have

$$\mathbf{diag}\left(\boldsymbol{l}(t-1)\right)\mathbf{G}(t) = \mathbf{diag}\left(\boldsymbol{l}(t)\mathbf{R}(t)^{-1}\right),$$

which implies

$$\mathbf{G}(t) = \left[\mathbf{diag}\left(\boldsymbol{l}(t-1)\right)\right]^{-1}\mathbf{diag}\left(\boldsymbol{l}(t)\mathbf{R}(t)^{-1}\right).$$

Thus, the matrix of state level intrinsic population growth rates, $\mathbf{G}(t)$, is estimated as

$$\hat{\mathbf{G}}(t) = \left[\mathbf{diag}\left(\boldsymbol{l}(t-1)\right)\right]^{-1}\mathbf{diag}\left(\boldsymbol{l}(t)\hat{\mathbf{R}}(t)^{-1}\right), \tag{A.26}$$

where $\hat{\mathbf{G}}(t) = \mathbf{diag}\left(\hat{g}_{l,1t}, \hat{g}_{l,2t}, ..., \hat{g}_{l,nt}\right)$ contains the estimates of state level intrinsic population growth rates, the state-level populations, $\boldsymbol{l}(t)$, are measured using Census data, and the migration probability matrix, $\mathbf{R}(t) = (\rho_{ij,t})$, is estimated using the migration probability equation (15):

$$\hat{\rho}_{ij,t} = \frac{\hat{\alpha}_{ij}^{-\psi}\left(q_{jt}/q_{it}\right)^{-\eta}\left(w_{jt}/w_{it}\right)}{\sum_{s=1}^{n} \hat{\alpha}_{is}^{-\psi}\left(q_{st}/q_{it}\right)^{-\eta}\left(w_{st}/w_{it}\right)},$$

where ψ was set to one and the migration costs, α_{ij}, were estimated in Section 5.2, and the incomes, w_{it}, and the annual housing rents, q_{it}, are from data.

B.1.2 Distance and population mobility

We now consider how the size of migration varies with the distance between origin and destination of the migration flows. The distance between two states is measured as the distance between their centers of population that are defined by Census.[A5] States that are within the x mile radius of State i are called the x-mile-neighbors of State i. Let $\mathcal{I}_i(x)$ be the collection of the indices of the x-mile-neighbors of State i. The number of migrants who migrate from State i to its x-mile-neighbors is denoted by $\mathfrak{m}_i(x)$. Thus, the share of migrants of State i who move to its x-mile-neighbors, denoted by $\pi_{it}(x)$, is given by

$$\pi_{it}(x) = \frac{\mathfrak{m}_{it}(x)}{\mathfrak{m}_{it}(\infty)}, \tag{A.27}$$

where $\mathfrak{m}_{it}(\infty)$ is the total number of migrants from State i in year t. Then, at the national level, the share of migrants who move to the x-mile-neighbor of the originating states is given by

$$\pi_t(x) = \frac{\sum_{i=1}^{n} \mathfrak{m}_{it}(x)}{\sum_{i=1}^{n} \mathfrak{m}_{it}(\infty)}. \tag{A.28}$$

Figure 15 plots the average of $\pi_t(x)$ over the 1990-2014 period against x, along with the 5 and 95 per cent quantile bands. As the figure shows, around 70% of the U.S. migrants move to a 1000-mile-neighbor of the originating states.

As an alternative measure, we also consider adjacency as the definition of neighborhood. A state is an *order-1* neighbor of State i if it is geographically adjacent to State i. A state is an *order-2* neighbor of State i if it is geographically adjacent to State i itself or its *order-1* neighbors. For example, Nevada is an order-1 neighbor of California, Utah is an order-1 neighbor of Nevada, and Utah is in an order-2 neighbor of California. As shown in Table 5, during 1990-2014, 50% of the U.S. migrants move to *order-2* neighbor of the originating states.

[A5] For further details about the definitions of population centers, see `https://www.census.gov/geo/reference/centersofpop.html`.

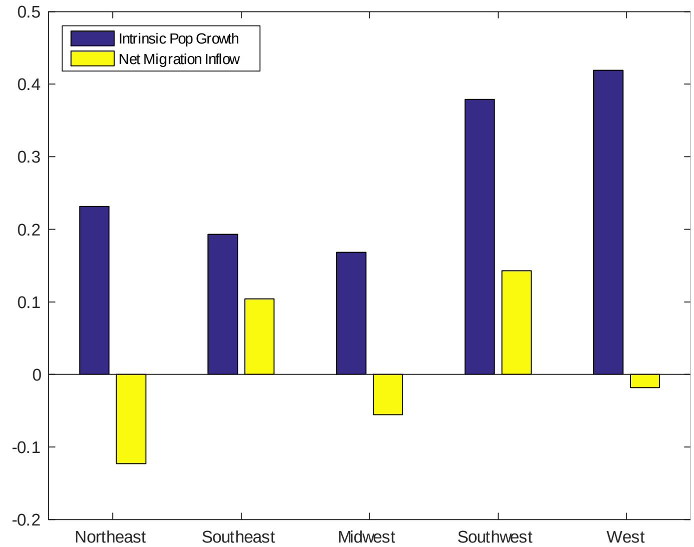

Figure 13: Decomposition of regional population growth during 1990-2014

Notes: This figure shows the decomposition of the cumulative population growth rates of U.S. regions during 1990-2014. The cumulative population growth rate of each region is decomposed into two parts: (1) the cumulative intrinsic population growth rate (blue bar) and (2) the ratio of the cumulative net migration inflow to the initial population (yellow bar).

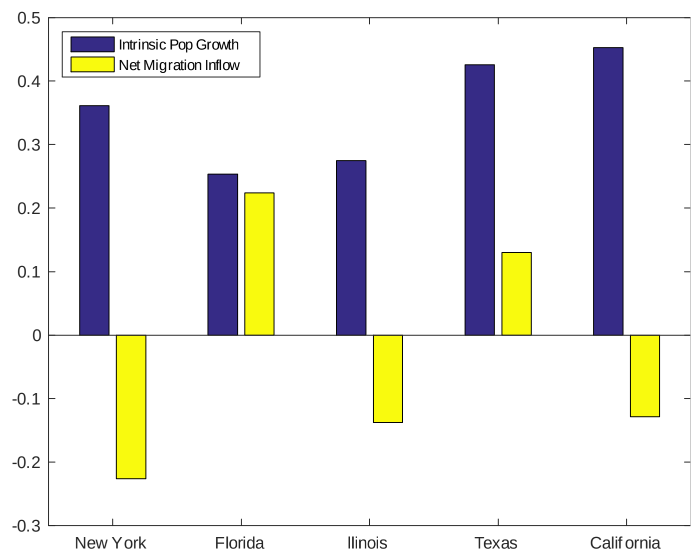

Figure 14: Decomposition of population growth for selected U.S. states during 1990-2014

Notes: This figure shows the decomposition of the cumulative population growth rates of NY, FL, IL, TX and CA during 1990-2014. The cumulative population growth rate of each State is decomposed into two parts: (1) the cumulative intrinsic population growth rate (blue bar) and (2) the ratio of the cumulative net migration inflow to the initial population (yellow bar).

Year		distance (miles) less than				adjacency	
		500	1000	1500		order-1	order-2
1990		43.36%	71.54%	86.30%		33.02%	49.82%
1991		43.27%	71.59%	86.13%		33.06%	49.94%
1992		43.16%	71.65%	86.03%		33.10%	50.12%
1993		43.50%	71.78%	86.15%		33.36%	50.34%
1994		43.49%	71.85%	86.28%		33.09%	50.10%
1995		43.79%	72.17%	86.37%		33.23%	50.37%
1996		44.04%	72.12%	86.29%		33.31%	50.31%
1997		44.03%	72.05%	86.29%		33.35%	50.29%
1998		44.53%	72.32%	86.37%		33.73%	50.66%
1999		44.42%	72.15%	86.17%		33.69%	50.57%
2000		44.03%	71.64%	85.92%		33.50%	50.19%
2001		44.06%	71.54%	86.07%		33.63%	50.13%
2002		44.29%	71.65%	86.11%		33.85%	50.27%
2003		44.06%	71.48%	86.14%		33.81%	50.03%
2004		43.79%	71.27%	86.15%		33.51%	49.68%
2005		44.38%	71.68%	86.34%		33.87%	50.12%
2006		43.94%	71.60%	86.27%		33.22%	49.84%
2007		43.76%	71.50%	86.03%		33.11%	49.68%
2008		43.36%	71.27%	85.88%		32.94%	49.52%
2009		42.94%	71.04%	85.85%		32.67%	49.18%
2010		42.67%	70.78%	85.65%		32.31%	48.78%
2011		41.98%	70.30%	85.56%		32.06%	48.13%
2012		41.50%	69.94%	85.44%		31.72%	47.78%
2013		41.19%	69.87%	85.70%		31.51%	47.57%
2014		41.57%	70.12%	86.12%		32.44%	48.03%
1990-2014		43.40%	71.40%	86.06%		33.08%	49.66%

Table 5: Patterns of migration of different distance categories

Notes: The first three columns show the shares of the U.S. migrants to states within 500 miles, 1000 miles, and 1500 miles of the states from which migrants originated. The last two columns show the shares of the U.S. migrants who move to an order-1 and order-2 neighbor of the origin states.

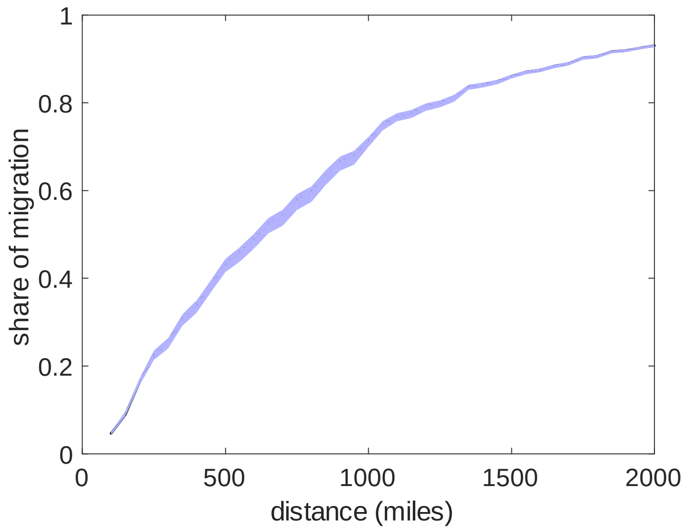

Figure 15: Patterns of migration and geographical distance

Notes: This figure plots $\pi_t(x)$ defined by (A.28) over the 1990-2014 period against x, along with its 5 and 95 per cent quantiles, where $\pi_t(x)$ is the share of the U.S. migrants who migrate to the x-miles of neighboring states.

B.2 State level real per capita incomes

The state level per capita annual disposable incomes are obtained from the Bureau of Economic Analysis (BEA).[A6] Real incomes are computed by dividing state level nominal incomes by state level prices of non-housing consumption goods. The relative prices of non-housing consumption goods across U.S. states for the year 2000 are estimated following the procedure in Holly et al. (2010) (see their Table A.1), where the American Chamber of Commerce Researchers Association (ACCRA) cost of living indices for non-housing items are used at the metropolitan statistical areas.[A7] Similarly, state level non-shelter Consumer Price Index (CPI) series are constructed using the U.S. Bureau of Labor Statistics (BLS) non-shelter CPIs of the cities and areas according to the Holly et al. (2010) procedure.[A8] Then, state level prices of non-housing consumption goods are complied by combining the relative prices of non-housing goods across U.S. states for 2000 and the state level non-shelter (CPI) series over 1976-2014.

[A6] For further information on the BEA state level per capita annual disposable income data (Table SA51), see `https://www.bea.gov/index.htm`.

[A7] The Cost of Living Index (COLI), formerly the ACCRA Cost of Living Index is a measure of living cost differences among urban areas in the United States compiled by the Council for Community and Economic Research. For further information, see `http://coli.org/`.

[A8] For further information on the BLS city level CPI data, see `https://www.bls.gov/data/`.

B.3 State level real house prices and rents

The state level median house prices for 1976-2014 are complied by combining the state level median house prices in 2000 obtained from the Historical Census of Housing Tables, and the state level House Price Index obtained from U.S. Federal Housing Finance Agency (FHFA).[A9] The FHFA House Price Index are available over the period $1976Q1$ to $2015Q4$. The annual house price index is computed using the simple average of the quarter indices over the year. Real house prices are obtained by dividing nominal house prices by prices of non-housing consumption goods.

The state level annual housing rents are computed for 1976-2014 by combing the state level annual housing rents for 2000 obtained from the Historical Census of Housing Tables, and the state level shelter-CPIs.[A10] We construct the state level shelter-CPI series based on the BLS shelter-CPI data and the procedure followed by Holly et al. (2010) (Table A.1).[A11] Real annual rents are obtained by dividing the nominal annual rents by the prices of non-housing consumption goods.

B.4 Land-use regulations and supplies

The state level Wharton Residential Land Use Regulatory Index is due to Gyourko et al. (2008), and the state level land share in house value is compiled by Davis and Heathcote (2007).[A12] The state-level data on urban area sizes are from the United States Department of Agriculture (USDA).[A13]

[A9] For further information on the Historical Census of Housing Tables of Home Values, see `https://www.census.gov/hhes/www/housing/census/historic/values.html`. For further information on the FHFA state level house price index, see `http://www.freddiemac.com/finance/fmhpi/archive.html`.

[A10] For further information on the Historical Census of Housing Tables of Housing Rents, see `https://www.census.gov/hhes/www/housing/census/historic/grossrents.html`.

[A11] For further information on the BLS city level CPI data, see `https://www.bls.gov/data/`.

[A12] For further information on the data of state level land share in house value, see `http://datatoolkits.lincolninst.edu/subcenters/land-values/land-prices-by-state.asp`.

[A13] For further information on the USDA land use data, see `https://www.ers.usda.gov/data-products/major-land-uses`.

C Calibration and estimation of parameters

Table 6: Benchmark calibration and estimation of parameters

		Value	Description
I. Preference			
η	Calibrated	0.240	Share of housing in consumption; Davis and Ortalo-Magné (2011).
β	Calibrated	0.980	Discount factor of landlords; Match the risk-free interest rate of 2%.
II. Migration and intrinsic population growth rates			
ψ	-	1.000	Weight of migration costs in utility function; Set to one.
α_{ij}	Estimated	See text	Route-specific migration costs.
g_l	Estimated	0.010	Intrinsic population growth rate; Match the U.S. average population growth rate over the period 1977-2014.
III. Housing supplies and investment			
α_l	Calibrated	0.430	Share of labor in residential structure values; Davis and Heathcote (2005).
α_m	Calibrated	0.570	Share of construction material in residential structure values; Davis and Heathcote (2005).
$\alpha_{\kappa,i}$	Estimated	See text	Location-specific shares of land in house values; Set to the state level average land values relative to total value of housing stocks over the period 1977-2014.
τ_i	Estimated	See text	Location-specific scalars in the housing supply functions.
θ_i	Estimated	See text	Location-specific housing investment costs; Match the state level average rent-to-price ratios over the period 1977-2014.
δ	Estimated	0.020	Depreciation rate of housing stocks; Set to the national housing stock depreciation rate over the period 1977-2014.
IV. Income processes			
a_i	Estimated	See text	Location-specific intercepts in the income processes.
g_a	Estimated	0.018	Income growth rate; Set to the U.S. average growth rate of real disposable per capita income over the period 1977-2014.
ρ_f	Estimated	0.950	AR(1) autoregressive coefficient for f_t.
σ_f	Estimated	0.017	Standard deviation of the innovation to f_t.
λ_i	Estimated	See text	Location-specific loading coefficients for f_t.
$\rho_{z_a,i}$	Estimated	See text	AR(1) autoregressive coefficients for $z_{a,it}$.
$\sigma_{z_a,i}$	Estimated	See text	Standard deviations of the innovations to $z_{a,it}$.
V. Land supply processes			
k_i	Estimated	See text	Location-specific intercepts in the land supply processes.
$g_{\kappa,i}$	Estimated	See text	Location-specific land supply growth rates.
$\rho_{z_\kappa,i}$	Estimated	See text	AR(1) autoregressive coefficients for $z_{\kappa,it}$.
$\sigma_{z_\kappa,i}$	Estimated	See text	Standard deviations of the innovations to $z_{\kappa,it}$.

Notes: This table reports the benchmark estimates of the parameters that are common to all locations. The estimates of the location-specific and route-specific parameters are reported in the remaining part of this appendix and the supplementary data files.

Table 7: Location-specific parameters related to housing supplies and investment

State		$\widehat{\alpha}_{\kappa,i}$	$\widehat{\theta}_i$			$\widehat{\alpha}_{\kappa,i}$	$\widehat{\theta}_i$
AL	Alabama	0.1063	0.0164	NE	Nebraska	0.0776	0.0265
AZ	Arizona	0.2084	0.0174	NV	Nevada	0.2389	0.0103
AR	Arkansas	0.0713	0.0270	NH	New Hampshire	0.2646	0.0147
CA	California	0.5653	0.0037	NJ	New Jersey	0.4637	0.0092
CO	Colorado	0.3383	0.0099	NM	New Mexico	0.1762	0.0067
CT	Connecticut	0.5106	0.0050	NY	New York	0.3090	0.0118
DE	Delaware	0.2474	0.0144	NC	North Carolina	0.2249	0.0230
DC	District of Columbia	0.6314	0.0045	ND	North Dakota	0.1198	0.0177
FL	Florida	0.2205	0.0279	OH	Ohio	0.1303	0.0191
GA	Georgia	0.1603	0.0231	OK	Oklahoma	0.0789	0.0267
ID	Idaho	0.1748	0.0125	OR	Oregon	0.2790	0.0102
IL	Illinois	0.2264	0.0133	PA	Pennsylvania	0.1651	0.0203
IN	Indiana	0.1013	0.0232	RI	Rhode Island	0.3079	0.0056
IA	Iowa	0.0977	0.0275	SC	South Carolina	0.1952	0.0198
KS	Kansas	0.1061	0.0280	SD	South Dakota	0.1430	0.0222
KY	Kentucky	0.0743	0.0218	TN	Tennessee	0.1379	0.0226
LA	Louisiana	0.1133	0.0187	TX	Texas	0.0845	0.0356
ME	Maine	0.2131	0.0153	UT	Utah	0.2816	0.0077
MD	Maryland	0.4418	0.0133	VT	Vermont	0.3082	0.0129
MA	Massachusetts	0.3971	0.0072	VA	Virginia	0.3833	0.0180
MI	Michigan	0.1321	0.0251	WA	Washington	0.3097	0.0079
MN	Minnesota	0.1127	0.0171	WV	West Virginia	0.0907	0.0221
MS	Mississippi	0.0746	0.0280	WI	Wisconsin	0.1410	0.0177
MO	Missouri	0.0838	0.0242	WY	Wyoming	0.2604	0.0044
MT	Montana	0.1857	0.0090				
Average across the U.S. states		0.2197	0.0169				

Table 8: Location-specific parameters of the income processes

State		$\hat{\lambda}_i$	SE	p-value	$\hat{\rho}_{z_a,i}$	SE	p-value	$\hat{\sigma}_{z_a,i}$
AL	Alabama	0.8389	0.1345	0.0000	0.9065	0.0631	0.0000	0.0109
AZ	Arizona	1.9745	0.2970	0.0000	0.9220	0.0583	0.0000	0.0221
AR	Arkansas	0.6650	0.0875	0.0000	0.5888	0.1342	0.0001	0.0148
CA	California	1.3070	0.2313	0.0000	0.9429	0.0372	0.0000	0.0110
CO	Colorado	1.3482	0.1137	0.0000	0.8190	0.0952	0.0000	0.0139
CT	Connecticut	0.8344	0.2165	0.0004	0.8192	0.0539	0.0000	0.0147
DE	Delaware	1.4805	0.1071	0.0000	0.6715	0.1218	0.0000	0.0168
DC	District of Columbia	0.1872	0.3245	0.5674	0.9475	0.0525	0.0000	0.0220
FL	Florida	1.6795	0.1588	0.0000	0.8117	0.0971	0.0000	0.0197
GA	Georgia	1.5342	0.1643	0.0000	0.9018	0.0610	0.0000	0.0129
ID	Idaho	1.6587	0.2335	0.0000	0.8097	0.0649	0.0000	0.0194
IL	Illinois	1.0512	0.0689	0.0000	0.7165	0.1134	0.0000	0.0101
IN	Indiana	1.1677	0.0987	0.0000	0.8994	0.0744	0.0000	0.0094
IA	Iowa	0.7934	0.1268	0.0000	0.6300	0.1234	0.0000	0.0202
KS	Kansas	0.8277	0.0832	0.0000	0.6348	0.1162	0.0000	0.0124
KY	Kentucky	0.9880	0.0843	0.0000	0.7777	0.1036	0.0000	0.0113
LA	Louisiana	-0.1423	0.1576	0.3723	0.8228	0.0950	0.0000	0.0192
ME	Maine	1.4355	0.0961	0.0000	0.7037	0.1115	0.0000	0.0138
MD	Maryland	1.0087	0.1398	0.0000	0.8963	0.0686	0.0000	0.0124
MA	Massachusetts	1.0243	0.2142	0.0000	0.8356	0.0569	0.0000	0.0155
MI	Michigan	1.9038	0.2224	0.0000	0.8979	0.0709	0.0000	0.0204
MN	Minnesota	1.1269	0.0750	0.0000	0.5065	0.1233	0.0002	0.0119
MS	Mississippi	0.5814	0.1384	0.0002	0.9136	0.0666	0.0000	0.0119
MO	Missouri	1.1063	0.0913	0.0000	0.8252	0.0851	0.0000	0.0100
MT	Montana	0.8539	0.2960	0.0064	0.8713	0.0530	0.0000	0.0200
NE	Nebraska	0.6417	0.0985	0.0000	0.3902	0.1544	0.0159	0.0193
NV	Nevada	2.5340	0.3188	0.0000	0.8506	0.0778	0.0000	0.0316
NH	New Hampshire	1.0080	0.2214	0.0001	0.7981	0.0609	0.0000	0.0170
NJ	New Jersey	1.1308	0.1538	0.0000	0.8188	0.0596	0.0000	0.0116
NM	New Mexico	1.2534	0.1735	0.0000	0.8832	0.0625	0.0000	0.0138
NY	New York	0.9135	0.1432	0.0000	0.8374	0.0746	0.0000	0.0137
NC	North Carolina	1.2796	0.1751	0.0000	0.9158	0.0542	0.0000	0.0122
ND	North Dakota	-1.1347	0.3293	0.0014	0.3877	0.1500	0.0139	0.0635
OH	Ohio	1.3093	0.1194	0.0000	0.8546	0.0841	0.0000	0.0130
OK	Oklahoma	0.2388	0.2373	0.3208	0.8940	0.0648	0.0000	0.0198
OR	Oregon	1.6539	0.2142	0.0000	0.8548	0.0594	0.0000	0.0162
PA	Pennsylvania	1.1937	0.0871	0.0000	0.7905	0.0998	0.0000	0.0112
RI	Rhode Island	1.1790	0.1414	0.0000	0.8035	0.0871	0.0000	0.0158
SC	South Carolina	1.0425	0.1161	0.0000	0.9168	0.0631	0.0000	0.0094
SD	South Dakota	0.2586	0.1963	0.1956	0.6065	0.1279	0.0000	0.0324
TN	Tennessee	1.0486	0.2565	0.0002	0.9529	0.0374	0.0000	0.0123
TX	Texas	0.3128	0.1613	0.0599	0.8861	0.0773	0.0000	0.0160
UT	Utah	1.2080	0.1230	0.0000	0.7789	0.0708	0.0000	0.0111
VT	Vermont	0.7823	0.1334	0.0000	0.7738	0.0825	0.0000	0.0140
VA	Virginia	0.8772	0.1175	0.0000	0.8658	0.0635	0.0000	0.0096
WA	Washington	1.2181	0.1300	0.0000	0.8574	0.0676	0.0000	0.0113
WV	West Virginia	0.5611	0.0853	0.0000	0.6727	0.1162	0.0000	0.0127
WI	Wisconsin	1.2577	0.1012	0.0000	0.8160	0.0845	0.0000	0.0110
WY	Wyoming	-0.0023	0.3465	0.9948	0.8952	0.0687	0.0000	0.0307
Average across the U.S. states		1.0000			0.7995			0.0164

Table 9: Location-specific parameters of the land supply processes

State		WRI	$\hat{g}_{K,i}$	SE	p-value	$\hat{\rho}_{z_K,i}$	SE	p-value	$\hat{\sigma}_{z_K,i}$
AL	Alabama	-1.1401	0.0662	0.0116	0.0000	0.9094	0.0593	0.0000	0.2910
AZ	Arizona	0.9917	0.0399	0.0126	0.0032	0.8726	0.0800	0.0000	0.4325
AR	Arkansas	-1.0279	0.1389	0.0172	0.0000	0.9160	0.0621	0.0000	0.4546
CA	California	1.0057	-0.0137	0.0057	0.0208	0.8560	0.0833	0.0000	0.2017
CO	Colorado	0.8514	0.0036	0.0055	0.5124	0.9315	0.0598	0.0000	0.1404
CT	Connecticut	0.7112	0.0059	0.0050	0.2468	0.8904	0.0768	0.0000	0.1608
DE	Delaware	0.8514	-0.0159	0.0071	0.0316	0.8855	0.0760	0.0000	0.2249
DC	District of Columbia		-0.0405	0.0049	0.0000	0.8960	0.0737	0.0000	0.1547
FL	Florida	0.6972	0.0130	0.0156	0.4091	0.8810	0.0768	0.0000	0.5099
GA	Georgia	-0.1163	0.0465	0.0085	0.0000	0.9061	0.0651	0.0000	0.2346
ID	Idaho	-0.7053	0.0305	0.0107	0.0070	0.8950	0.0713	0.0000	0.3251
IL	Illinois	-0.0882	0.0013	0.0080	0.8693	0.9089	0.0733	0.0000	0.2438
IN	Indiana	-1.2383	0.0633	0.0106	0.0000	0.9070	0.0712	0.0000	0.3218
IA	Iowa	-1.2102	0.0710	0.0186	0.0005	0.9039	0.0586	0.0000	0.4639
KS	Kansas	-1.4066	0.0862	0.0150	0.0000	0.9364	0.0524	0.0000	0.3346
KY	Kentucky	-0.6212	0.0331	0.0136	0.0193	0.9135	0.0648	0.0000	0.3699
LA	Louisiana	-1.3084	0.0843	0.0182	0.0000	0.9535	0.0515	0.0000	0.3982
ME	Maine	1.1319	-0.0277	0.0085	0.0023	0.8908	0.0770	0.0000	0.2756
MD	Maryland	1.2862	-0.0109	0.0058	0.0674	0.8942	0.0767	0.0000	0.1872
MA	Massachusetts	2.3661	-0.0322	0.0069	0.0000	0.9211	0.0670	0.0000	0.1932
MI	Michigan	0.2063	-0.0028	0.0168	0.8705	0.9441	0.0613	0.0000	0.4320
MN	Minnesota	0.2904	-0.0122	0.0173	0.4858	0.9353	0.0603	0.0000	0.4429
MS	Mississippi	-0.9718	0.1578	0.0193	0.0000	0.9104	0.0579	0.0000	0.4756
MO	Missouri	-1.2663	0.0436	0.0153	0.0072	0.9117	0.0663	0.0000	0.4292
MT	Montana	-0.3267	-0.0220	0.0105	0.0437	0.9110	0.0657	0.0000	0.2949
NE	Nebraska	-0.7755	0.0854	0.0170	0.0000	0.9170	0.0616	0.0000	0.4476
NV	Nevada	-0.4529	0.0613	0.0121	0.0000	0.8557	0.0840	0.0000	0.4332
NH	New Hampshire	2.0856	-0.0014	0.0098	0.8859	0.9044	0.0725	0.0000	0.3013
NJ	New Jersey	1.4124	-0.0169	0.0057	0.0050	0.9048	0.0754	0.0000	0.1788
NM	New Mexico	0.0240	0.0298	0.0073	0.0002	0.8828	0.0797	0.0000	0.2471
NY	New York	0.1642	-0.0382	0.0074	0.0000	0.9220	0.0703	0.0000	0.2186
NC	North Carolina	-0.3126	0.0295	0.0047	0.0000	0.9104	0.0703	0.0000	0.1389
ND	North Dakota	-0.5791	0.0740	0.0167	0.0001	0.8452	0.0915	0.0000	0.6301
OH	Ohio	-0.3267	0.0473	0.0116	0.0002	0.9401	0.0614	0.0000	0.2956
OK	Oklahoma	-0.8035	0.1860	0.0235	0.0000	0.9373	0.0596	0.0000	0.5935
OR	Oregon	0.2904	-0.0407	0.0095	0.0001	0.9094	0.0672	0.0000	0.2724
PA	Pennsylvania	0.6972	-0.0154	0.0089	0.0908	0.8829	0.0753	0.0000	0.2800
RI	Rhode Island	2.3942	-0.0296	0.0088	0.0019	0.9168	0.0758	0.0000	0.2786
SC	South Carolina	-0.8877	0.0241	0.0063	0.0005	0.9278	0.0543	0.0000	0.1449
SD	South Dakota	-1.2804	0.0269	0.0095	0.0077	0.8468	0.0789	0.0000	0.3200
TN	Tennessee	-0.7755	0.0401	0.0081	0.0000	0.8960	0.0678	0.0000	0.2327
TX	Texas	-0.4529	0.1510	0.0183	0.0000	0.9511	0.0592	0.0000	0.4514
UT	Utah	0.0801	0.0139	0.0070	0.0534	0.9036	0.0695	0.0000	0.2065
VT	Vermont	0.6691	-0.0069	0.0055	0.2146	0.8379	0.0889	0.0000	0.2061
VA	Virginia	-0.0882	-0.0039	0.0056	0.4936	0.8980	0.0705	0.0000	0.1669
WA	Washington	1.2161	-0.0250	0.0062	0.0003	0.8715	0.0843	0.0000	0.2201
WV	West Virginia	-1.0840	0.1298	0.0213	0.0000	0.9296	0.0563	0.0000	0.5113
WI	Wisconsin	0.2764	-0.0025	0.0130	0.8507	0.9255	0.0624	0.0000	0.3397
WY	Wyoming	-0.4529	0.0238	0.0098	0.0203	0.9442	0.0506	0.0000	0.2115
Average across the U.S. states		0.0000	0.0296			0.9049			0.3127

Notes: The average WRI is computed across the 48 states on the U.S. mainland, since Alaska and Hawaii are excluded from our analyses. The WRIs of the states we included are re-scaled such that the mean and the standard deviation of the sub-sample are zero and one, respectively.

D Supplementary results

D.1 House price dispersion between U.S. states

We divide the District of the Columbia and the 48 states on the U.S. main land (referred to as 49 U.S. states for short) into five regions following the regional categorization by National Geographic Society. The time series plots of log house price-to-income ratios during 1976-2014 for the 49 U.S. states separately are displayed in Figure 16. As can be seen the house price-to-income ratios of states within the same region share similar dynamic patterns. Figure 17 shows the log house price-to-income ratios aggregated at the five U.S. regions. Regional-level house price-to-income ratio is measured as the population weighted average of state level house price-to-income ratios, where the population weights are computed based on state level population data over the period 1976-2014. This figure shows that house price-to-income ratio has significantly increased in the West, and considerably dropped in the Southwest and the Southeast. The difference in house price-to-income ratio between the Southwest and the West is increasing overtime. In addition, a dispersion decomposition shows that around 70% of the between-state variance is due to the between-region differences (Figure 18).

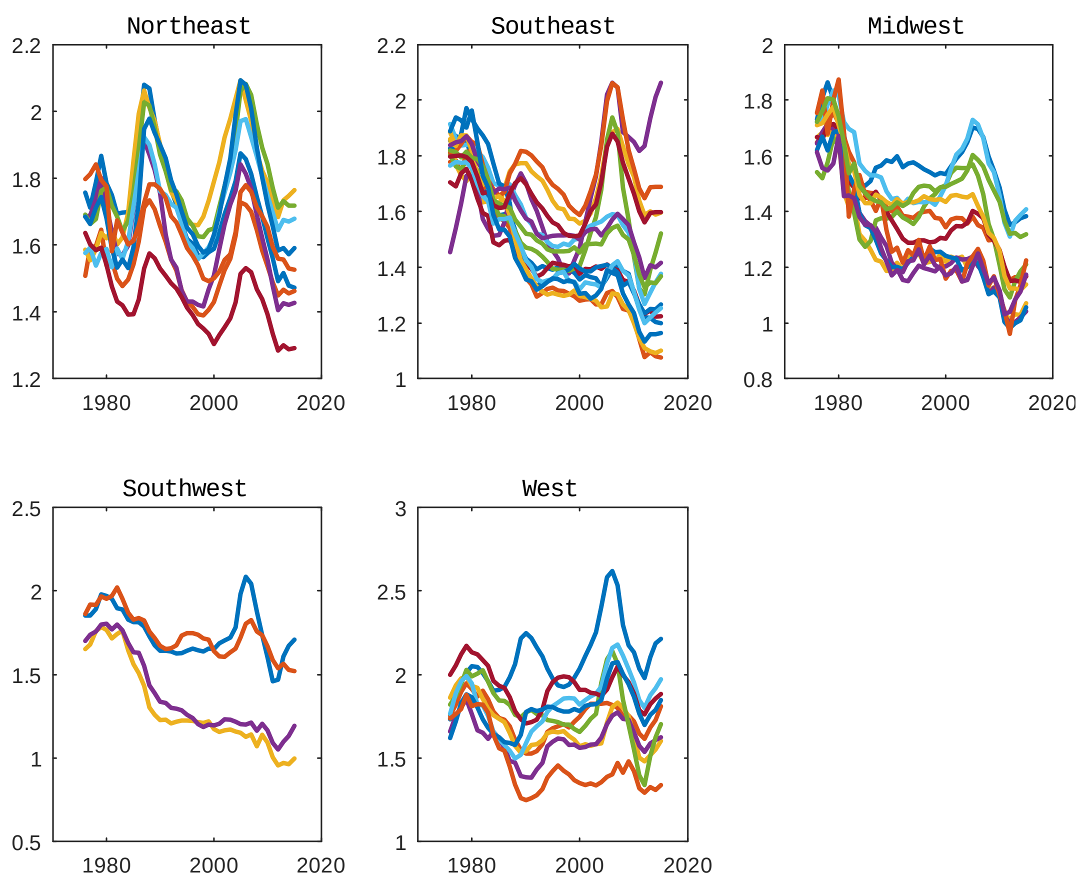

Figure 16: State level log house price-to-income ratios (grouped in to five U.S. regions)

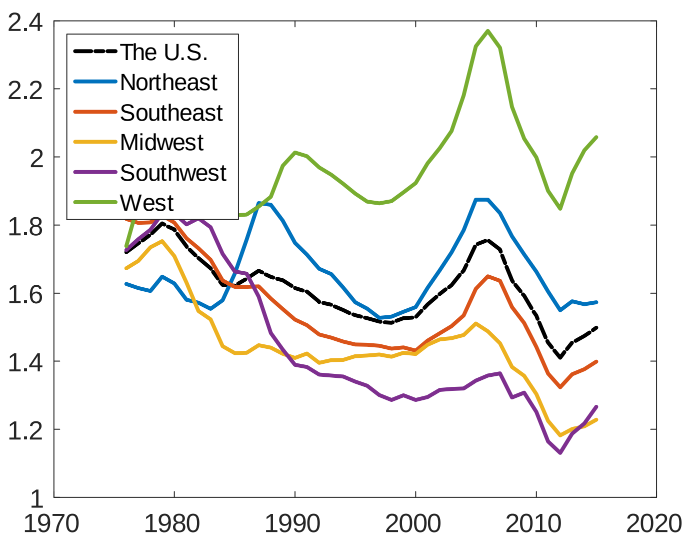

Figure 17: Log house price-to-income ratios of U.S. regions

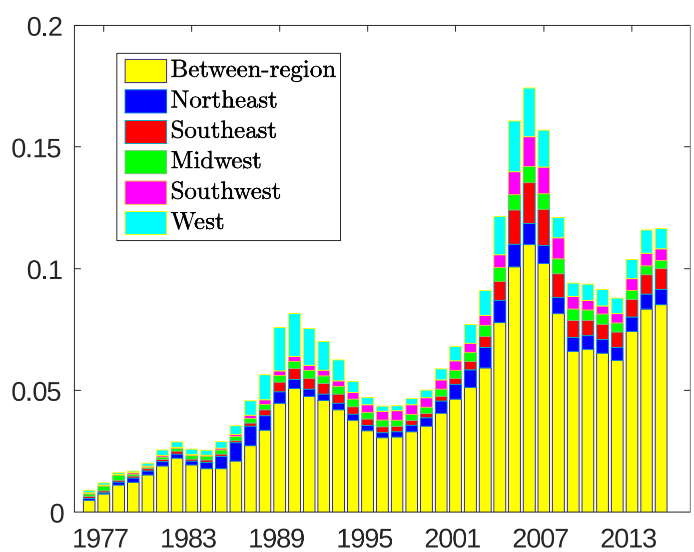

Figure 18: Regional decomposition of log house price-to-income ratio dispersion

Notes: This figure shows the decomposition of the variance of log house price-to-income ratio across U.S. states. The between-state variance is decomposed into between-region variance (yellow) and weighted within-region variances (blue, green, red, pink, cyan).

D.2 House price dispersion between MSAs

We investigate the patterns of house price dispersions between Metropolitan Statistical Areas (MSAs) using data from Van Nieuwerburgh and Weill (2010). As shown in Figure 19, the dispersion of log house price-to-income ratios across MSAs has significantly increased during 1975-2007. We then decomposed the house price-to-income ratio dispersion between MSAs into within- and between- state dispersion. In doing so, we group the MSAs in the U.S. mainland by state. A multi-state MSA is equally split across the states shared by the MSA in question.[A14] For instance, Kansas city, which is on the Kansas-Missouri boarder, is equally divided between Kansas and Missouri. A "state" is considered as a group of MSAs,[A15] and the dispersion across these groups is referred to as *between-state dispersion* and the dispersion across MSAs within a group is referred to as *within-state dispersion*. Figure 19 shows the decomposition of between-MSA dispersion of log house price-to-income ratios. It is clear that increases in within-state dispersions contributed very little to the increases in the between-MSA dispersions during 1975-2007.

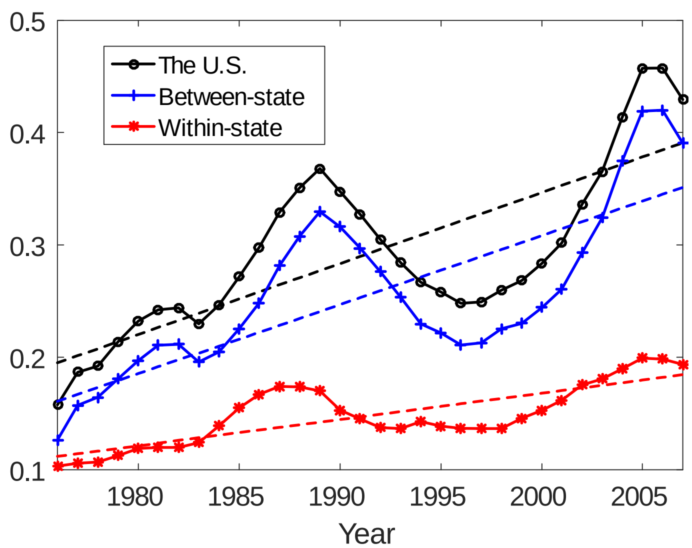

Figure 19: Dispersion of log house price-to-income ratios between- and within- U.S. states

Notes: The line designated with 'o' shows the dispersion of log house price-to-income ratio across all MSAs. The line designated with '+' shows the dispersion of log house price-to-income ratio across the U.S. states. The line designated with '*' shows the average of within-state dispersions, where within-state dispersion is the standard deviation of log house price-to-income ratio across the MSAs that are within a given state.

[A14] In the sample, around 10% of the MSAs are multi-state MSAs.

[A15] In the US, around 86% of its population live in MSAs. In the most populated states, such as, California, New York, Texas, Illinois, and Florida, more than 95% of their population live in MSAs.

D.3 Results of the baseline simulation

Figure 20 shows the realized and the model simulated log populations of U.S. states. Figure 21 shows the realized and the model simulated log annual housing rents of U.S. states. Figure 22 shows the realized and the model simulated log house prices of U.S. states.

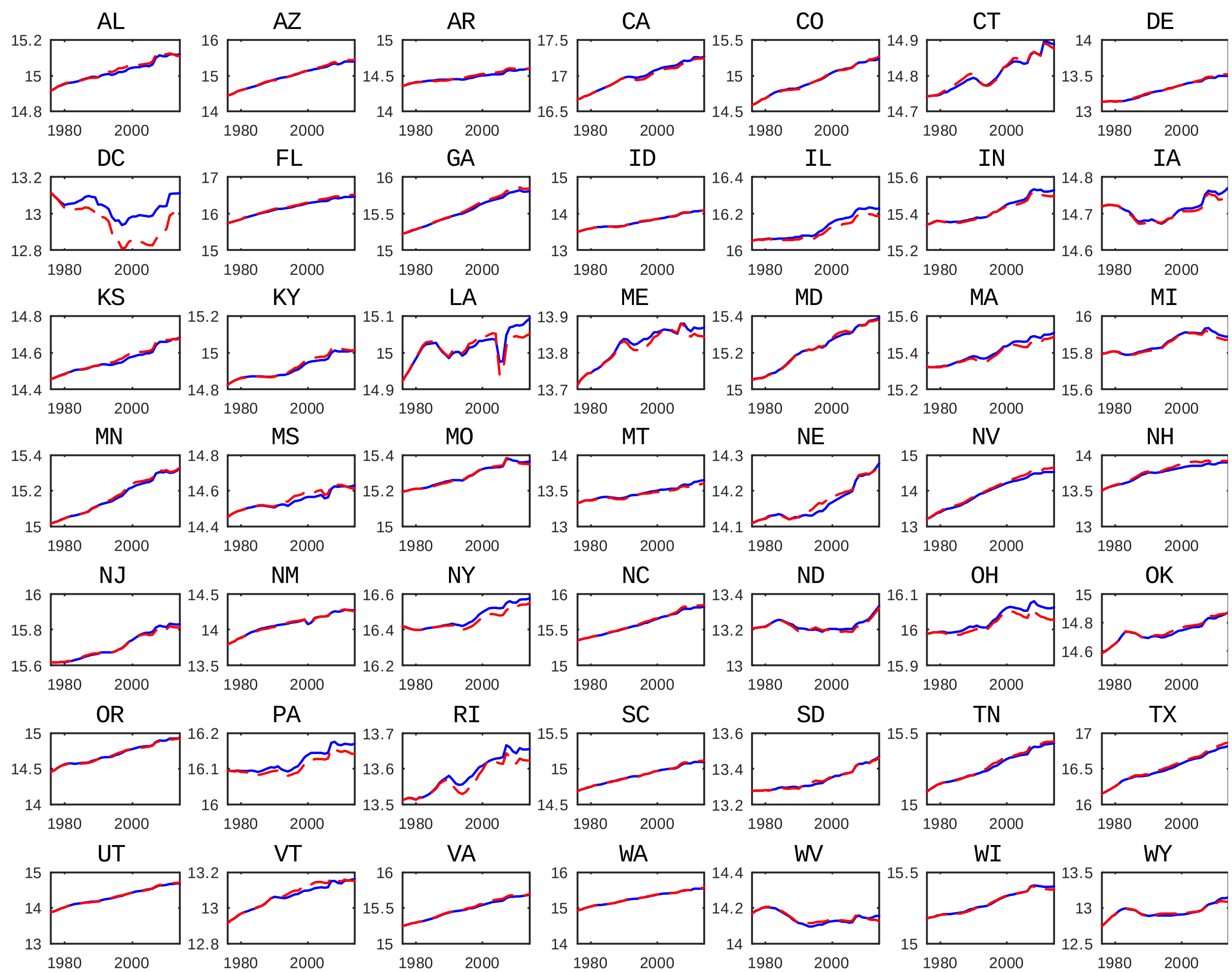

Figure 20: Log populations of U.S. states (Solid-blue: model; Dashed-red: data)

Notes: This figure plots the realized and the model simulated log populations of U.S. states.

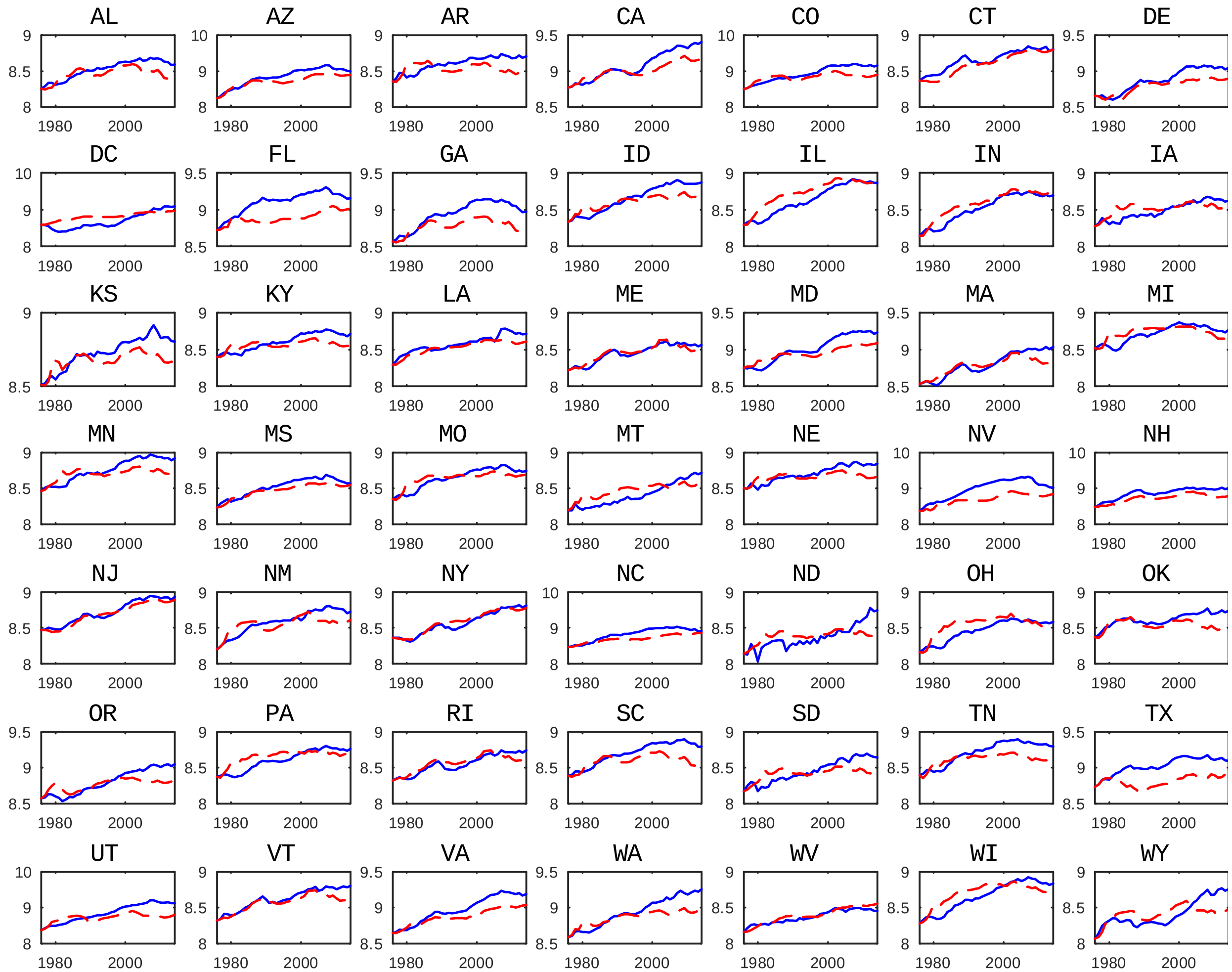

Figure 21: Log annual housing rents of U.S. states (Solid-blue: model; Dashed-red: data)

Notes: This figure plots the realized and the model simulated log annual housing rents of U.S. states.

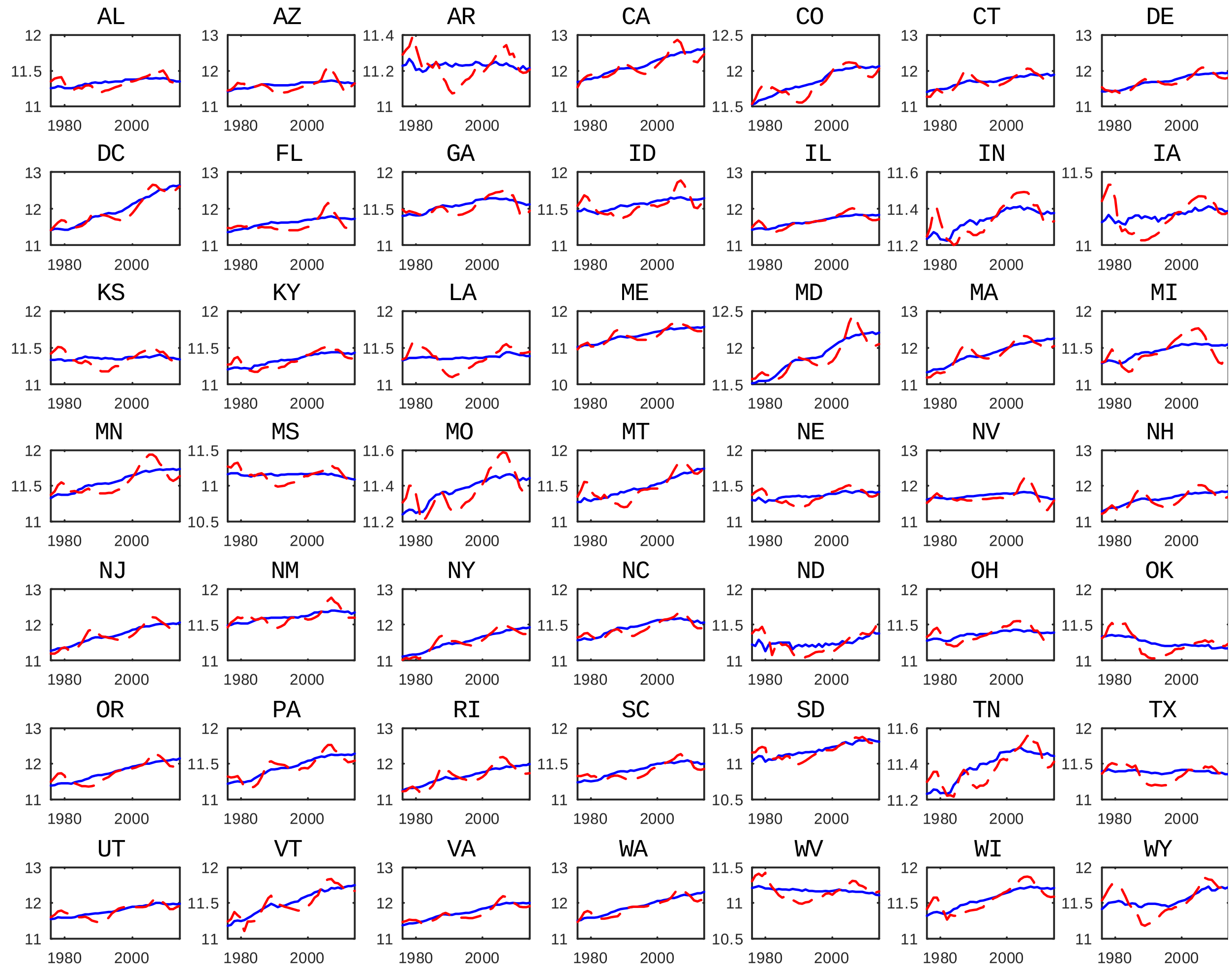

Figure 22: Log house prices of U.S. states (Solid-blue: model; Dashed-red: data)

Notes: This figure plots the realized and the model simulated log house prices of U.S. states.

References

Bailey, N., Holly, S., and Pesaran, M.H. (2016). A two-stage approach to spatio-temporal analysis with strong and weak cross-sectional dependence. *Journal of Applied Econometrics*, 31, 249–280.

Ciccone, A. and Hall, R.E. (1996). Productivity and the density of economic activity. *The American Economic Review*, 86, 54–70.

Cohen, J.P., Ioannides, Y.M., and Thanapisitikul, W.W. (2016). Spatial effects and house price dynamics in the usa. *Journal of Housing Economics*, 31, 1–13.

Cotter, J., Gabriel, S.A., and Roll, R. (2011). Integration and contagion in us housing markets. Available at SSRN: https://ssrn.com/abstract=2017793.

Davis, M.A., Fisher, J.D., and Veracierto, M. (2013). Gross migration, housing and urban population dynamics. FRB of Chicago Working Paper No. 2013-19. Available at SSRN: https://ssrn.com/abstract=2366922.

Davis, M.A., Fisher, J.D., and Whited, T.M. (2014). Macroeconomic implications of agglomeration. *Econometrica*, 82, 731–764.

Davis, M.A. and Heathcote, J. (2005). Housing and the business cycle. *International Economic Review*, 46, 751–784.

Davis, M.A. and Heathcote, J. (2007). The price and quantity of residential land in the united states. *Journal of Monetary Economics*, 54, 2595–2620.

Davis, M.A. and Ortalo-Magné, F. (2011). Household expenditures, wages, rents. *Review of Economic Dynamics*, 14, 248–261.

DeFusco, A., Ding, W., Ferreira, F., and Gyour, J. (2017). The role of contagion in the last american housing cycle. Available at SSRN: https://ssrn.com/abstract=2696695.

Favara, G. and Imbs, J. (2015). Credit supply and the price of housing. *The American Economic Review*, 105, 958–992.

Favilukis, J., Ludvigson, S.C., and Van Nieuwerburgh, S. (2017). The macroeconomic effects of housing wealth, housing finance, and limited risk sharing in general equilibrium. *Journal of Political Economy*, 125, 140–223.

Ferreira, F., Gyourko, J., and Tracy, J. (2010). Housing busts and household mobility. *Journal of urban Economics*, 68, 34–45.

Fuguitt, G.V. (1965). The growth and decline of small towns as a probability process. *American Sociological Review*, 30, 403–411.

Glaeser, E.L. and Gyourko, J. (2003). The impact of building restrictions on housing affordability. *Federal Reserve Bank of New York Economic Policy Review*, 9, 21–39.

Glaeser, E.L., Gyourko, J., and Saks, R.E. (2005). Why have housing prices gone up? *The American Economic Review*, 95, 329–333.

Glaeser, E.L. and Tobio, K. (2008). The rise of the sunbelt. *Southern Economic Journal*, 74, 610–643.

Gyourko, J., Mayer, C., and Sinai, T. (2010). Dispersion in house price and income growth across markets: Facts and theories. In *Agglomeration Economics*, pages 67–104. University of Chicago Press.

Gyourko, J., Mayer, C., and Sinai, T. (2013). Superstar cities. *American Economic Journal: Economic Policy*, 5, 167–199.

Gyourko, J., Molloy, R., et al. (2015). Regulation and housing supply. *Handbook of Regional and Urban Economics*, 5, 1289–1337.

Gyourko, J., Saiz, A., and Summers, A. (2008). A new measure of the local regulatory environment for housing markets: The wharton residential land use regulatory index. *Urban Studies*, 45, 693–729.

Head, A. and Lloyd-Ellis, H. (2012). Housing liquidity, mobility, and the labour market. *Review of Economic Studies*, 79, 1559–1589.

Herkenhoff, K.F., Ohanian, L.E., and Prescott, E.C. (2018). Tarnishing the golden and empire states: Land-use restrictions and the us economic slowdown. *Journal of Monetary Economics*, 93, 89–109.

Holly, S., Pesaran, M.H., and Yamagata, T. (2010). A spatio-temporal model of house prices in the usa. *Journal of Econometrics*, 158, 160–173.

Hsieh, C.T. and Moretti, E. (2015). Housing constraints and spatial misallocation. Working Paper 21154, National Bureau of Economic Research.

Koop, G., Pesaran, M.H., and Potter, S.M. (1996). Impulse response analysis in nonlinear multivariate models. *Journal of econometrics*, 74, 119–147.

Mcfadden, D. (1978). Modelling the Choice of Residential Location. In *Spatial Interaction Theory and Planning Models*, pages 75–96. North-Holland Publishing Company.

Mian, A. and Sufi, A. (2009). The consequences of mortgage credit expansion: Evidence from the u.s. mortgage default crisis. *Quarterly Journal of Economics*, 124, 1449–1496.

Nenov, P.T. (2015). Regional reallocation and housing markets in a model of frictional migration. *Review of Economic Dynamics*, 18, 863–880.

Ortalo-Magne, F. and Rady, S. (2006). Housing market dynamics: On the contribution of income shocks and credit constraints. *The Review of Economic Studies*, 73, 459–485.

Ouazad, A. and Ranciere, R. (2017). City equilibrium with borrowing constraints: Structural estimation and general equilibrium effects. Working Paper 23994, National Bureau of Economic Research.

Parkhomenko, A. (2016). The rise of housing supply regulation in the us: Local causes and aggregate implications. Technical report, mimeo.

Philippon, T. and Midrigan, V. (2016). Household leverage and the recession. Working Paper 16965, National Bureau of Economic Research.

Quigley, J.M. and Raphael, S. (2005). Regulation and the high cost of housing in california. *The American Economic Review*, 95, 323–328.

Roback, J. (1982). Wages, rents, and the quality of life. *Journal of political economy*, 90, 1257–1278.

Rosen, S. (1979). Wage-based indexes of urban quality of life. In *Current issues in urban economics*, pages 74–104. Johns Hopkins University Press.

Sinai, T. (2012). House price moments in boom-bust cycles. In *Housing and the Financial Crisis*, pages 19–68. University of Chicago Press.

Sterk, V. (2015). Home equity, mobility, and macroeconomic fluctuations. *Journal of Monetary Economics*, 74, 16–32.

Tarver, J.D. and Gurley, W.R. (1965). A stochastic analysis of geographic mobility and population projections of the census divisions in the united states. *Demography*, 2, 134–139.

Valentinyi, A. and Herrendorf, B. (2008). Measuring factor income shares at the sectoral level. *Review of Economic Dynamics*, 11, 820–835.

Van Nieuwerburgh, S. and Weill, P.O. (2010). Why has house price dispersion gone up? *The Review of Economic Studies*, 77, 1567–1606.

Online Supplement to

"Land Use Regulations, Migration and Rising House Price Dispersion in the U.S."

by

Wukuang Cun

USC Dornsife INET, University of Southern California

M. Hashem Pesaran

Department of Economics & USC Dornsife INET, University of Southern California, USA and Trinity College, Cambridge, UK

S1 Existence and uniqueness of short-run equilibrium

Proposition S1 *Consider the dynamic spatial equilibrium model set up in Section 3 by (6), (15), (18), (22), (28), (35) and (37). Suppose that the vectors of exogenous processes for labor productivities, $\boldsymbol{a}_t$, land supplies, $\boldsymbol{\kappa}_t$, and intrinsic population growth rates, $\boldsymbol{g}_{lt}$, for $t = 1, 2, ...,$ are given by (39)-(41), condition (42) holds, and the initial values for local population and housing stocks ($\boldsymbol{l}_0$ and $\boldsymbol{h}_0$) are strictly positive. Then the model has a unique short-run equilibrium in the sense set out in Definition 1.*

Proof: To prove the existence and uniqueness of the short-run equilibrium, we show that given $\boldsymbol{l}^*_{t-1}$ and $\boldsymbol{h}^*_{t-1}$, then $\boldsymbol{w}^*_t, \boldsymbol{q}^*_t, \boldsymbol{p}^*_t, \boldsymbol{l}^*_t, \boldsymbol{x}^*_t, \boldsymbol{h}^*_t$ and $\mathbf{R}^*_t$ are uniquely determined by equations (43) to (49), which are the equilibrium conditions (6), (15), (18), (22), (28), (35) and (37) re-written in terms of detrended variables.

We first show that $l^*_{\cdot i}(t) > 0$, and hence $1 > \rho^*_{ij}(t) > 0$, for all i and $j \in \mathcal{I}_n$. Consider a population vector $\boldsymbol{l}^*_t$ that solves (43) to (49). Note that $\sum_{i=1}^n l^*_{\cdot i}(t) > 0$, and $l^*_{\cdot i}(t)$ is non-negative for any $i \in \mathcal{I}_n$. Thus, $l^*_{\cdot i}(t) > 0$ has to hold for at least one i. Without loss of generality, we assume

$$l^*_{\cdot 1}(t) > 0. \tag{S.1}$$

Note also that since $l^*_{\cdot 1}(t)$ is the first element in $\boldsymbol{l}^*_t$, then from (43) we have

$$l^*_{\cdot 1}(t) = \sum_{i=1}^n \rho^*_{i1}(t) l^*_{\cdot i}(t-1), \tag{S.2}$$

where, upon using (44), (47) and (49), $\rho^*_{i1}(t)$ is given by

$$\rho^*_{i1}(t) = \frac{\alpha_{i1}^{-\psi} a_1^{1-\eta} \left(h^*_{1,t-1}\right)^{\eta} \left(l^*_{\cdot 1}(t)\right)^{-\eta}}{\sum_{s=1}^n \alpha_{is}^{-\psi} a_s^{1-\eta} \left(h^*_{s,t-1}\right)^{\eta} \left(l^*_{\cdot s}(t)\right)^{-\eta}} \tag{S.3}$$

which implies

$$\rho^*_{i1}(t) = \frac{1}{1 + \sum_{s \neq i} \left(\frac{\alpha_{is}^{-\psi} a_s^{1-\eta} \left(h^*_{s,t-1}\right)^{\eta}}{\alpha_{i1}^{-\psi} a_1^{1-\eta} \left(h^*_{1,t-1}\right)^{\eta}} \right) \frac{\left(l^*_{\cdot 1}(t)\right)^{\eta}}{\left(l^*_{\cdot s}(t)\right)^{\eta}}}, \text{ for } i = 1, 2, ..., n. \tag{S.4}$$

Note that since η, α_{is} and $a_s > 0$ by assumption, and that also $h^*_{s,t-1} > 0$, for $t = 1, 2, ...,$ since $h_{s0} > 0$ and the depreciation rate of housing stock δ is less than one. Thus, $\alpha_{is}^{-\psi} a_s^{1-\eta} \left(h^*_{s,t-1}\right)^{\eta} > 0$. In addition, it is supposed that $l^*_{\cdot 1}(t) > 0$. Hence, if $l^*_{\cdot s}(t) = 0$, for any $s \in \{2, 3, ..., n\}$, then $\rho^*_{i1}(t) = 0$, for all $i \in \mathcal{I}_n$, and using (S.4) it follows that $l^*_{\cdot 1}(t) = 0$, which contradicts our supposition. The same line of reasoning can be applied to any other elements of $\boldsymbol{l}^*_t$, and we must have $l^*_{\cdot 1}(t) > 0$, for any $i \in \mathcal{I}_n$.

Second, let $\mathcal{L}_t(\epsilon)$ with $\epsilon > 0$, be a set of population vector:

$$\mathcal{L}_t(\epsilon) \equiv \left\{ (l^*_{\cdot 1}(t), ..., l^*_{\cdot n}(t)) \,\middle|\, L_0 \geq l^*_{\cdot i}(t) \geq \epsilon \text{ for any } i, \text{ where } \epsilon > 0, \sum_{i=1}^{n} l^*_{\cdot i}(t) = L_0 \right\}$$

Consider a mapping F, define

$$F(\boldsymbol{l}^*_t) = \boldsymbol{l}^*_{t-1} \mathbf{R}(\boldsymbol{l}^*_t; \boldsymbol{h}^*_{t-1}),$$

where $\boldsymbol{l}^*_{t-1}$ and $\boldsymbol{h}^*_{t-1}$ are given, and $\mathbf{R}(\boldsymbol{l}^*_t, \boldsymbol{h}^*_{t-1})$ is the migration probability matrix with typical element $\rho^*_{ij}(t)$, which is given by (S.3). Thus, for (43) to hold, the above mapping should have a fixed point. Consider a $\boldsymbol{l}^*_t \in \mathcal{L}_t(\epsilon)$. Note that $l^*_{\cdot i}(t)$ is the ith element of $\boldsymbol{l}^*_t$ and satisfies $L_0 \geq l^*_{\cdot i}(t) \geq \epsilon$, for $i = 1, 2, ..., n$. Then, by using (S.3), we have

$$\begin{aligned}
\rho^*_{ij}(t) &= \frac{\alpha_{ij}^{-\psi} a_j^{1-\eta} \left(h^*_{j,t-1}\right)^{\eta} \left(l^*_{\cdot j}(t)\right)^{-\eta}}{\sum_{s=1}^{n} \alpha_{is}^{-\psi} a_s^{1-\eta} \left(h^*_{s,t-1}\right)^{\eta} \left(l^*_{\cdot s}(t)\right)^{-\eta}} \\
&> \frac{\alpha_{ij}^{-\psi} a_j^{1-\eta} \left(h^*_{j,t-1}\right)^{\eta} (L_0)^{-\eta}}{\sum_{s=1}^{n} \alpha_{is}^{-\psi} a_s^{1-\eta} \left(h^*_{s,t-1}\right)^{\eta} (\epsilon)^{-\eta}} = \frac{\alpha_{ij}^{-\psi} a_j^{1-\eta} \left(h^*_{j,t-1}\right)^{\eta} (L_0)^{1-\eta}}{\sum_{s=1}^{n} \alpha_{is}^{-\psi} a_s^{1-\eta} \left(h^*_{s,t-1}\right)^{\eta} (\epsilon)^{1-\eta}} \frac{\epsilon}{L_0}.
\end{aligned}$$

Since $\eta \in (0, 1)$, then $1 - \eta > 0$. Suppose ϵ is small enough such that

$$\rho^*_{ij}(t) > \frac{\epsilon}{L_0}, \text{ for } i \text{ and } j \in \mathcal{I}_n.$$

Define $\boldsymbol{l}^{*'}_t = F(\boldsymbol{l}^*_t) = \boldsymbol{l}^*_{t-1} \mathbf{R}(\boldsymbol{l}^*_t; \boldsymbol{h}^*_{t-1})$. Thus we have

$$l^{*'}_{\cdot j}(t) = \sum_{i=1}^{n} \rho^*_{ij}(t) l^*_{\cdot i}(t-1) > \sum_{i=1}^{n} \left(\frac{\epsilon}{L_0} \right) L_0 = \epsilon \qquad \text{for any } j \in \mathcal{I}_n.$$

In addition,

$$\sum_{j=1}^{n} l^{*'}_{\cdot j}(t) = \sum_{j=1}^{n} \sum_{i=1}^{n} \rho^*_{ij}(t) l^*_{\cdot i}(t-1) = \sum_{i=1}^{n} l^*_{\cdot i}(t-1) \sum_{j=1}^{n} \rho^*_{ij}(t) = \sum_{i=1}^{n} l^*_{\cdot i}(t-1) = L_0.$$

Therefore, when ϵ is small enough such that $\rho^*_{ij}(t) > \epsilon/L_0$ for any $i, j \in \mathcal{I}_n$, then $\boldsymbol{l}^*_t \in \mathcal{L}_t(\epsilon) \Rightarrow \boldsymbol{l}^{*'}_t = F(\boldsymbol{l}^*_t) \in \mathcal{L}_t(\epsilon)$. Thus, F is a continuous mapping from $\mathcal{L}_t(\epsilon)$ to itself, where $\mathcal{L}_t(\epsilon)$ is a compact convex set. Thus, Brouwer Fix Point Theorem is applicable to ensure the existence of fixed point. Then, using the solution of $\boldsymbol{l}^*_t$, the other variables of the model, namely, $\boldsymbol{p}^*_t, \boldsymbol{q}^*_t, \boldsymbol{x}^*_t, \boldsymbol{h}^*_t$and $\mathbf{R}^*_t$, can be solved for using equations (44) to (49).

Third, to show the uniqueness, suppose there are $\boldsymbol{l}^{*(1)}_t, \boldsymbol{l}^{*(2)}_t \in \mathcal{L}_t(\epsilon)$, with $\boldsymbol{l}^{*(1)}_t \neq \boldsymbol{l}^{*(2)}_t$, and $\boldsymbol{l}^{*(1)}_t = F(\boldsymbol{l}^{*(1)}_t)$, $\boldsymbol{l}^{*(2)}_t = F(\boldsymbol{l}^{*(2)}_t)$. Define $\mathcal{I}^+_n \equiv \{j |\ l^{*(2)}_{\cdot j}(t) > l^{*(1)}_{\cdot j}(t),\ j \in \mathcal{I}_n\}$ and $\mathcal{I}^-_n \equiv \{j |\ l^{*(2)}_{\cdot j}(t) \leq l^{*(1)}_{\cdot j}(t),\ j \in \mathcal{I}_n\}$. Thus, neither $\mathcal{I}^+_n$ nor $\mathcal{I}^-_n$ is empty, and we have

$$\sum_{j \in \mathcal{I}^+_n} l^{*(2)}_{\cdot j}(t) > \sum_{j \in \mathcal{I}^+_n} l^{*(1)}_{\cdot j}(t). \tag{S.5}$$

Note that by using (S.3), we have

$$\begin{aligned}
\frac{\sum_{j \in \mathcal{I}^+_n} \rho^{*(2)}_{ij}(t)}{\sum_{j \in \mathcal{I}^-_n} \rho^{*(2)}_{ij}(t)} &= \frac{\sum_{j \in \mathcal{I}^+_n} \alpha_{ij}^{-\psi} a_j^{1-\eta} \left(h^*_{j,t-1}\right)^\eta \left(l^{*(2)}_{\cdot j}(t)\right)^{-\eta}}{\sum_{j \in \mathcal{I}^+_n} \alpha_{ij}^{-\psi} a_j^{1-\eta} \left(h^*_{j,t-1}\right)^\eta \left(l^{*(2)}_{\cdot j}(t)\right)^{-\eta}}, \\
&< \frac{\sum_{j \in \mathcal{I}^+_n} \alpha_{ij}^{-\psi} a_j^{1-\eta} \left(h^*_{j,t-1}\right)^\eta \left(l^{*(1)}_{\cdot j}(t)\right)^{-\eta}}{\sum_{j \in \mathcal{I}^+_n} \alpha_{ij}^{-\psi} a_j^{1-\eta} \left(h^*_{j,t-1}\right)^\eta \left(l^{*(1)}_{\cdot j}(t)\right)^{-\eta}}, \\
&= \frac{\sum_{j \in \mathcal{I}^+_n} \rho^{*(1)}_{ij}(t)}{\sum_{j \in \mathcal{I}^-_n} \rho^{*(1)}_{ij}(t)}.
\end{aligned}$$

Note also that

$$\sum_{j \in \mathcal{I}^+_n} \rho^{*(2)}_{ij}(t) + \sum_{j \in \mathcal{I}^-_n} \rho^{*(2)}_{ij}(t) = \sum_{j \in \mathcal{I}^+_n} \rho^{*(1)}_{ij}(t) + \sum_{j \in \mathcal{I}^-_n} \rho^{*(1)}_{ij}(t) = 1.$$

Thus,

$$\sum_{j \in \mathcal{I}^+_n} \rho^{*(2)}_{ij}(t) < \sum_{j \in \mathcal{I}^+_n} \rho^{*(1)}_{ij}(t) \qquad \text{for any } i \in \mathcal{I}_n. \tag{S.6}$$

Since $\boldsymbol{l}^{*(1)}_t = F(\boldsymbol{l}^{*(1)}_t)$, $\boldsymbol{l}^{*(2)}_t = F(\boldsymbol{l}^{*(2)}_t)$, thus for any $j \in I$

$$l^{*(2)}_{\cdot j}(t) = \sum_{i \in I} \rho^{*(2)}_{ij}(t) l^*_{\cdot i}(t-1) \qquad \text{and} \qquad l^{*(1)}_{\cdot j}(t) = \sum_{i \in I} \rho^{*(1)}_{ij}(t) l^*_{\cdot i}(t-1)$$

Then, we have

$$\begin{aligned}\sum_{j\in\mathcal{I}_n^+}(l_{\cdot j}^{*(2)}(t)-l_{\cdot j}^{*(1)}(t)) &= \sum_{j\in\mathcal{I}_n^+}\sum_{i\in I}\rho_{ij}^{*(2)}(t)l_{\cdot i}^{*}(t-1)-\sum_{j\in\mathcal{I}_n^+}\sum_{i\in I}\rho_{ij}^{*(1)}(t)l_{\cdot i}^{*}(t-1)\\ &=\sum_{i\in I}\sum_{j\in\mathcal{I}_n^+}\left(\rho_{ij}^{*(2)}(t)-\rho_{ij}^{*(1)}(t)\right)l_{\cdot i}^{*}(t-1)\\ &=\sum_{i\in I}\left(\sum_{j\in\mathcal{I}_n^+}\rho_{ij}^{*(2)}(t)-\sum_{j\in\mathcal{I}_n^+}\rho_{ij}^{*(1)}(t)\right)l_{\cdot i}^{*}(t-1)\\ &<0\end{aligned}$$

Thus, the above contradicts with (S.5), which implies that $\boldsymbol{l}_t^{*(1)} \neq \boldsymbol{l}_t^{*(2)}$ cannot be true. ■

S2 Extended model with endogenously determined wages

S2.1 Theoretical derivations

In the baseline model, wage rates are exogenously determined and pinned down by local labor productivities, as shown by (18). This section extends the analysis by explicitly modelling the determination of wage rates and investigates the conditions under which the extended model has a unique long run equilibrium. We follow Davis et al. (2014) and Herkenhoff et al. (2018), and introduce capital, denoted by χ_{it}, land for production, denoted by $\kappa_{y,i}$, and allow for agglomeration effects in the production function, and instead of (17) we assume:

$$y_{it}=\psi_{it}\left[(\chi_{it})^{1-\lambda_\kappa}(\kappa_{y,i})^{\lambda_\kappa}\right]^{1-\upsilon_l}\left[a_{it}l_{\cdot i}^{y}(t)\right]^{\upsilon_l}, \tag{S.7}$$

where as before $l_{\cdot i}^{y}(t)$ is the labor used in the production sector and a_{it} is the exogenous labor productivity, $\upsilon_l \in (0,1)$ is the share of labor in production costs, $\lambda_\kappa \in [0,1)$ is the share of land in non-labor costs, and ψ_{it} stands for total factor productivity given by

$$\psi_{it}=\bar{\psi}_i y_{it}^{\lambda_\psi}, \tag{S.8}$$

where $\bar{\psi}_i > 0$, and $\lambda_\psi \in [0,1)$. It is assumed that total factor productivity increases with production scale, which captures agglomeration effects of production. Parameter λ_ψ governs the magnitude of agglomeration effects, with $\lambda_\psi = 0$ corresponding to no agglomeration effect. Individual firms are assumed to take ψ_{it} as given.

The representative goods production firm of location i is endowed with $\kappa_{y,i}$ units of production land, where $\kappa_{y,i} > 0$. It is assumed that capital can be relocated without any cost, and thus goods production firms rent capital in a national market and face the same common rental rate nationally. In addition, they hire labor only from local markets. The profit of the representative firm in location i is given as

$$\pi_{it}^{y}=y_{it}-\bar{r}_x\chi_{it}-w_{it}l_{\cdot i}^{y}(t), \tag{S.9}$$

where w_{it} is the wage rate in location i as before, and $\bar{r}_x > 0$ is the capital rental rate that is common to all locations and is assumed to be time invariant. The representative firm chooses χ_{it} and $l^y_{\cdot i}(t)$ to maximize its profits (S.9) subject to (S.7). The resultant demand functions are:

$$\chi_{it} = (1-\lambda_\kappa)(1-\upsilon_l)\frac{y_{it}}{\bar{r}_x}, \tag{S.10}$$

$$l^y_{\cdot i}(t) = \upsilon_l \left(\frac{y_{it}}{w_{it}}\right). \tag{S.11}$$

By substituting (S.10) and (S.8) into (S.7), we obtain

$$y_{it} = \tau_{y,i}\left[a_{it} l^y_{\cdot i}(t)\right]^{\frac{\upsilon_l}{(1-\lambda_\psi)-(1-\lambda_\kappa)(1-\upsilon_l)}}, \tag{S.12}$$

where $\tau_{y,i}$ is a scalar given by

$$\tau_{y,i} = \left(\bar{\psi}_i \kappa_{y,i}^{\lambda_\kappa(1-\upsilon_l)}\right)^{\frac{1}{(1-\lambda_\psi)-(1-\lambda_\kappa)(1-\upsilon_l)}} \left[\frac{(1-\lambda_\kappa)(1-\upsilon_l)}{\bar{r}_x}\right]^{\frac{(1-\lambda_\kappa)(1-\upsilon_l)}{(1-\lambda_\psi)-(1-\lambda_\kappa)(1-\upsilon_l)}}. \tag{S.13}$$

It is easily seen that $\tau_{y,i} > 0$, since $\bar{\psi}_i, \bar{r}_x$ and $\kappa_{y,i} > 0$, and λ_κ and $\upsilon_l \in [0,1)$. By substituting (S.12) into (S.11), we obtain:

$$w_{it} = \upsilon_l \tau_{y,i} (a_{it})^{\tau_a} \left(l^y_{\cdot i}(t)\right)^{-\tau_l}. \tag{S.14}$$

where

$$\tau_a = \frac{\upsilon_l}{\lambda_\kappa(1-\upsilon_l) - \lambda_\psi + \upsilon_l}, \tag{S.15}$$

$$\tau_l = \frac{\lambda_\kappa(1-\upsilon_l) - \lambda_\psi}{\lambda_\kappa(1-\upsilon_l) - \lambda_\psi + \upsilon_l}. \tag{S.16}$$

To ensure that wage rates, w_{it}, increase with productivities, a_{it}, and decrease with labor inputs, $l^y_{\cdot i}(t)$, we assume

$$\lambda_\kappa(1-\upsilon_l) - \lambda_\psi \geq 0, \tag{S.17}$$

which in turn implies $\tau_a > 0$ and $\tau_l \geq 0$.

As can be seen, the main difference between the baseline model in the paper and the extended model is in the specification of the labor demand function, which is now given by (S.14) instead of (18). All other equilibrium conditions continue to have the same form as before. It is also worth noting that when we exclude production land and agglomeration effects by setting,

$$\lambda_\kappa = 0 \text{ and } \lambda_\psi = 0, \tag{S.18}$$

then $\tau_a = 1$ and $\tau_l = 0$ (see (S.15) and (S.16)), and (S.14) simplifies to

$$w_{it} = \tilde{a}_{it}, \tag{S.19}$$

where $\tilde{a}_{it} = \upsilon_l \tau_{y,i} a_{it}$ is the rescaled version of a_{it}. The same simplified outcome follows even if λ_κ and $\lambda_\psi > 0$, so long as

$$\lambda_\psi = \lambda_\kappa \left(1 - \upsilon_l\right). \tag{S.20}$$

Under (S.20), when labor inputs increase, the agglomeration effects that tends to raise productivity are exactly offset by the diminishing marginal productivity of labor. In short, when either (S.18) or (S.20) is satisfied, $w_{it} = \tilde{a}_{it} = \upsilon_l \tau_{y,i} a_{it}$. In these cases, the extended and the baseline models have the same equilibrium conditions.

Note that, according to the estimates obtained by Valentinyi and Herrendorf (2008), the share of land in non-labor costs, λ_κ, is around 0.15, and the share of labor in production costs is around 0.67, which yields an estimate of 0.05 for $\lambda_\kappa (1 - \upsilon_l)$. Also, estimates of the agglomeration effect, λ_ψ, ranges from 0.02 (Davis et al. (2014)) to 0.06 (Ciccone and Hall (1996)). As a result, condition (S.17) holds for any estimate of λ_ψ within the interval $[0.02, 0.05]$, and we have $\tau_a \in [0.96, 1]$ and $\tau_l \in [0, 0.04]$ (see (S.15) and (S.16)), which suggest wage rates, w_{it}, are mainly driven by productivities, a_{it}, and are not that responsive to worker population, $l^y_{\cdot i}(t)$. Therefore, allowing for capital and agglomeration effects in the production function are not likely to significantly alter our main empirical conclusions.

In addition, we are able to show that the non-stochastic version of the extended model has a unique balanced growth path under assumption (S.17). In addition, we are able to show that the non-stochastic version of the extended model has a unique balanced growth path under condition (S.17). To see this, note that on the balanced growth path, the ratio of labor force employed in local production sectors, $l^y_{\cdot i}(t)$, to local populations, $l_{\cdot i}(t)$, should be constant overtime, with $l_{\cdot i}(t)$ and a_{it} growing at the common rates of g_l and g_a, respectively. Also, local housing service prices, q_{it}, house prices, p_{it}, and wage rates, w_{it}, should all grow at the same rate. Denoting this rate by g_w, and using (S.14) it is easily seen that

$$g_w = \tau_a g_a - \tau_l g_l. \tag{S.21}$$

As a result, to ensure the existence of a balanced growth path, location-specific land supply growth rates (which were given by (42) in the baseline model) must now be changed to

$$\tilde{g}^*_{\kappa,i} = g_l - \frac{(1 - \alpha_{\kappa,i})\alpha_m}{\alpha_{\kappa,i}} g_w, \text{ for } i = 1, 2, ..., n. \tag{S.22}$$

Thus, in the non-stochastic version of the extended model, local productivities, a_{it}, intrinsic population growth rates, $g_{l,it}$, are given by (39) and (40) as before, and land supplies, κ_{it}, are given by

$$\kappa_{it} = e^{\tilde{g}^*_{\kappa,i} t} \kappa_i, \text{ for } i = 1, 2, ...n, \text{ and } t = 1, 2, ..., \tag{S.23}$$

where $\tilde{g}^*_{\kappa,i}$ is given by (S.22).

Proposition S2 ***(Existence and uniqueness)*** *Consider the extended version of the dynamic spatial equilibrium model set out in Section 3, and given by equations (6), (15), (22), (27), (28), (35), (37), (38) and (S.14). Suppose labor productivities, land supplies and intrinsic population growth rates across locations, i.e.,* $\boldsymbol{a}_t$, $\boldsymbol{\kappa}_t$ *and* $\boldsymbol{g}_{lt}$, *are given deterministically by (39), (S.23) and (40), and parameters* $\lambda_\kappa \geq 0$, $\lambda_\psi \geq 0$ *and* $\upsilon_l > 0$ *satisfy (S.17). Then,* *there exists a unique balanced growth path, on which prices* $[\boldsymbol{p}_t, \boldsymbol{q}_t, \boldsymbol{w}_t]$ *grow at the common rate of* g_w*, where* g_w *is given by (S.21), and quantities* $[\boldsymbol{l}(t), \boldsymbol{l}^y(t), \boldsymbol{l}^c(t), \boldsymbol{x}_t, \boldsymbol{h}_t]$ *grow at the common rate of* g_l*.*

Proof. The existence of the balanced growth path of the extended model can be proved following the same line of reasoning as in the proof of the existence of the balanced growth path of the baseline model. To establish the uniqueness of the equilibrium, we denote the detrended vectors on the balanced growth path by $\boldsymbol{p}^* = \lim_{t\to\infty} \boldsymbol{p}_t^*$, and $\mathbf{q}^* = \lim_{t\to\infty} \boldsymbol{q}_t^*$, etc. Recall that the detrended aggregate population remains constant over time, as shown in (52). Also recall that by imposing the balance growth path conditions, the equilibrium conditions (6), (15), (22), (28), (35) and (37) can be written in terms of the detrended variables as (55)-(60) as shown in Section 4. In addition, the equilibrium conditions (27), (38) and (S.14) can be written in terms of the detrended variables as

$$
\begin{aligned}
l_{\cdot i}^* &= l_{\cdot i}^{y*} + l_{\cdot i}^{c*}, && \text{(S.24)}\\
w_i^* &= \frac{\alpha_l(1-\alpha_{\kappa,i})x_i^* p_i^*}{l_{\cdot i}^{c*}}, && \text{(S.25)}\\
w_i^* &= \upsilon_l \tau_{y,i} \left(a_i\right)^{\tau_a} \left(l_{\cdot i}^{y*}\right)^{-\tau_l}. && \text{(S.26)}
\end{aligned}
$$

In the rest of the proof, we show that given $L_0, \boldsymbol{\kappa}$ and $\boldsymbol{a}$, then $\boldsymbol{w}^*, \boldsymbol{p}^*, \boldsymbol{q}^*, \boldsymbol{x}^*, \boldsymbol{h}^*, \boldsymbol{l}^*, \boldsymbol{l}^{y*}, \boldsymbol{l}^{c*}$ and $\mathbf{R}^*$ are uniquely determined by (52), (55)-(60), and (S.24)-(S.26).[S1] First, recall that for given values of $\boldsymbol{l}^*, \boldsymbol{\kappa}$ and $\boldsymbol{w}^*$, the solution for $\boldsymbol{p}^*, \boldsymbol{q}^*, \boldsymbol{x}^*$ and $\boldsymbol{h}^*$ is unique and can be obtained using (57), (58), (59) and (60), which is given by (66)-(69). Then, by using (66) and (69), we have

$$
x_i^* p_i^* = \frac{\delta \eta l_{\cdot i}^* w_i^*}{\Gamma_i},
$$

where as before Γ_i is given by

$$
\Gamma_i = \frac{1}{\beta\left(1-\theta_i\right)} - (1-\delta). \tag{S.27}
$$

Note that β and $\theta_i \in (0,1)$, which implies $\beta^{-1}\left(1-\theta_i\right)^{-1} > 1$. Since $\delta > 0$, it follows that $\Gamma_i > \delta > 0$. Using the above equation in (S.25) to eliminate $x_i^* p_i^*$, we have

$$
\frac{l_{\cdot i}^{c*}}{l_{\cdot i}^*} = \frac{\alpha_l(1-\alpha_{\kappa,i})\eta\delta}{\Gamma_i}. \tag{S.28}
$$

Let γ_i be the equilibrium share of labor used in the production sector. Then by (S.24) and (S.28), we have

$$
\gamma_i = \frac{l_{\cdot i}^{y*}}{l_{\cdot i}^*} = 1 - \frac{l_{\cdot i}^{c*}}{l_{\cdot i}^*} = 1 - \frac{\alpha_l(1-\alpha_{\kappa,i})\eta\delta}{\Gamma_i}. \tag{S.29}
$$

[S1] For the baseline model, since wage rates are exogenously determined, i.e., $\boldsymbol{w}^* = \boldsymbol{a}^*$, then $\boldsymbol{p}^*$, $\boldsymbol{x}^*$ and $\boldsymbol{l}^*$ can be solved for given $\boldsymbol{w}^*$. Then, using the solution of $\boldsymbol{p}^*$, $\boldsymbol{x}^*$ and $\boldsymbol{l}^*$, the balanced growth path labor allocations between production and housing sectors, i.e., $\boldsymbol{l}^{y*}$ and $\boldsymbol{l}^{c*}$, can be solved for using (S.24) and (S.25). However, for the extended model, $\boldsymbol{l}^{y*}$, $\boldsymbol{l}^{c*}$, and $\boldsymbol{w}^*$ are jointly determined with all the other variables.

Note that $\alpha_l, \alpha_{\kappa,i}$ and η all lie in the interval $(0,1)$, and hence $\alpha_l(1-\alpha_{\kappa,i})\eta \in (0,1)$. Recall also that $\Gamma_i > \delta > 0$ as previously shown. It follows that $\gamma_i \in (0,1)$. Thus, (S.26) can be written as

$$w_i^* = \varpi_i \left(l_{\cdot i}^*\right)^{-\tau_l}. \tag{S.30}$$

where

$$\varpi_i = \upsilon_l \tau_{y,i} \left(a_i\right)^{\tau_a} \gamma_i^{-\tau_l}. \tag{S.31}$$

It is now easily seen that $\varpi_i > 0$, since $\tau_{y,i}$ and γ_i, given by (S.13) and (S.29), are strictly positive as previously shown. Using (S.30) in (67) to eliminate w_i^*, we obtain

$$q_i^* = \left(\frac{\delta\eta}{\tau_i \kappa_i}\right)^{\alpha_{\kappa,i}} \Gamma_i^{1-\alpha_{\kappa,i}} \left(l_{\cdot i}^*\right)^{\alpha_{\kappa,i}-\tau_l[\alpha_{\kappa,i}+\alpha_l(1-\alpha_{\kappa,i})]} \left(\varpi_i\right)^{\alpha_{\kappa,i}+\alpha_l(1-\alpha_{\kappa,i})}. \tag{S.32}$$

By substituting (S.30) and (S.32) into (56) to eliminate w_i^* and q_i^*, then ρ_{ij}^* can be written as a function of $\boldsymbol{l}^*$:

$$\rho_{ij}^* = \frac{\tilde{\psi}_{ij} \left(l_{\cdot j}^*\right)^{-\tilde{\varphi}_j}}{\sum_{s=1}^n \tilde{\psi}_{is} \left(l_{\cdot s}^*\right)^{-\tilde{\varphi}_s}}, \tag{S.33}$$

where

$$\begin{aligned}
\tilde{\varphi}_j &= \eta\alpha_{\kappa,j} + \tau_l \left\{1 - \eta\left[\alpha_{\kappa,j} + \alpha_l(1-\alpha_{\kappa,j})\right]\right\}, \\
\tilde{\psi}_{ij} &= \alpha_{ij}^{-\psi} \left(\frac{\delta\eta}{\tau_j \kappa_j}\right)^{-\eta\alpha_{\kappa,j}} \Gamma_j^{-\eta(1-\alpha_{\kappa,j})} \left(\varpi_j\right)^{1-\eta[\alpha_{\kappa,j}+\alpha_l(1-\alpha_{\kappa,j})]}.
\end{aligned}$$

Note that $\eta, \alpha_{\kappa,j}$ and α_l all lie in the interval $(0,1)$, and under assumption (S.17) τ_l, given by (S.16) is non-negative. It follows that $\tilde{\varphi}_j > 0$, for any $i \in \mathcal{I}_n$.[S2] In addition, note that $\tilde{\psi}_{ij} > 0$, for any i and $j \in \mathcal{I}_n$, since α_{ij},δ, η,τ_j and $\kappa_j > 0$, and Γ_j and ϖ_j, given by (S.27) and (S.31), are strictly positive as previously shown. Recall that $\mathbf{R}^*$ is the migration probability matrix on the balanced growth path, with a typical element ρ_{ij}^* given by (S.33). Thus, $\mathbf{R}^*$ can be written as a function of $\boldsymbol{l}^*$, namely $\mathbf{R}^* \equiv \mathbf{R}(\boldsymbol{l}^*)$. Then, (55) can be written more compactly as

$$\boldsymbol{l}^* = \boldsymbol{l}^* \mathbf{R}(\boldsymbol{l}^*), \tag{S.34}$$

which is a system of non-linear equations in $\boldsymbol{l}^*$. Lemma A1 in the Appendix establishes that there exists a $\boldsymbol{l}^*$ that solves (S.34). Lemma A2 establishes that (S.34) cannot have more than one solution. Therefore, $\boldsymbol{l}^*$ exists and is unique. Then, using the solution of $\boldsymbol{l}^*$, the other variables of the model, namely, $\boldsymbol{w}^*, \boldsymbol{p}^*, \boldsymbol{q}^*, \boldsymbol{x}^*, \boldsymbol{h}^*, \boldsymbol{l}^{y*}, \boldsymbol{l}^{c*}$ and $\mathbf{R}^*$, can be solved for using equations (66) to (69), (S.24)-(S.26) and (S.33).■

S2.2 Quantitative differences between models with and without endogenously determined wages

To examine how the extended model quantitatively differs from the base-line model, we carried out the simulations presented in Section 7.1 and the counterfactual experiments

[S2] Note that for any a and $b \in (0,1)$, it follows that $a + b(1-a) \in (0,1)$.

reported in Section 7.4 using the extended model. We calibrated the extended model by setting the share of labor in production costs, υ_l, to 0.67, according to the estimates obtained by Valentinyi and Herrendorf (2008). To distinguish between scale effects of ψ_{it} and a_{it} in (S.7), we set $\bar{\psi}_i$ defined by (S.8) such that $\tau_{y,i} = 1$, where $\tau_{y,i}$ is given by (S.13). We experimented with different values of λ_ψ and λ_κ. In particular, we considered the values $\lambda_\psi = (0, 0.02, 0.05)$, and $\lambda_\kappa =$ (0.15, 0.2, 0.25 and 0.3). Given λ_ψ and λ_κ, the values of τ_a and τ_l are then set by (S.15) and (S.16). For each pair of λ_ψ and λ_κ, we infer w_{it} using (S.11), where the worker population, $l^y_{\cdot i}(t)$, is measured using the actual state-level population, and the state-specific output, y_{it}, is measured by multiplying realized real per capita disposable income of the state by its population. Labor productivities, a_{it}, are then inferred using (S.14). The rest of the parameters are calibrated and estimated as before (see Section 5). The comparative simulation results for dispersion of house price-to-income ratios are reported in Table S1, and the results of counterfactual exercises on the effects of changes in land-use regulations in California and Texas are summarized in S2. As can be seen from these results, allowing for capital and agglomeration effects in production have little effects on the simulation and counterfactual outcomes. Also as to be expected when $\lambda_\psi = 0.05$ and $\lambda_\kappa = 0.15$, which implies $\tau_a = 1$ and $\tau_l = 0$, the results of our model and the extend model are identical. In particular, the results for the baseline and extended models are very close even if one considers the combination of $(\lambda_\psi, \lambda_\kappa) = (0.02, 0.3)$ which results in the largest differences in the outcomes. For example, for this parametrization the dispersion of house price-to-income ratio in the U.S. falls from 0.39251 (baseline model) to 0.39232 (extended model), with very similar small changes obtained for between and within region dispersions. Similarly, the effects of changes to land-use regulations in California and Texas are only marginally affected when we allow wages to be determined endogenously.

Table S1: Dispersions of house price-to-income ratios for 2014 simulated by the baseline model and the extended model with endogenously determined wages

	Baseline model	Extended model with endogenous wages					
	(1)	(2)	(3)	(4)	(5)	(6)	(7)
λ_ψ		0.05	0.02	0	0.02	0.02	0.02
λ_K		0.15	0.15	0.15	0.2	0.25	0.3
τ_l		0	0.042	0.069	0.064	0.085	0.105
τ_a		1	0.958	0.931	0.936	0.915	0.895
The U.S.	0.39251	0.39251	0.39243	0.39239	0.39240	0.39236	0.39232
Between-region	0.32576	0.32576	0.32573	0.32570	0.32571	0.32569	0.32567
Northeast	0.21205	0.21205	0.21192	0.21184	0.21186	0.21180	0.21174
Southeast	0.21530	0.21530	0.21510	0.21498	0.21500	0.21490	0.21481
Midwest	0.15766	0.15766	0.15765	0.15764	0.15764	0.15763	0.15763
Southwest	0.26416	0.26416	0.26429	0.26438	0.26436	0.26443	0.26449
West	0.26744	0.26744	0.26737	0.26732	0.26733	0.26729	0.26726

Notes: This table reports the dispersions of log house price-to-income ratios for 2014 simulated by the baseline model defined in Section 3, and the extended model with endogenously determined wages defined in Section S2. Columns 2 to 7 report the simulation results of the extended model for different λ_ψ and λ_κ. Given λ_ψ and λ_κ, the values of τ_a and τ_l are then set by (S.15) and (S.16).

Table S2: Effects of land-use regulation changes in California and Texas simulated by the baseline model and the extended model with endogenously determined wages

	Baseline model	Extended model with endogenous wages					
	(1)	(2)	(3)	(4)	(5)	(6)	(7)
λ_ψ		0.05	0.02	0	0.02	0.02	0.02
λ_K		0.15	0.15	0.15	0.2	0.25	0.3
τ_l		0	0.042	0.069	0.064	0.085	0.105
τ_a		1	0.958	0.931	0.936	0.915	0.895
I. Counterfactual increases in land supply growth in California							
Actual land growth:							
Population (millions)	31.400	31.400	31.378	31.365	31.367	31.357	31.347
House price (Thousands $)	302.056	302.056	301.802	301.650	301.675	301.560	301.453
National average land growth:							
Population (millions)	32.667	32.667	32.631	32.609	32.612	32.595	32.579
House price (Thousands $)	129.330	129.330	129.023	128.836	128.868	128.722	128.585
II. Counterfactual decreases in land supply growth in Texas							
Actual land growth:							
Population (millions)	20.254	20.254	20.272	20.282	20.280	20.288	20.296
House price (Thousands $)	85.159	85.159	85.254	85.312	85.302	85.348	85.390
National average land growth:							
Population (millions)	19.639	19.639	19.664	19.680	19.677	19.689	19.701
House price (Thousands $)	123.700	123.700	123.931	124.074	124.050	124.161	124.266

Notes: This table shows (I) the impacts of loosening of land-use regulations in California and (II) the impacts of tightening of land-use regulations in Texas on the local house prices and population, simulated by the baseline model defined in Section 3, and the extended model with endogenously determined wages defined in Section S2. Columns 2 to 7 report the simulation results of the extended model for different λ_ψ and λ_κ. Given λ_ψ and λ_κ, the values of τ_a and τ_l are then set by (S.15) and (S.16).

S3 Extended model with mortgage loans

The cyclical fluctuations in house prices can have important implications for the macro economy and thus have long been a topic of interest of economists. In particular, Ortalo-Magne and Rady (2006), Mian and Sufi (2009), Favilukis et al. (2017), and Favara and Imbs (2015), have shown that the supplies of mortgage credit have played an important role in driving fluctuations in the aggregate house prices. However, much less attention is paid to the cyclical fluctuations in house price dispersions. We contribute to this strand of literature by examining the role of credit supply shocks in generating fluctuations in house price dispersions using an extended version of our baseline model in which landlords are allowed to borrow mortgage loans.

S3.1 Theoretical derivations

In this extended version of the baseline model, only the optimization problems of landlords are changed, while all the other components are kept the same. Recall that the life time utility of landlords in location i is given by

$$E_t \sum_{s=0}^{\infty} (\beta e^{g_l})^s \ln(c^o_{i,t+s}), \tag{S.35}$$

and that the realized net return on housing investment in location i in period t is given by

$$r^o_{it} = (1-\theta_i)\left[\frac{q_{it} + (1-\delta)p_{it}}{p_{i,t-1}}\right]. \tag{S.36}$$

We introduce mortgage loans by assuming that landlords can finance housing investment by borrowing from outside lenders, who passively lend at a time-invariant and exogenously determined interest rate r. We assume that $e^{-r} > \beta$, which implies that the subjective discount rate of landlords, β, is lower than the discount rate implied by the interest rate, e^{-r}. Thus, landlords tend to borrow as much as possible until their borrowing constraints bind. The outstanding balance of the mortgage debts owed by the landlord in period t is denoted by d_{it}. Let b_{it} denote the amount of new mortgage loans obtained by the landlord.[S3] Thus, the landlords' outstanding balance of mortgage debts evolves as:

$$d_{it} = e^r d_{i,t-1} + b_{it} \tag{S.37}$$

Furthermore, following Philippon and Midrigan (2016), we assume a borrowing constraint that limits the landlords' ability to obtain new mortgage loans:

$$b_{it} \le \phi_t p_{it} h_{it}, \tag{S.38}$$

where ϕ_t is the required loan-to-value (LTV henceforth) ratio for new mortgage loans, which is assumed to be common to all locations and follow the following exogenous stochastic process:

$$\phi_t - \phi^* = \rho_\phi \left(\phi_{t-1} - \phi^*\right) + \sigma_\phi \varepsilon_{\phi,t}, \tag{S.39}$$

[S3] We allow b_{it} to be negative, and when $b_{it} < 0$, the landlord is making net repayments.

where $\phi^* > 0$ is the long-run LTV, $\rho_\phi \in (0,1)$, and $\varepsilon_{\phi,t} \sim IIDN(0,1)$. As argued by Philippon and Midrigan (2016), this assumption of borrowing constraints captures the idea that a tightening of the credit limit precludes agents from obtaining new loans, but does not force them to prepay old debts. We consider only the cases in which the borrowing constraint (S.38) always binds in equilibrium. Thus, credit supply shocks, which refer to the exogenous changes in ϕ_t, can affect the landlords' demand for housing via tightening or loosening the borrowing constraint.[S4]

Then, the landlords' flow of funds constraint is given by

$$c_{it}^o l_{it}^o + p_{it} h_{it} = r_{it}^o \left(p_{i,t-1} h_{i,t-1}\right) + \left(d_{it} - e^r d_{i,t-1}\right). \tag{S.40}$$

As compared to the baseline model (see (33)), the landlord now has an additional source of funds for housing investment, which is the net borrowing from the outside lenders, i.e., $d_{it} - e^r d_{i,t-1}$. Recall that the borrowing constraint (S.38) is assumed to always bind. Thus, using (S.37) and the binding borrowing constraint (S.38) in (S.40) to replace d_{it}, we have

$$c_{it}^o l_{it}^o + \left(1 - \phi_t\right) p_{it} h_{it} = r_{it}^o \left(p_{i,t-1} h_{i,t-1}\right). \tag{S.41}$$

Thus, the landlords' optimization problem is reduced to the following: choosing c_{it}^o and h_{it} to maximize the life time utility (S.35) subject to (S.41). Similarly to the baseline model, the optimal housing investment of the landlord is given by

$$p_{it} h_{it} \left(1 - \phi_t\right) = \beta e^{g_l} \left(1 - \theta_i\right) \left[q_{it} + (1-\delta) p_{it}\right] h_{i,t-1}. \tag{S.42}$$

As compared to the baseline model (see (35)), the credit supply shock, ϕ_t, now has a role in determining housing investment.

S3.2 Calibration

The values of the parameters that are common in the baseline model and the extended model are kept the same. We only calibrate the parameters that are specific to the extended model. The long-run ratio of new mortgage loan to house value, ϕ^*, in (S.39), is calibrated as follows. Note that using (S.37), d_{it} can be re-written as

$$d_{it} = b_{it} + e^r b_{i,t-1} + e^{2r} b_{i,t-2} ..., + e^{tr} b_{i0}. \tag{S.43}$$

Recall that the borrowing constraint (S.38) is assumed to always bind. Using the binding (S.38) in (S.43) to replace b_{it}, we have

$$d_{it} = \phi_t p_{it} h_{it} + e^r \phi_{t-1} p_{i,t-1} h_{i,t-1} + e^{2r} \phi_{t-2} p_{i,t-2} h_{i,t-2} + ... + e^{tr} \phi_0 p_{i0} h_{i0}. \tag{S.44}$$

Consider the non-stochastic version of the extended model in which $\phi_t = \phi^*$ for any t. On the balanced growth path, the detrended outstanding mortgage debts, housing stocks, and house

[S4] We focus on the role of borrowing constraints rather than that of mortgage rates in driving fluctuations in house price dispersions because recent literature, such as, Favilukis et al. (2017), have shown that relaxation of financing constraints can lead to booms in house prices; however, low interest rates cannot explain high house values.

prices are time invariant, and denoted by $d_i^* \equiv \lim_{t\to\infty} e^{-(g_a+g_l)t} d_{it}$, $h_i^* \equiv \lim_{t\to\infty} e^{-g_l t} h_{it}$ and $p_i^* \equiv \lim_{t\to\infty} e^{-g_a t} p_{it}$. Thus, as $t \to \infty$, (S.44) can be written as

$$\begin{aligned} d_i^* &= \phi^* h_i^* p_i^* \sum_{s=0}^{\infty} e^{-s(g_a+g_l-r)}, \\ &= \frac{\phi^* h_i^* p_i^*}{1-e^{-(g_a+g_l-r)}}, \end{aligned} \tag{S.45}$$

which can be re-written as

$$\frac{d_i^*}{h_i^* p_i^*} = \frac{\phi^*}{1-e^{-(g_a+g_l-r)}} \quad \text{for all} \quad i = 1, 2, ..., n,$$

and since $d_i^* / (h_i^* p_i^*)$ is constant across i, then we have

$$\frac{\sum_{i=1}^n d_i^*}{\sum_{i=1}^n h_i^* p_i^*} = \frac{\phi^*}{1-e^{-(g_a+g_l-r)}}. \tag{S.46}$$

where $\sum_{i=1}^n d_i^* / (\sum_{i=1}^n h_i^* p_i^*)$ is the balanced growth path ratio of aggregate outstanding mortgage debt to aggregate house value. Note that the average ratio of the aggregate outstanding mortgage debt to the aggregate house value of the U.S. over the period 1976-2014 is around 40%, and recall that g_a and g_l are calibrated to 1.94% and 1% as discussed in Section 5. Recall that r is assumed to be small enough such that $e^{-r} > \beta$ holds. Specifically, we set r to 0. Thus, (S.46) implies that $\phi^* = 0.01$.

Recall that in the model, ϕ_t is the ratio of new mortgage loan to house value in period t, which is common to all locations. Thus, the series of ϕ_t are measured using the ratios of the realized increases in the aggregate outstanding mortgage debt to the realized aggregate house value, which are scaled to ensure that $\frac{1}{T}\sum_{t=1}^T \hat{\phi}_t = \phi^*$:

$$\hat{\phi}_t = \phi^* \left(\frac{mort_t - mort_{t-1}}{hval_t} \right) \left[\frac{1}{T} \sum_{s=1}^{T} \left(\frac{mort_s - mort_{s-1}}{hval_s} \right) \right]^{-1}$$

where ϕ^* is calibrated to 0.01 as previously discussed, $mort_t$ is the realized aggregate outstanding mortgage debt in year t, and $hval_t$ is the realized aggregate house value.[S5] Figure S1 plots the growth rates of the national house price index and the estimated credit supply shocks $\hat{\phi}_t$. To estimate the autoregression coefficient ρ_ϕ and the standard deviation of innovation σ_ϕ in (S.39), we regress $\hat{\phi}_t - \phi^*$ on $\hat{\phi}_{t-1} - \phi^*$, and the estimated ρ_ϕ and σ_ϕ are 0.94 and 0.004, respectively.

[S5] Aggregate home value and aggregate outstanding mortgage debt correspond to the line 4 and 34 of Table B.101 in the Financial Accounts of the United States data from the Federal Reserve Board's Z.1 release. For further information, see `https://www.federalreserve.gov/releases/z1/current/`.

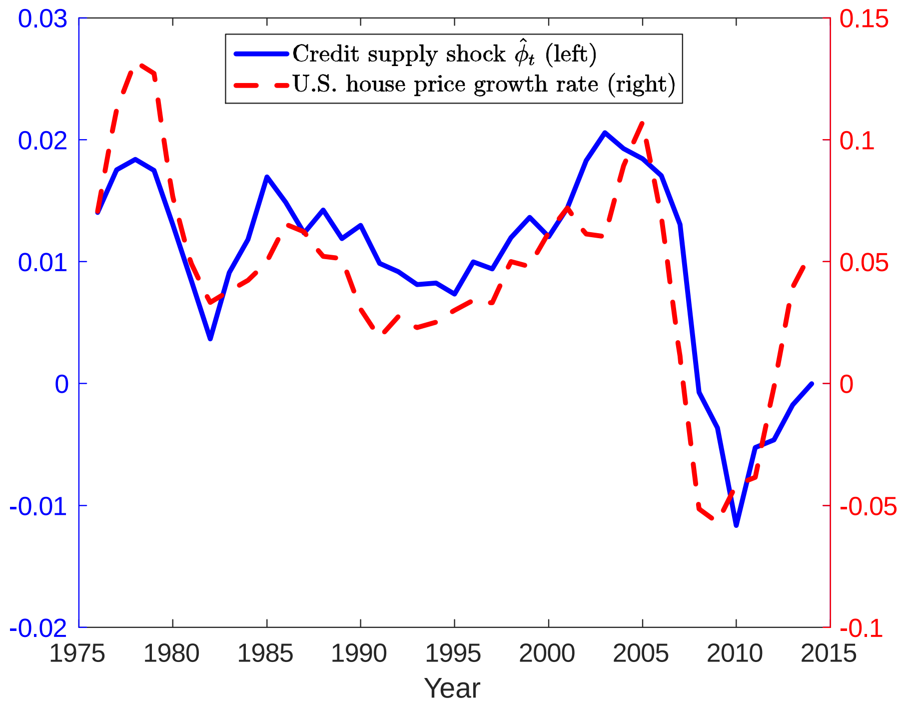

Figure S1: Measured credit supply shock $\hat{\phi}_t$ and growth rate of aggregate house price

S3.3 Cyclical fluctuations of house price dispersion

Note that the extended model is exactly the same as the baseline model except that (35) is replaced by (S.42). In addition, the stochastic processes of credit supply shock, ϕ_t, is given by (S.39).

To examine the extended model's ability in explaining the cyclical fluctuations of house price dispersion during the period 1976-2014, we simulate the extended model using the realized productivity and credit supply shocks. Though $\boldsymbol{a}_t, \boldsymbol{\kappa}_t$ and ϕ_t, are stochastic in the model, we take them as deterministic variables in the following simulations, and set $\boldsymbol{a}_t$ and ϕ_t to their actual values, and $\boldsymbol{\kappa}_t$ as

$$\boldsymbol{\kappa}_t = \hat{\boldsymbol{\kappa}}\ \mathbf{diag}(e^{\hat{g}_{\kappa,1}t}, e^{\hat{g}_{\kappa,2}t}, ...e^{\hat{g}_{\kappa,n}t}), \text{ for } t = 0, 1, ..., T,$$

where $\hat{\boldsymbol{\kappa}}$ and $\hat{\boldsymbol{g}}_\kappa$, are estimated in Section 5.5. The realized national credit supply shock, ϕ_t, is measured using the national mortgage data in Section S3.2. In addition, as in the baseline simulation in Section 7.1, the state level intrinsic population growth rates, $\boldsymbol{g}_{l,t}$, are set to their actual values, which are estimated in Section 5.2. The initial values, $\boldsymbol{l}(0)$ and $\boldsymbol{q}_0$ correspond to the actual 1976 economy.

Figure S2 shows the realized and the model simulated series of the aggregate house price and the dispersion of house prices across U.S. states. As shown in the figure, the extended model can capture a substantial part of the cyclical fluctuations in the aggregate house price and the dispersion of house prices.

To investigate the impacts of a national credit supply shock on the state level house prices, we analyze the impulse responses of the economy to a one standard deviation expansionary national credit supply shock.[S6] Figure S3 shows the response of the dispersion of house price-to-income ratio across U.S. states to the shock. Figures S4 and S5 show the responses of house price-to-income ratios and housing stocks in U.S. states to the shock. States, ordered by their housing supply elasticities, $1 - \alpha_{\kappa,i}$, are given from top to bottom and from left to right. As shown in the figures, states with lower housing supply elasticities experience relatively larger increases in house prices and smaller increases in housing stocks, while those with lower supply elasticities experienced smaller increases in prices and larger increases in housing stocks.

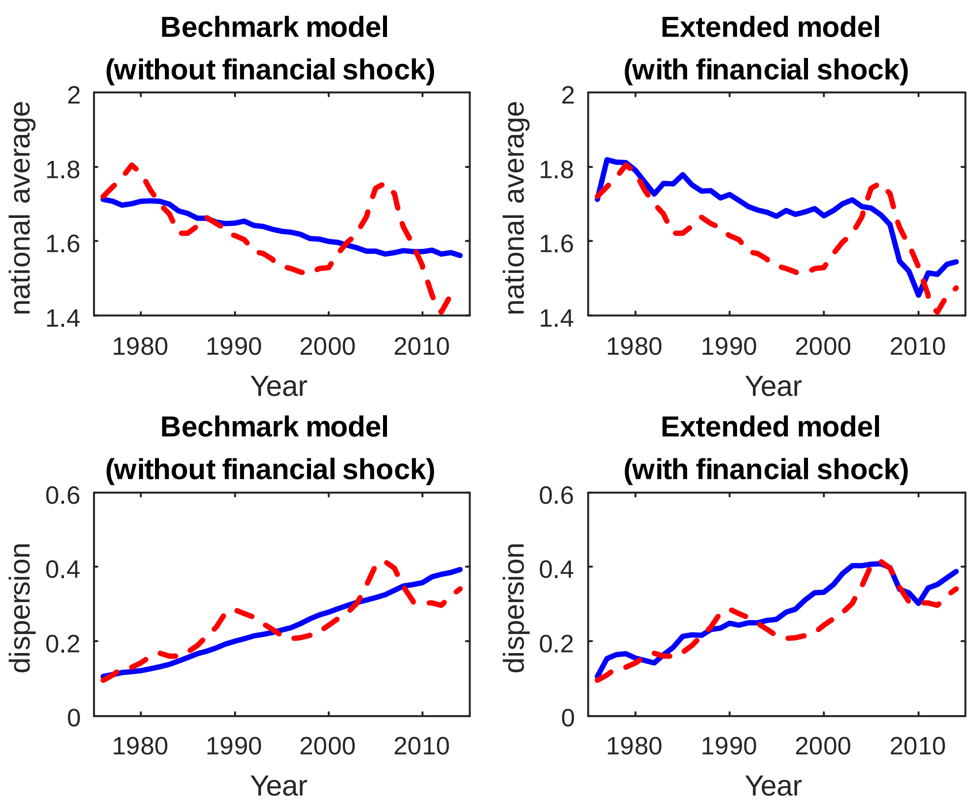

Figure S2: Log house price-to-income ratio of the U.S. and the dispersion of log house price-to-income ratios across U.S. states (Solid-blue: simulated; Dashed-red: data)

[S6]For the details of the computation of the impulse responses, please see Section S4 of the online supplement.

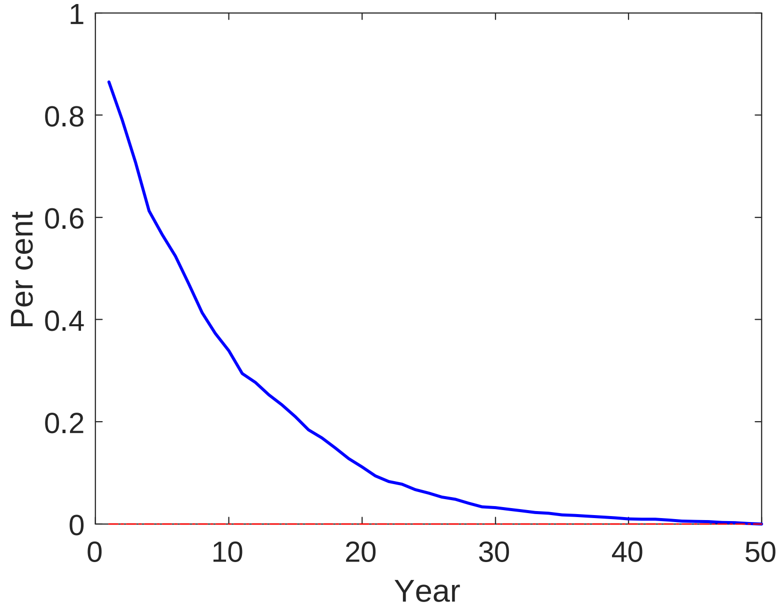

Figure S3: Reponses of the dispersion of log house price-to-income ratios across U.S. states to a national expansionary credit supply shock

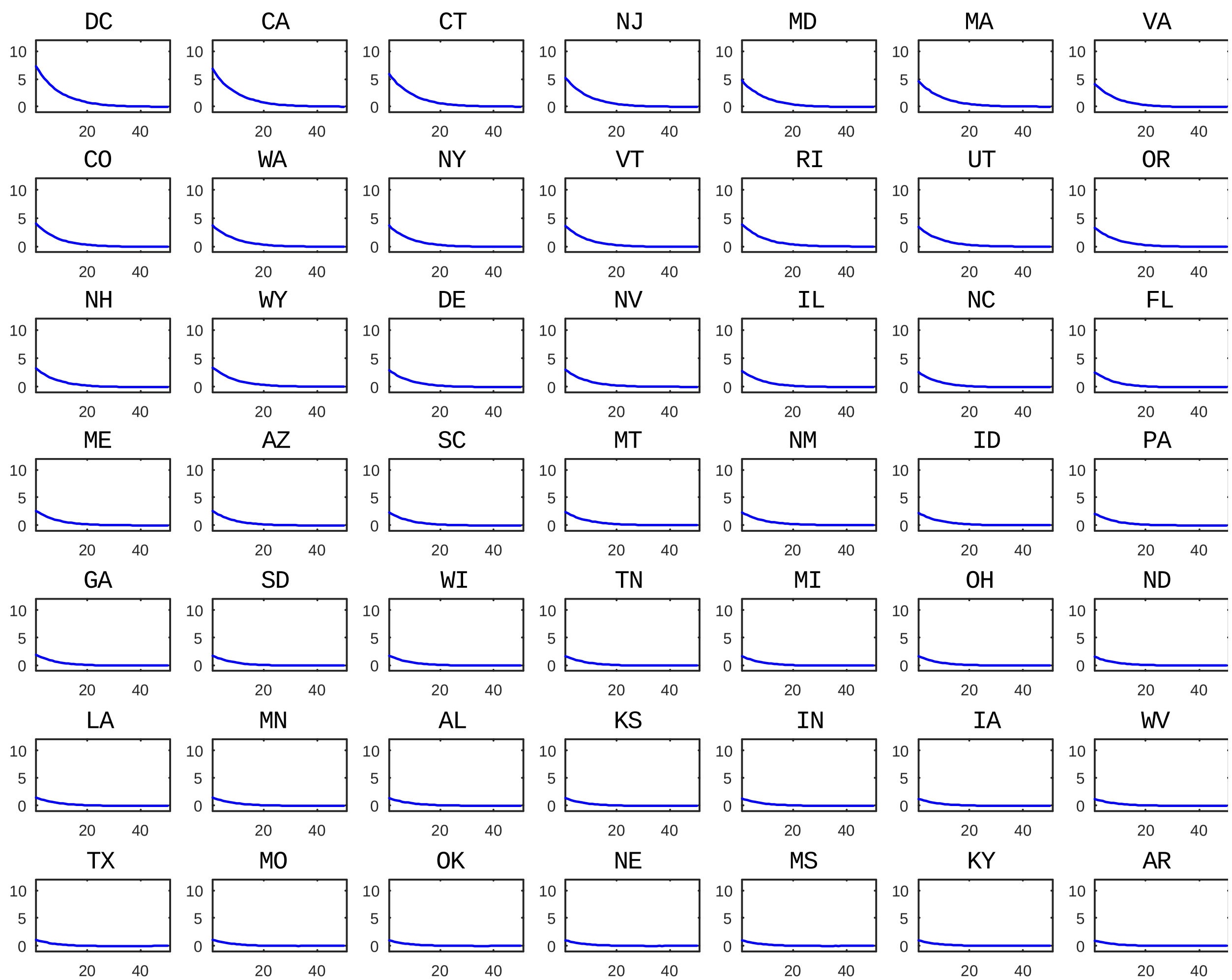

Figure S4: Reponses of log house price-to-income ratios of U.S. states to a national expansionary credit supply shock

Notes: This figure shows the responses of house price-to-income ratios of U.S. states to a one standard deviation expansionary national credit supply shock. States are ordered ascendingly by their housing supply elasticities, $1-\alpha_{\kappa,i}$, from top to bottom and left to right. The unit on the horizontal axis is year. The unit on the vertical axis is per cent.

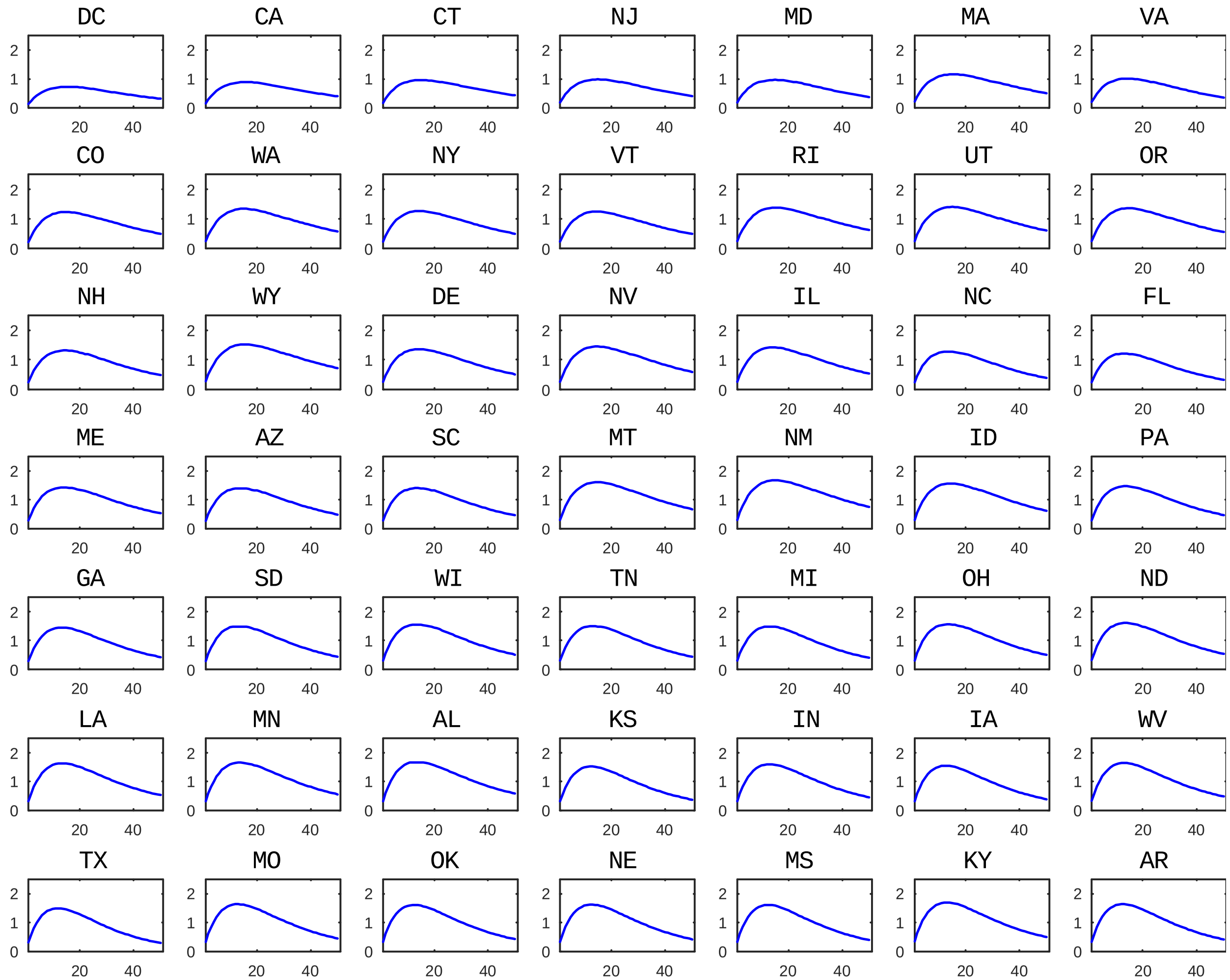

Figure S5: Responses of log housing stocks of U.S. states to a national expansionary credit supply shock

Notes: This figure shows the responses of housing stocks of U.S. states to a one standard deviation expansionary national credit supply shock. States are ordered ascendingly by their housing supply elasticities, $1 - \alpha_{\kappa,i}$, from top to bottom and left to right. The unit on the horizontal axis is year. The unit on the vertical axis is per cent.

S4 Computation of the impulse responses

The impulse responses reported in the paper are computed using the Monte Carlo techniques developed by Koop et al. (1996). As discussed in Section 6, the model economy set out in Section 3 can be written in a compact form as:

$$\boldsymbol{\zeta}_t = \boldsymbol{f}\left(\boldsymbol{\zeta}_{t-1}, \boldsymbol{a}_t, \boldsymbol{a}_{t-1}, \boldsymbol{\kappa}_{t-1}, \boldsymbol{g}_{l,t}; \Theta\right), \tag{S.47}$$

where Θ is a row vector that contains all the parameters, $\boldsymbol{\zeta}_t = [\boldsymbol{l}(t), \boldsymbol{q}_t]$ is a $1 \times 2n$ vector, and

$$\boldsymbol{\chi}_t = \boldsymbol{g}\left(\boldsymbol{\zeta}_t, \boldsymbol{a}_t, \boldsymbol{\kappa}_t; \Theta\right), \tag{S.48}$$

where $\boldsymbol{\chi}_t = [\boldsymbol{p}_t, \boldsymbol{h}_t]$ is a $1 \times 2n$ vector.

Define $\boldsymbol{\xi}_t = [\boldsymbol{\zeta}_t, \boldsymbol{\chi}_t]$, which is a $1\times 4n$ vector. Then, the (S.47) and (S.48) can be combined and written as

$$\boldsymbol{\xi}_t = \boldsymbol{\psi}\left(\boldsymbol{\xi}_{t-1}, \boldsymbol{a}_t, \boldsymbol{a}_{t-1}, \boldsymbol{\kappa}_t, \boldsymbol{\kappa}_{t-1}, \boldsymbol{g}_{l,t}; \Theta\right). \tag{S.49}$$

The stochastic processes of $\boldsymbol{a}_t$ and $\boldsymbol{\kappa}_t$, are given by

$$\begin{aligned}
\ln \boldsymbol{a}_t &= \ln \boldsymbol{a} + \boldsymbol{g}_a t + \boldsymbol{\lambda} f_t + \boldsymbol{z}_{a,t}, && \text{(S.50)}\\
f_t &= \rho_f f_{t-1} + \sigma_f \varepsilon_{f,t}, && \text{(S.51)}\\
\boldsymbol{z}_{a,t} &= \boldsymbol{z}_{a,t-1}\mathbf{diag}(\rho_{z_a,1}, \rho_{z_a,2}, ...\rho_{z_a,n}) + \boldsymbol{\varepsilon}_{z_a,t}\mathbf{diag}(\sigma_{z_a,1}, \sigma_{z_a,2}, ...\sigma_{z_a,n}), && \text{(S.52)}
\end{aligned}$$

and

$$\begin{aligned}
\ln \boldsymbol{\kappa}_t &= \ln \boldsymbol{\kappa} + \boldsymbol{g}_\kappa t + \boldsymbol{z}_{\kappa,t}, && \text{(S.53)}\\
\boldsymbol{z}_{\kappa,t} &= \boldsymbol{z}_{\kappa,t-1}\mathbf{diag}(\rho_{z_\kappa,1}, \rho_{z_\kappa,2}, ...\rho_{z_\kappa,n}) + \boldsymbol{\varepsilon}_{z_\kappa,t}\mathbf{diag}(\sigma_{z_\kappa,1}, \sigma_{z_\kappa,2}, ...\sigma_{z_\kappa,n}), && \text{(S.54)}
\end{aligned}$$

and the values of state level intrinsic population growth rates, $\boldsymbol{g}_{l,t}$, for $t = 0, 1, 2, ...,$ are exogenously given.

Impulse response function: To illustrate the computation algorithm, we take the computation of the impulse responses to a standard deviation negative productivity shock to State i^* as an example. Note that the model is Markovian. Thus, the relevant history is only the period before the start of simulation. Let the shock hits the economy in period 1. Then, the impulse response function is given by

$$\begin{aligned}
GI_\xi(t, \varepsilon_{z_a,i^*1}, \boldsymbol{\xi}_0, \boldsymbol{a}_0, \boldsymbol{\kappa}_0) &= E(\boldsymbol{\xi}_t | \varepsilon_{z_a,i^*1}, \boldsymbol{\xi}_0, \boldsymbol{a}_0, \boldsymbol{\kappa}_0) - E(\boldsymbol{\xi}_t | \boldsymbol{\xi}_0, \boldsymbol{a}_0, \boldsymbol{\kappa}_0)\\
\text{for } t &= 1, 2, ..., T,
\end{aligned}$$

where T is the horizon of the impulse response analyses, $E(\boldsymbol{\xi}_t | \boldsymbol{\xi}_0, \boldsymbol{a}_0, \boldsymbol{\kappa}_0)$ is the expectation of $\boldsymbol{\xi}_t$ conditional only on $\boldsymbol{\xi}_0$, $\boldsymbol{a}_0$ and $\boldsymbol{\kappa}_0$, and $E(\boldsymbol{\xi}_t | \varepsilon_{z,i^*1}, \boldsymbol{\xi}_0, \boldsymbol{a}_0, \boldsymbol{\kappa}_0)$ is the expectation of $\boldsymbol{\xi}_t$ conditional on both $\boldsymbol{\xi}_0, \boldsymbol{a}_0, \boldsymbol{\kappa}_0$ and ε_{z,i^*1}. Recall that ε_{z,i^*1} is the innovation to the local productivity shock in State i^* in period 1.

Initial values: In our impulse response simulations, we assume that the economy is on the balanced growth path when $t = 0$. Recall that in Section 4, we established the uniqueness of the balanced growth path by showing that for given values of $L_0, \boldsymbol{\kappa}$ and $\boldsymbol{a}$, the steady states of the detrended variables are uniquely determined by the equation system (54)-(61). Note that detrended variables equal non-detrended variables when $t = 0$. Thus, we use the steady state values of the detrended variables as the initial values for the corresponding non-detrended variable in the impulse response simulations, which implies that the economy is on the balanced growth path when $t = 0$.

Deterministic variables: The intrinsic population growth rates of all states are set equal to the balanced growth path level given by (40):

$$\boldsymbol{g}_{l,t} = [\hat{g}_l, \hat{g}_l, ..., \hat{g}_l], \text{ for } t = 1, 2, ..., T,$$

where g_l is the balanced growth path intrinsic population growth rate, which is assumed to be common to all states, and estimated as the average growth rate of the national population over the period 1976-2014.

Stochastic processes: The state level productivities and land supplies, $\boldsymbol{a}_t$ and $\boldsymbol{\kappa}_t$, are simulated using the estimated (S.50) - (S.54), where f_0, $\boldsymbol{z}_{a0}$ and $\boldsymbol{z}_{\kappa 0}$ are set to 0.

We set the numbers of replications and horizons to R and T, and independently draw innovations from the standard normal distribution. Let $\varepsilon_{f,t}^{(r)}$, $\boldsymbol{\varepsilon}_{z_a,t}^{(r)}$ and $\boldsymbol{\varepsilon}_{z_\kappa,t}^{(r)}$ denote the simulated $\varepsilon_{f,t}$, $\boldsymbol{\varepsilon}_{z,t}$ and $\boldsymbol{\varepsilon}_{z_\kappa,t}$, for replication r, where $\boldsymbol{\varepsilon}_{z_a,t}^{(r)} = \left[\varepsilon_{z_a,1t}^{(r)}, \varepsilon_{z_a,2t}^{(r)}, ..., \varepsilon_{z_a,nt}^{(r)}\right]$ and $\boldsymbol{\varepsilon}_{z_\kappa,t}^{(r)} = \left[\varepsilon_{z_\kappa,1t}^{(r)}, \varepsilon_{z_\kappa,2t}^{(r)}, ..., \varepsilon_{z_\kappa,nt}^{(r)}\right]$. The innovations, $\varepsilon_{f,t}^{(r)}$, $\varepsilon_{z_a,it}^{(r)}$ and $\varepsilon_{z_\kappa,it}^{(r)}$, for $i = 1, 2, ..., n$, $t = 1, 2., ..., T$ and $r = 1, 2., ..., R$, are independently drawn from the standard normal distribution.

Productivity processes without shock: When there is no shock, for each replication r, we plug the simulated innovations, $\varepsilon_{f,t}^{(r)}$ and $\boldsymbol{\varepsilon}_{z_a,t}^{(r)}$, into (S.50) - (S.52), and obtain a series of simulated productivities, $\boldsymbol{a}_t^{(r)}$, for $t = 1, 2., ..., T$.

Productivity processes with shock: When there is shock, for each replication r, we plug the simulated innovations, $\varepsilon_{f,t}^{(r)}$ and $\boldsymbol{\varepsilon}_{z_a,t}^{(r)}$, with the i^*th element of $\boldsymbol{\varepsilon}_{z_a,1}^{(r)}$, i.e., $\varepsilon_{z_a,i^*1}^{(r)}$, being replaced by -1 (a negative shock), into (S.50) - (S.52), and obtain another series of simulated productivities, $\check{\boldsymbol{a}}_t^{(r)}$, for $t = 1, 2., ..., T$.

Land supply processes: For both the cases with and without shock, for each replication r, we plug the simulated innovations, $\boldsymbol{\varepsilon}_{z_\kappa,t}^{(r)}$, into (S.53) - (S.54), and obtain a series of simulated productivities, $\boldsymbol{\kappa}_t^{(r)}$, for $t = 1, 2., ..., T$.

Computation: To compute $E(\boldsymbol{\xi}_t|\boldsymbol{\xi}_0, \boldsymbol{a}_0, \boldsymbol{\kappa}_0)$ and $E(\boldsymbol{\xi}_t|\varepsilon_{z,i^*1}, \boldsymbol{\xi}_0, \boldsymbol{a}_0, \boldsymbol{\kappa}_0)$ numerically, we conduct the following two simulations.

- *Simulation 1 (no shock):* For each replication r, given the initial values, $\boldsymbol{\xi}_0, \boldsymbol{a}_0$ and $\boldsymbol{\kappa}_0$, and the deterministic processes of $\boldsymbol{g}_{l,t}$, we simulate the model (S.49) using the simulated productivity processes, $\boldsymbol{a}_t^{(r)}$ and $\boldsymbol{\kappa}_t^{(r)}$, for $t = 1, 2, ..., T$, and obtain a series of realized $\boldsymbol{\xi}_t$, i.e., $\boldsymbol{\xi}_t^{(r)}$, for $t = 1, 2, ..., T$:

$$\boldsymbol{\xi}_t^{(r)} = \boldsymbol{\psi}\left(\boldsymbol{\xi}_{t-1}^{(r)}, \boldsymbol{a}_t^{(r)}, \boldsymbol{a}_{t-1}^{(r)}, \boldsymbol{\kappa}_t^{(r)}, \boldsymbol{\kappa}_{t-1}^{(r)}, \boldsymbol{g}_{l,t}; \Theta\right).$$

- *Simulation 2 (with shock):* For each replication r, given the initial values, $\boldsymbol{\xi}_0$, $\boldsymbol{a}_0$ and $\boldsymbol{\kappa}_0$, and the deterministic processes of $\boldsymbol{g}_{l,t}$, we simulate the model (S.49) using the simulated productivity processes, $\breve{\boldsymbol{a}}_t^{(r)}$ and $\boldsymbol{\kappa}_t^{(r)}$, for $t = 1, 2, ..., T$, and obtain a series of realized $\boldsymbol{\xi}_t$, i.e., $\breve{\boldsymbol{\xi}}_t^{(r)}$, for $t = 1, 2, ..., T$:

$$\breve{\boldsymbol{\xi}}_t^{(r)} = \boldsymbol{\psi}\left(\breve{\boldsymbol{\xi}}_{t-1}^{(r)}, \breve{\boldsymbol{a}}_t^{(r)}, \breve{\boldsymbol{a}}_{t-1}^{(r)}, \boldsymbol{\kappa}_t^{(r)}, \boldsymbol{\kappa}_{t-1}^{(r)}, \boldsymbol{g}_{l,t}; \Theta\right).$$

Here, $\boldsymbol{\xi}_t^{(r)}$ and $\breve{\boldsymbol{\xi}}_t^{(r)}$ are the simulated $\boldsymbol{\zeta}_t$ in replication r in Simulation 1 and Simulation 2, respectively. Then, the two expectations, $E(\boldsymbol{\xi}_t|\boldsymbol{\xi}_0, \boldsymbol{a}_0, \boldsymbol{\kappa}_0)$ and $E(\boldsymbol{\xi}_t|\varepsilon_{z_a,i^*1}, \boldsymbol{\xi}_0, \boldsymbol{a}_0, \boldsymbol{\kappa}_0)$, are approximated as the averages across replications:

$$\hat{E}(\boldsymbol{\xi}_t|\boldsymbol{\xi}_0, \boldsymbol{a}_0, \boldsymbol{\kappa}_0) = \frac{1}{R}\sum_{r=1}^{R} \boldsymbol{\xi}_t^{(r)} \quad \text{and} \quad \hat{E}(\boldsymbol{\xi}_t|\varepsilon_{z_a,i^*1}, \boldsymbol{\xi}_0, \boldsymbol{a}_0, \boldsymbol{\kappa}_0) = \frac{1}{R}\sum_{r=1}^{R} \breve{\boldsymbol{\xi}}_t^{(r)}.$$

Thus, the approximated impulse response in period t is given as

$$GI_{\boldsymbol{\xi}}(t, \varepsilon_{z,i^*1}, \boldsymbol{\xi}_0, \boldsymbol{a}_0, \boldsymbol{\kappa}_0) = \frac{1}{R}\sum_{r=1}^{R} \breve{\boldsymbol{\xi}}_t^{(r)} - \frac{1}{R}\sum_{r=1}^{R} \boldsymbol{\xi}_t^{(r)}.$$

S5 Derivation of dispersion decomposition formula

Let U.S. states be indexed by i, and denote the collection of all states by $\mathcal{I}$, where $i \in \mathcal{I}$, and $\mathcal{I} = \{1, 2, ..., 49\}$. Let j denote the index for regions and $\mathcal{J}$ be the collection of all regions, where $j \in \mathcal{J}$ and $\mathcal{J} = \{1, 2, ..., 5\}$. Let $\mathcal{I}_j$ be the collection of the indices of the states in region j, with $\mathcal{I} = \cup_{j\in\mathcal{J}}\mathcal{I}_j$, and $\mathcal{I}_{j_1} \cap \mathcal{I}_{j_2} = \emptyset$, if $j_1 \neq j_2$. Further, let ω_i be the population share of State i. Define $\nu_j \equiv \sum_{i\in\mathcal{I}_j} \omega_i$ to be the weight of region j in the U.S. mainland, with $\sum_{j\in\mathcal{J}} \nu_j = 1$. It is now easily seen that the weight of State i in region j is ω_i/ν_j, with $i \in \mathcal{I}_j$, and $\sum_{i\in\mathcal{I}_j} \omega_i/\nu_j = 1$.

The dispersion of log house price-to-income ratios across all states is given by

$$\hat{\sigma}_{xt}^2 \equiv \sum_{i\in\mathcal{I}} \omega_i(x_{it} - \bar{x}_t)^2, \qquad \text{where} \qquad \bar{x}_t \equiv \sum_{i\in\mathcal{I}} \omega_i x_{it}.$$

The dispersion of log house price-to-income ratios within region j is given by

$$\hat{\sigma}_{xjt}^2 \equiv \sum_{i\in\mathcal{I}_j} \frac{\omega_i}{\nu_j}(x_{it} - \bar{x}_{jt})^2, \qquad \text{where} \qquad \bar{x}_{jt} \equiv \sum_{i\in\mathcal{I}_j} \frac{\omega_i}{\nu_j} x_{it},$$

and the dispersion of log house price-to-income ratios across regions is given by

$$\hat{\sigma}_{xrt}^2 \equiv \sum_{j\in\mathcal{J}} \nu_j(\bar{x}_{jt} - \bar{x}_t)^2.$$

It is easy to see that the following decomposition of variance holds:

$$\begin{aligned}
\hat{\sigma}_{xt}^2 &= \sum_{j\in\mathcal{J}}\sum_{i\in\mathcal{I}_j}\omega_i(x_{it}-\bar{x}_{jt}+\bar{x}_{jt}-\bar{x}_t)^2 \\
&= \sum_{j\in\mathcal{J}}\sum_{i\in\mathcal{I}_j}\omega_i\left[(x_{it}-\bar{x}_{jt})^2+(\bar{x}_{jt}-\bar{x}_t)^2+2\left(x_{it}-\bar{x}_{jt}\right)\left(\bar{x}_{jt}-\bar{x}_t\right)\right] \\
&= \sum_{j\in\mathcal{J}}\sum_{i\in\mathcal{I}_j}\omega_i\left(\bar{x}_{jt}-\bar{x}_t\right)^2+\sum_{j\in\mathcal{J}}\nu_j\sum_{i\in\mathcal{I}_j}\frac{\omega_i}{\nu_j}\left(x_{it}-\bar{x}_{jt}\right)^2 \\
&\quad +2\sum_{j\in\mathcal{J}}\left(\bar{x}_{jt}-\bar{x}_t\right)\sum_{i\in\mathcal{I}_j}\omega_i\left(x_{it}-\bar{x}_{jt}\right)\left(\bar{x}_{jt}-\bar{x}_t\right) \\
&= \sum_{j\in\mathcal{J}}\nu_j\left(\bar{x}_{jt}-\bar{x}_t\right)^2+\sum_{j\in\mathcal{J}}\nu_j\hat{\sigma}_{xjt}^2 \\
&= \hat{\sigma}_{xrt}^2+\sum_{j\in\mathcal{J}}\nu_j\hat{\sigma}_{xjt}^2.
\end{aligned}$$

Finally, the average within-region dispersion, $\hat{\sigma}_{xwt}$, is given by

$$\hat{\sigma}_{xwt} \equiv \left(\sum_{j\in\mathcal{J}}\nu_j\hat{\sigma}_{xjt}^2\right)^{0.5},$$

where $\hat{\sigma}_{xjt}$ is the standard deviation of log house price-to-income ratios across states within region j, and ν_j is the population weight of region j.

S6 Baseline model with costless migration

In the baseline model, we allow for route-specific migration costs by assuming $\alpha_{ii}=1$ and $\alpha_{ij}>1$ for all i and $j\in\mathcal{I}_n$, and $i\neq j$, (see equation (9)). To examine the importance of migration costs in determining house price dispersions, we consider a scenario where the migration costs, $\ln\alpha_{ij}$, are set to zero, namely,

$$\alpha_{ij}=1 \text{ for any } i \text{ and } j\in\mathcal{I}_n, \text{ and } i\neq j. \tag{S.55}$$

The values of all other parameters are kept the same as before. Note that the estimation or calibration of other parameters do not depend on the values of α_{ij} as shown in Section 5. We then implement the baseline simulations, presented in Section 7.1, under (S.55). As shown in Figure S6, dispersions of house price to income ratios jump in the second period and remain relatively stable throughout the rest of the periods, regardless of the spatial heterogeneity in land supply growth rates. These results indicate that migration can immediately equilibrate local housing markets when it is costless. Therefore, spatial heterogeneity in land-use regulation can lead to a secular rise in dispersion only in the presence of non-zero migration costs.

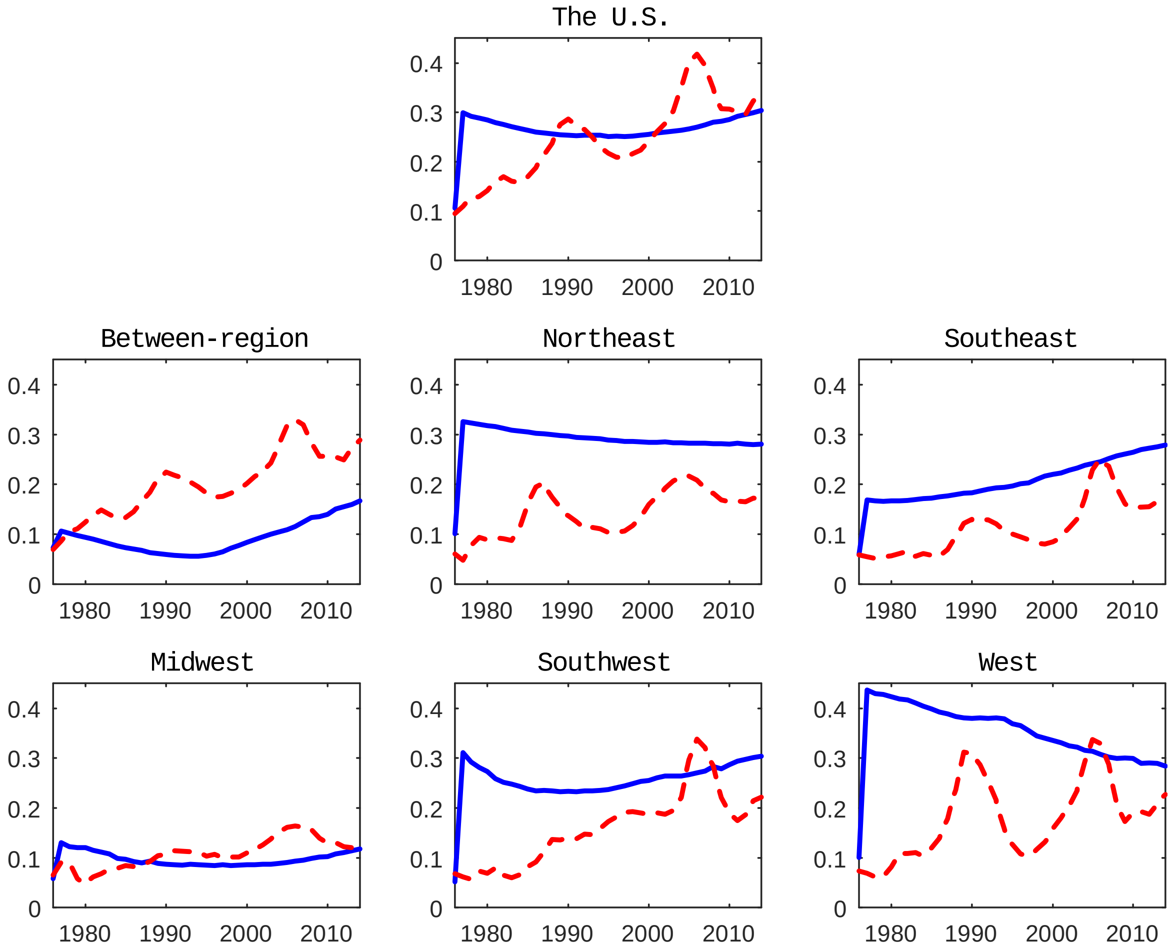

Figure S6: Dispersions of log house price-to-income ratios between- and within- U.S. regions (Solid-blue: simulated by model with costless migration; Dashed-red: data)

Notes: This figure compares the realized values of the dispersions of log house price-to-income ratios between- and within- U.S. regions with the simulated values under the baseline model with costless migration as in (S.55).

S7 Baseline model with homogeneous housing supply elasticity

In the baseline model, we allow $\alpha_{\kappa,i}$ to vary across locations, where $1-\alpha_{\kappa,i}$ is the location-specific elasticity of housing supply with respect to non-land inputs. To examine the effects of spatial heterogeneity in $\alpha_{\kappa,i}$ on the dispersion of house price-to-income ratio, we simulate the baseline model while assuming $\alpha_{\kappa,i}$ is the same across i, and set it to the national average estimate:

$$\alpha_{\kappa,i} = \bar{\hat{\alpha}}_{\kappa} = n^{-1} \sum_{s=1}^{n} \hat{\alpha}_{\kappa,s}, \text{ for } i = 1, 2, ..., n, \tag{S.56}$$

where $\hat{\alpha}_{\kappa,i}$ are obtained in Section 5.3. Note that $\hat{\gamma}_{it}$, and thus the estimation of κ_i and $g_{\kappa,i}$, depend on the values of $\alpha_{\kappa,i}$ (see Section 5.5). Thus, we re-estimate κ_i and $g_{\kappa,i}$, for $i = 1, 2, ..., n$, following the same steps as in Section 5.5, and re-do the baseline simulations using the re-estimated model. The results are summarized in Panel (3) of Table S3, and as can be seen, they are quite close to the results obtained when $\alpha_{\kappa,i}$ are allowed to differ across i. Thus, we conclude that spatial heterogeneity in housing supply elasticity is not an important reason for the rising house price dispersion.

Table S3: The level and the dispersion of realized and simulated log house price-to-income ratios

	Actual		**Simulated**			
	(1) Data		(2) Baseline simulation		(3) Homogeneous housing supply elasticities	
Year	*1976*	*2014*	*1976*	*2014*	*1976*	*2014*
			I. Level			
The U.S.	1.72	1.47	1.71	1.56	1.71	1.56
Northeast	1.63	1.57	1.67	1.73	1.67	1.72
Southeast	1.82	1.38	1.74	1.44	1.74	1.44
Midwest	1.67	1.21	1.62	1.30	1.62	1.30
Southwest	1.73	1.22	1.75	1.14	1.75	1.16
West	1.74	2.02	1.83	2.14	1.83	2.12
			II. Disperison			
The US	0.09	0.34	0.11	0.39	0.11	0.38
Between-region	0.07	0.29	0.07	0.33	0.07	0.32
Northeast	0.06	0.18	0.10	0.21	0.10	0.21
Southeast	0.06	0.17	0.06	0.22	0.06	0.21
Midwest	0.06	0.12	0.06	0.16	0.06	0.16
Southwest	0.07	0.22	0.05	0.26	0.05	0.26
West	0.07	0.23	0.10	0.27	0.10	0.26

Notes: This table reports the levels and the dispersions of realized and simulated log house price-to-income ratios at different geographical levels. Panel (2) reports the results from the baseline simulations. Panel (3) reports the simulation results of the alternative model in which state level housing supply elasticity, i.e., $\alpha_{\kappa,i}$, is assumed to be the same across locations, and set to the national average $\bar{\hat{\alpha}}_{\kappa}$, defined by (S.56).

Reference

Ciccone, A. and Hall, R.E. (1996). Productivity and the density of economic activity. *The American Economic Review*, 86, 54–70.

Davis, M.A., Fisher, J.D., and Whited, T.M. (2014). Macroeconomic implications of agglomeration. *Econometrica*, 82, 731–764.

Favara, G. and Imbs, J. (2015). Credit supply and the price of housing. *The American Economic Review*, 105, 958–992.

Favilukis, J., Ludvigson, S.C., and Van Nieuwerburgh, S. (2017). The macroeconomic effects of housing wealth, housing finance, and limited risk sharing in general equilibrium. *Journal of Political Economy*, 125, 140–223.

Herkenhoff K.F., Ohanian, L.E., and Prescott, E.C. (2018). Tarnishing the golden and empire states: Land-use restrictions and the us economic slowdown. *Journal of Monetary Economics*, 93, 89–109.

Koop, G., Pesaran, M.H., and Potter, S.M. (1996). Impulse response analysis in nonlinear multivariate models. *Journal of econometrics*, 74, 119–147.

Mian, A. and Sufi, A. (2009). The consequences of mortgage credit expansion: Evidence from the u.s. mortgage default crisis. *Quarterly Journal of Economics*, 124, 1449–1496.

Ortalo-Magne, F. and Rady, S. (2006). Housing market dynamics: On the contribution of income shocks and credit constraints. *The Review of Economic Studies*, 73, 459–485.

Philippon, T. and Midrigan, V. (2016). Household leverage and the recession. Working Paper 16965, National Bureau of Economic Research.

Valentinyi, A. and Herrendorf, B. (2008). Measuring factor income shares at the sectoral level. *Review of Economic Dynamics*, 11, 820–835.